Performance Evaluation of High Strength Concrete Using Natural Aggregates

Thesis Submitted for the Award of the Degree of

DOCTOR OF PHILOSOPHY

in

Civil Engineering

By

Akshat Mahajan

Registration Number: 41800626

Supervised By

Dr. Pushpendra Kumar Sharma

(34640)

Professor, School of Civil Engineering

LOVELY PROFESSIONAL UNIVERSITY, PUNJAB

2025

DECLARATION

I, **Akshat Mahajan**, bearing Registration No. **41800626**, hereby declare that the research work embodied in the Ph.D. thesis titled "**Performance Evaluation of High Strength Concrete Using Natural Aggregates**" submitted to Lovely Professional University is the original and bonafide work carried out by me under the supervision of **Dr. Pushpendra Kumar Sharma**, Professor, School of Civil Engineering, Lovely Professional University.

I further declare that:

a) The work presented in this thesis is a genuine contribution to the field of research and is a result of investigations carried out by me during the period of my doctoral study.

b) The research work has been conducted in accordance with the academic and ethical standards prescribed by the university.

c) Due acknowledgements and references have been duly given wherever the work of others has been cited or used.

d) The thesis has not been submitted either partly or fully to any other university or institution for the award of any degree or diploma.

I understand that any violation of the above declarations may lead to the cancellation of my degree by the university at any stage.

Signature of Scholar

Name: Akshat Mahajan

Registration Number:41800626

Date: 15-12-2025

CERTIFICATE

This is to certify that the work reported in the Ph. D. thesis entitled "**Performance Evaluation of High Strength Concrete Using Natural Aggregates**" submitted in fulfillment of the requirement for the award of degree of **Doctor of Philosophy (Ph.D.)** in the **School of Civil Engineering**, is a research work carried out by Akshat Mahajan (41800626), is bonafide record of his/her original work carried out under my supervision and that no part of thesis has been submitted for any other degree, diploma or equivalent course.

Dr. Pushpendra Kumar Sharma
Professor,
UID:34640
School of Civil Engineering,
Lovely Professional University
Punjab, India

ABSTRACT

High-strength concrete (HSC) has become an essential material for modern infrastructure due to its superiority in mechanical performance and durability; however, its large-scale application raises concerns related to the intensive consumption of natural aggregates and environmental sustainability. In this specific perspective, the present research investigates the performance of high-strength concrete produced using natural coarse aggregates limestone and granite in combination with alternative fine aggregates, namely silica sand (SS) and quarry sand (QS), as partial replacements for natural river sand. The study aims to evaluate the mechanical behaviour, durability characteristics, and cost implications of these material substitutions in order to identify best and practically viable HSC mixes.

A comprehensive experimental programme was designed in which four series of concrete mixes were formulated based on the type of coarse aggregate (limestone or granite) and fine aggregate replacement (silica sand or quarry sand). The replacement levels of fine aggregates were varied systematically, while all mixes were proportioned to achieve high strength and incorporated SCM's, specifically silica fume and metakaolin, to enhance matrix densification and long-term durability. Standard curing practices were followed, and tests were conducted at multiple curing ages to overview both early-age and prolonged performance.

The mechanical properties of the developed mixes were evaluated through compressive strength, split tensile strength, and flexural strength tests. Durability performance was assessed using water absorption, abrasion resistance, and RCPT. The results demonstrated that replacement of natural coarse aggregates with limestone and granite significantly enhanced the mechanical performance of HSC, with granite-based mixes consistently exhibiting higher strength due to improved aggregate hardness, angularity, and aggregate–paste interlock. Silica sand replacement showed optimum performance at 60%, leading to marked improvements in strength and durability owing to refined particle packing and reduced pore connectivity. Quarry sand exhibited optimal behaviour at 40%

replacement, beyond which excess fines adversely affected workability and durability.

Durability investigations revealed substantial reductions in water absorption, chloride permeability, and abrasion loss for best mixes, particularly those incorporating granite aggregates and silica sand. Granite-based mixes showed superior resistance to aggressive environments compared to limestone mixes, highlighting the influence of intrinsic aggregate properties on transport mechanisms. Based on combined mechanical and durability performance, selected optimum mixes from each series were further evaluated for cost. The cost analysis indicated that the performance gains were achieved with only marginal increases in material cost, demonstrating favourable cost–performance efficiency.

Overall, this research establishes that the judicious use of alternative fine aggregates and natural coarse aggregates can produce high-strength concrete with enhanced performance, durability, and economic feasibility, while reducing reliance on natural river sand. The findings contribute valuable insights for sustainable material selection in developing the better performing high-strength concrete.

Keywords: High strength concrete, granite aggregates, Silica Fume, Metakaolin, Limestone aggregates.

GRAPHICAL ABSTRACT

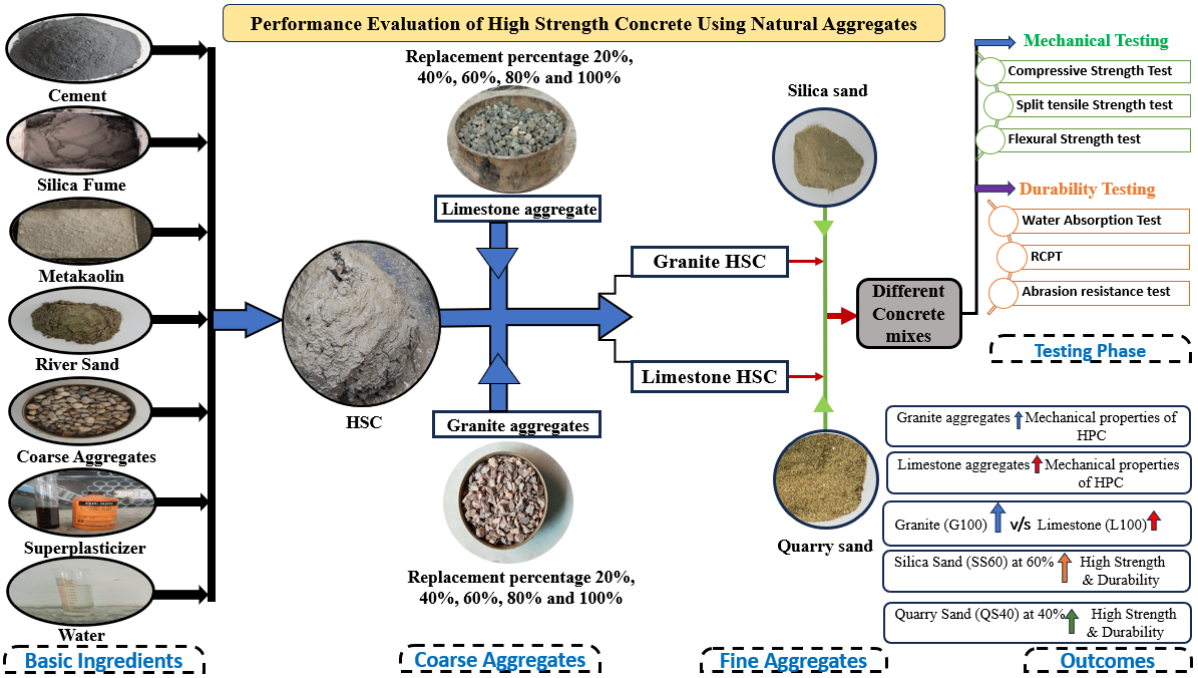

ACKNOWLEDGEMENT

First and foremost, I express my deepest gratitude to the Almighty God for granting me the strength, patience, and wisdom throughout the journey.

I would like to convey my sincere and heartfelt thanks to my esteemed research supervisor, Dr. Pushpendra Kumar Sharma, Professor, School of Civil Engineering, Lovely Professional University, for his invaluable guidance, constructive suggestions, and continuous encouragement, which were instrumental in shaping this research work.

I owe my profound gratitude to my parents, Mrs. Veena Mahajan and Mr. Rajan Mahajan, for their unconditional love, sacrifices, and constant encouragement throughout my academic journey. I also sincerely acknowledge my respected grandmother and grandfather for their blessings, motivation, and moral support.

I extend my heartfelt thanks to my wife, Megha Gupta, for her patience, understanding, and unwavering support, and to my sister, Akriti Mahajan, for her motivation and timely help. Special thanks to my beloved son, Taksh Mahajan, whose presence has been a constant source of joy and stress relief during this journey.

I would be lacking behind if I do not express my sincere gratitude to my uncles, Mr. Rajesh Kumar and Mr. Arun Mahajan, who were there to support me at every time.

A Special to my friends Dr. Ganesh S., Mr. Sahil Jaggi, Dr. Tarunbir Singh, Mohd. Latif, and Mr. Satwinder Singh for their friendship, encouragement, and support during my Ph.D. journey.

Finally, I acknowledge all those who have directly or indirectly contributed to this academic journey.

Akshat Mahajan

Research Scholar

Lovely Professional University

Contents

LIST OF ABBREVIATIONS

High Strength concrete.	HSC
Silica Fume	SF
Fly ash	FA
Calcium Silicate Hydrate	CSH
Non-Destructive Testing	NDT
Supplementary Cementitious Materials	SCM
Self-compacting concrete	SCC
Metakaolin	MK
Polyvinyl Alcohol	PVA
Interfacial Transition Zone	ITZ
Scanning Electron Microscopy	SEM
Ultra-High Perfromance concrete	UHPC
Condensed Silica Fume	CSF
high-performance concrete	HPC
Ground Granulated Blast Furnace Slag	GGBFS
Rice Husk ash	RHA
no-fines concrete	NFC
Water by binder	w/b
Water by cement	w/c
X-ray Diffraction	XRD
Linz-Donawitz	LD
Polypropylene	PP
Recycled Coarse Aggregates	RCA
Recycled Aggregates	RA
Construction and Demolition	C&D
Rapid chloride permeability testing	RCPT
Compression Testing Machine	CTM
Megapascal	MPa
Sodium Chloride	NaCl
Sodium Hydroxide	NaOH

Non-Destructive Techniques	NDT
Ultrasonic Pulse Velocity	UPV
Oyster shell powder	OSP
Coal bottom ash	CBA
Recycled concrete Aggregates	RCA
Ferronickel slag	FNS
Los Angeles	LA

LIST OF FIGURES

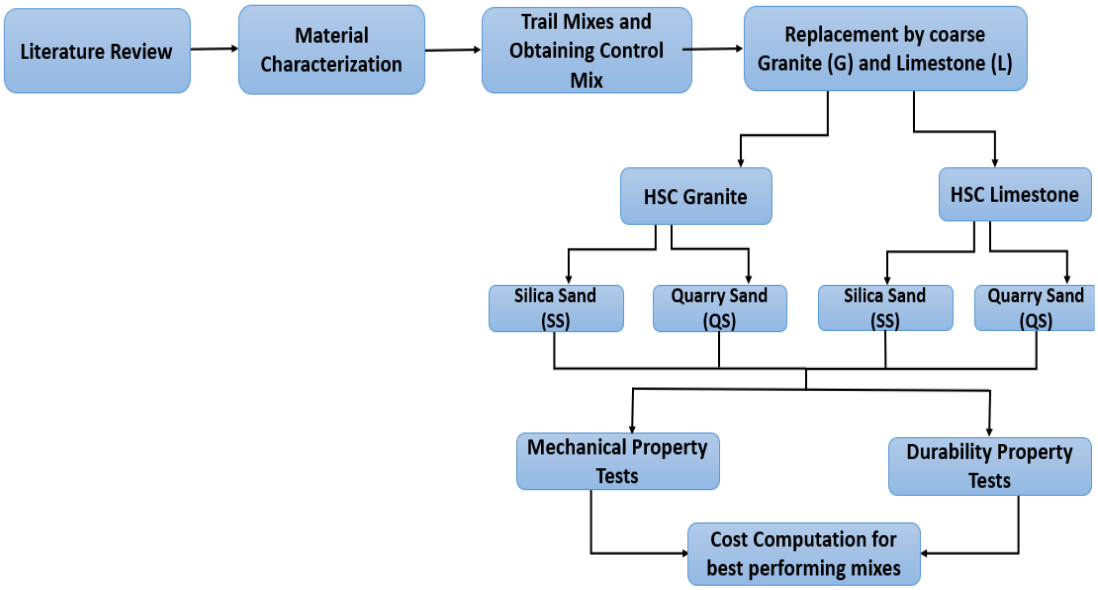

LIST OF TABLES

CHAPTER 1 INTRODUCTION

1.1 GENERAL

Concrete is one of the most essential resources in modern construction, widely regarded as the second most used material globally after water. Its every year production is estimated at 25-30 billion tons, driven by its affordability, versatility, and ability to be moulded into various forms for infrastructure projects such as buildings, roads, bridges, and dams [1], [2]. Concrete's widespread use stems from its basic composition of cement, aggregates, water, and sometimes admixtures, which together create a durable and strong material. As urbanisation and population growth accelerate, particularly in developing nations like China and India, which consume billions tons of concrete annually, the demand for this material continues to rise[3],[4].The rise in megacities, the growth of transport infrastructure, and the increasing preference for high-rise buildings have intensified the reliance on concrete. This growing need highlights the importance of understanding concrete and its ingredients' role in construction and the challenges associated with its production and supply.

The composition of concrete makes it adaptable to a range of applications. Cement, typically Ordinary Portland Cement (OPC), acts as a binder, while aggregates comprising 60-75% of concrete's volume provide strength and stability[5]. Coarse aggregates, which included gravel or crushed stone, and fine aggregates, like river sand, are critical to concrete's mechanical charactestics, including compressive strength and durability. Water eases the hydration reaction that hardens the cement paste, and admixtures can enhance properties like workability or setting time[6],[7].

In addition to these advantages, concrete's compatibility with reinforcing steel makes it a preferred material for enhancing its tensile capacity in structural systems. Its inherent fire resistance, thermal mass, and ability to undergo long-term strength gain further contribute to its suitability for critical infrastructure projects [8], [9]. As performance requirements continue to evolve, especially with higher expectations for durability, sustainability, and service life

The ability to adjust these components allows concrete to meet diverse needs, from standard mixes for residential structures to HSC (HSC) for specialized projects like high-rise buildings and sea bridges, which require compressive strengths above 60 MPa[10]-[13]. However, the massive scale of concrete production to meet global infrastructure demands has raised significant concerns about resource availability and environmental impacts.

1.2 Present scenario

The increasing demand for concrete has led to a surge in the extraction of its raw materials, particularly aggregates and cement. Global aggregate consumption is estimated at 32-50 billion tons per year, with natural sand and gravel being mined from riverbeds and quarries at unsustainable rates [14],[15].The United Nations Environment Programme (UNEP) in its *Sand and Sustainability* report (2019) warns that excessive sand mining disrupts ecosystems, erodes riverbanks, and threatens biodiversity in regions like Southeast Asia and Africa [16]. For example, sand extraction in rivers such as the Mekong has caused significant environmental damage, including habitat loss and altered water flows [17] .Similarly, cement production is a major environmental concern, contributing 8-9% of global CO_2 emissions. Production of approximately one ton cement releases around one ton of CO_2, with worldwide production emitting 1.6 billion metric ton of CO_2 in 2022 [18]-[20],[21]. These environmental challenges highlight the urgent need for sustainable practices in concrete production.

Sustainability concerns are further compounded by the supply-demand dynamics of concrete's raw materials [22], [23].The rapid pace of urbanization, especially in emerging economies, has outstripped the natural replenishment of aggregates, leading to shortages in some regions. For instance, sand scarcity in parts of India and the Middle East has driven up construction costs and prompted illegal mining activities [24]-[26]. Cement production, meanwhile, relies on energy-intensive processes and finite resources like limestone, contributing to both environmental degradation and resource depletion. These supply constraints underscore the need for alternatives, such as using SCM's like SF and MK to reduce cement content,

or replacing natural aggregates with locally available materials like crushed aggregates [27]-[29].

The growing demand for concrete, coupled with its environmental footprint, has spurred research into sustainable solutions. Alternatives like recycled aggregates, industrial by-products, and SCMs can reduce reliance on natural resources and lower CO_2 emissions. For example, SF and MK improve concrete's strength and durability while decreasing the need for cement, potentially reducing emissions by up to 30% in some mixes [30]. Similarly, using alternative aggregates like limestone or granite can alleviate pressure on overexploited natural sand and gravel reserves [16]. These strategies align with global sustainability goals, such as those outlined in the UNEP's *Sand and Sustainability* report and the COP21 Paris Agreement, which call for resource-efficient construction practices. Addressing these challenges is critical to ensuring that concrete production meets the needs of modern infrastructure without compromising environmental integrity.

Rapid infrastructure development, has significantly strained the supply chain of its raw materials, particularly aggregates and cement. The construction boom in urbanizing regions, such as Asia and Africa, has led to localized shortages of high-quality aggregates, with countries like India facing challenges in securing consistent supplies of river sand due to regulatory restrictions and environmental concerns [Zhang et al., 2022]. These supply constraints have increased construction costs and prompted exploration of alternative materials to ensure a stable supply chain. For instance, the use of manufactured aggregates, such as quarry sand, and recycled materials from C&Dwaste has gained traction as a means to address aggregate scarcity while promoting a circular economy [Gholampour et al., 2023]. However, the adoption of such alternatives requires careful evaluation to ensure they meet the performance standards of conventional concrete, particularly for specialized applications requiring enhanced strength and durability as required in HSC.

1.3 High Strength Concrete

Defining HSC has evolved significantly over the decades in response to advancements in material science and changing structural demands. In the early

years of concrete development, any concrete achieving a compressive strength beyond 40 MPa was considered high strength, primarily because conventional mixes rarely exceeded this range [31],[32]. During the 1960s and 1970s, with the introduction of better cement quality, improved aggregate selection, and chemical admixtures, compressive strength targets of 60 MPa became increasingly achievable. Consequently, codes and researchers began referring to concrete with a compressive strength more than 55 or 60 Megapascal as HSC. As per the American Concrete Institute (ACI 363R-92), HSC is demarcated as concrete with a strength in compression higher than 55 MPa (8000 psi)[31]. Thus, the term HSC is now context-dependent and dynamic, generally applied to concretes that surpass the strength range of normal structural concrete and are tailored for demanding structural. HSC as per the Indian standards, is the concrete which is having strength more than 65 MPa[33].

1.4 Composition of High-Strength Concrete

The successful formulation of HSC depends on a scientific combination of constituents, each selected and proportioned to enhance various properties of concrete.

(a) Cementitious binder

HSC uses cement of higher grade and cementitious binders, including SCM's, with low alkali content and high early strength. To improve strength and durability, HSC incorporates different type of SCMs such as:

Silica Fume: An extremely fine secondary product generated while production of silicon and ferrosilicon alloys, it contains over 90% amorphous silica and acts as a micro-filler and pozzolan, refining the pore structure and improving the ITZ.

Metakaolin: A highly reactive pozzolan derived from calcined kaolinite clay, it enhances early strength and chemical resistance.

Fly Ash and GGBFS: Occasionally used in combination, these improve long-term strength and workability but are more common in High-Performance Concrete (HPC).

These cementitious materials contribute to formation of additional CSH gel through pozzolanic reactions, which contribute to reduce porosity and enhance microstructural density[27], [29].

(b) Aggregates

Aggregates form the skeleton of concrete and are significantly crucial for achieving higher strength. For HSC, the Coarse Aggregates preferably be clean, strong, angular, and free from deleterious substances. Fine Aggregates are equally significant for the HSC. In a nutshell, aggregate's selection along with the type of aggregate have a very conciderable part in imparting the desirable properties to the HSC. While selecting the coarse aggregates for HSC, properties including crushing strength, abrasion value, specific gravity etc share a major contribution in strength properties of HSC.

(c) Water and Water-binder ratio

Water content in HSC is tightly controlled. A low w/b is preferred for the HSC, as it essentially reduces porosity and achieves high strength. However, a lower w/b ratio negatively affects workability, which necessitates the use of superplasticizers.

(d) Chemical Admixtures

To compensate for low workability and enhance performance, superplasticisers are employed. Modern admixtures based on polycarboxylate ether (PCE) are highly effective in dispersing cement particles, enabling the use of very low w/b ratios.

1.5 Applications of High-Strength Concrete

The superior mechanical and durability properties of HSC make it extremely suitable, specifically for structural applications. With advancements in material design and placement techniques, HSC is now widely used in diverse sectors of civil engineering.

(a) In high-rise construction and Skyscrapers, HSC enables the use of smaller and more efficient structural elements, particularly columns and core walls, by offering increased compressive strength and stiffness[34]. This leads to reduced

cross-sectional area of vertical load-bearing members, more usable floor space, lower self-weight of the structure, reducing foundation loads.

Iconic structures like Petronas Towers (Malaysia) utilize HSC grades for vertical elements to meet structural performance criteria.

(b) Long-Span Bridges and Flyovers, especially in bridge engineering, HSC is preferred in prestressed gir0ders, box segments, and piers, where high compressive strength and durability are critical. The increased strength allows for

- Longer spans with reduced member depth,
- Decreased deflections,
- Enhanced fatigue performance in dynamic loading condition3s.

Segmental precast box girder bridges and cable-stayed bridges benefit significantly from HSC, particularly when exposed to harsh environments.

(c) In Precast and Prestressed Elements, HSC is widely used in precast structural components which includes beams, slabs, wall panels, & bridge segments.

The early strength gain due to SCMs accelerates demolding and allows faster production cycles. In prestressed concrete applications, the high compressive strength of HSC enhances stress transfer efficiency.

(d) For Marine and Coastal structures, due to its low permeability and high resistance to chloride penetration, HSC is ideal for marine structures, including seawalls, piers, offshore platforms, and port infrastructure to enhance the durability and increase the life of these coastal structures.

(e) Industrial Floors and Heavy-Duty Pavements in warehouses, industrial floors, and container yards, HSC is used for slabs subjected to heavy wheel loads and abrasion. The high flexural and compressive strength ensures resistance against cracking and surface wear.

(f) In case of Nuclear and Defence structures, HSC is employed in nuclear containment vessels, defence bunkers, and blast-resistant structures, where low permeability, radiation shielding, and impact resistance are required.

(g) Repair and retrofitting applications, due to its high strength and compatibility with existing structures, HSC is also used in jacketing of columns, overlay systems, and retrofit interventions where space is limited but high strength is necessary.

1.6 Role of Aggregates in Concrete

Aggregates serve as core ingredient in concrete mixtures, occupying approximately 60% to 80% of its total volume, and significantly influence its mechanical, durability, and rheological properties. The proper selection and proportioning of aggregates are crucial in producing concrete with the desired strength, workability, and long-term performance. Aggregates provide a rigid skeleton in the concrete matrix and act as economic fillers that reduce the demand for cement paste, thereby influencing cost and shrinkage behavior.

The contribution of coarse aggregates to the HSC has been considered as a factor of paramount significance, as different characteristics of coarse aggregates govern the various aspects of the performance of HSC. Many aggregate characteristics, including strength, stiffness, abrasion and many other factors, profoundly influence the strength, stiffness, fracture and long-term durability of the HSC. Early studies established that coarse aggregate type and quality govern the failure mechanism of HSC far more significantly than in normal-strength concrete. It can be stated that different types of aggregates have different influences on compressive, tensile strengths, durability and many other long-term properties largely due to variations in characteristics of coarse aggregates[35],[36]. Subsequent studies confirmed that high-quality aggregates with low porosity and high intrinsic strength are essential for achieving high compressive strengths beyond 60 MPa, as failure often shifts from the matrix to the aggregate particles themselves[37]

Past studies demonstrated that aggregate hardness, roughness, and surface texture significantly affect the stress transfer efficiency at the ITZ, with stronger aggregates contributing to higher load-carrying capacity, specifically in the case of HSC [37],[38],[39]. Around the same period, Kilic et al. reported that high-strength mixtures incorporating dense and angular aggregates achieve superior abrasion resistance and improved post-peak behaviour, underscoring the role of aggregate morphology in imparting toughness and resistance to surface deterioration.

More recent studies examined aggregate effects from both mechanical and durability perspectives. Beushausen and Dittmer observed that the elastic modulus

of HSC is strongly influenced by aggregate stiffness, noting that aggregate selection becomes especially critical when designing concretes for high-rise or prestressed applications where deformation control is essential[40]. Research on alternative aggregate types, including recycled and ceramic aggregates, further highlighted that deviations in aggregate strength or absorption characteristics can alter shrinkage behaviour, permeability, and microcracking in HSC.[41]

Advances in material science have also expanded the focus toward optimizing coarse aggregate characteristics for UHPC. For instance, Li et al. demonstrated that the incorporation of coarse basalt aggregates enhances both compressive strength and fracture resistance due to their superior elastic properties and strong bond with the matrix [42]. Studies on aggregate behaviour under rate-dependent loading additionally revealed that aggregate stiffness governs crack propagation and energy absorption mechanisms in high-performance concretes[37], [38].

Collectively, the literature underscores that coarse aggregate selection is not merely a volumetric consideration but a decisive factor that controls the structural reliability and durability of HSC[43],[44].Appropriate aggregate choice considering, texture, stiffness, abrasion, toughness and strength is therefore fundamental factor for achieving the targeted performance levels in advanced concrete systems.

1.7 Role of Fine Aggregates in HSC

Fine aggregates form an essential component of HSC, fundamentally influencing its packing density, cohesiveness, and overall performance. Because HSC is proportioned with low water-binder ratios and higher binder contents, the grading, texture, and mineralogical characteristics of the fine aggregates become more critical than in normal-strength concrete. Variations in fineness or angularity directly affect the compactness of the matrix, thereby influencing strength development and long-term durability[45], [46].

Well-graded fine aggregates contribute to a denser particle arrangement, resulting in reduced voids and improved structural integrity. Many of the past studies have shown that improvements in packing reduce pathways for moisture ingress, leading to better resistance against chemical deterioration[47], [48]. Similarly,

optimized fine aggregate proportions support enhanced tensile response when used alongside reactive pozzolans like SF, as noted by Bhanja and Sengupta [49]. This improvement is attributed mainly to better grain-to-grain interaction and the stabilization of the cementitious matrix.

The type and quality of fine aggregates also play a substantial role when SCM are incorporated. Research has shown that compatibility between fine aggregates and pozzolanic materials affects the degree of microstructural refinement achieved in HSC mixtures. For instance, the work of Khatib and Hibbert highlighted that aggregate characteristics influence how effectively MK-modified mixes consolidate and gain strength. More recent findings suggest that fine aggregates with suitable mineralogy and surface texture facilitate better dispersion of SCMs and lead to improved homogeneity in high-strength mixes[27], [50] .

In addition, modern studies such as those by Kim et al.[51]v indicate that the mechanical performance of HSC, particularly under abrasion and environmental exposure, is closely linked to the physical attributes of the fine aggregate fraction. Angular and dense fine aggregates assist in forming a more compact surface layer, contributing to improved wear resistance and reduced permeability.

Overall, fine aggregates do not merely serve as inert fillers in HSC; they actively influence its performance by refining packing structure, improving cohesiveness, and enhancing durability[52]. Their selection must therefore be guided by particle size distribution, shape characteristics, and mineralogical compatibility to fully realize the benefits of HSC systems.

1.8 Need for alternatives to Natural aggregates

The steady rise in concrete consumption across residential, commercial, and infrastructure projects has placed significant strain on the natural sources of aggregates used in HSC. While the structural performance of HSC makes it indispensable for modern construction, its traditional reliance on river sand and crushed stone is becoming increasingly unsustainable. This situation has created a pressing need to identify alternative aggregates that can deliver comparable performance while reducing pressure on natural ecosystems and supply chains.

Rapid depletion of natural aggregate reserves

River sand and quarry stone are being extracted at rates far beyond natural replenishment, particularly in fast-urbanizing regions. This leads to long-term scarcity and inconsistent availability of quality aggregates.

- **Environmental degradation from excessive mining**
  Unregulated removal of river sand causes riverbank erosion, habitat loss, and lowered groundwater levels, disrupting entire ecological systems.
- **Quarrying impacts on terrain and biodiversity**
  Continuous extraction of crushed stone weakens slopes, generates dust pollution, and affects local flora and fauna, raising concerns about landscape stability.
- **Increasing restrictions on sand mining**
  Governments in regions such as India, the Middle East, and Southeast Asia have imposed strict controls on sand extraction, causing supply shortages and project delays. This compels the industry to seek viable alternatives.
- **Rising transportation costs and embodied energy**
  As nearby natural deposits become exhausted, aggregates must be transported from distant locations, increasing fuel consumption, environmental footprint, and overall construction costs.
- **High carbon footprint of aggregate production**
  Drilling, blasting, crushing, and screening operations rely heavily on fossil fuels, resulting in significant CO_2 emissions and dust pollution during aggregate processing [47].
- **Need for material supply chain stability**
  Dependence on limited natural sources can disrupt continuous construction activity. Alternative aggregates help stabilize supply chains, especially for large-scale HSC projects.
- **Support for green building certification requirement**
  Sustainable rating systems like LEED and GRIHA encourage the use of low-impact materials and locally sourced alternatives to reduce embodied energy.
- **Reduction of construction costs in the long term**

Alternative aggregates, when sourced locally, can significantly cut down transportation costs, making them economically attractive for high-volume concrete production.

- **Encouragement of sustainable infrastructure policies**
  Modern construction policies promote reducing dependence on river sand and raw crushed stone. Alternative aggregates align with national and global sustainability mandates (e.g., UNEP sand sustainability principles).
- **Preparing for future material scarcity**
  Urban expansion and megaproject development will intensify aggregate demand. Diversifying aggregate sources today helps mitigate future shortages and ensures resilience in construction material supply.

This promotion to move towards sustainable development parallelly also aligns with Sustainable Development Goals (SDGs)

The construction sector's shift toward alternative materials aligns with several **United Nations SDGs**, notably:

Goal 9 (Industry, Innovation, and Infrastructure): Encouraging the creation of robust infrastructure using local materials

Goal 11 (Sustainable Cities and Communities): Promoting environmentally conscious urban development.

Goal 12 (Responsible Consumption and Production): Minimizing overuse of finite natural resources.

Adoption of alternative natural aggregates like limestone and granite in HSC supports these global targets by reducing the dependency on conventional resources and improving the overall environmental performance of concrete.

1.9 Supplementary Cementitious Materials

SCM's are finely divided mineral constituents that possess either pozzolanic reactivity or latent hydraulic properties and are added to concrete to partially replace Ordinary Portland Cement (OPC). Such materials chemically engage with the $Ca(OH)_2$ generated in the course of cement hydration, yielding additional CSH,the principal binding phase responsible for strength development in concrete. Typical SCMs include SF, FA, GGBFS, and calcined clays such as MK. Their

incorporation modifies the hydration mechanism, improves particle packing, and enhances the physical, mechanical, and durability features of the cementitious system. The technical importance of SCMs has been demonstrated over decades of research, particularly in high-performance and high-strength applications where conventional cement alone may not meet the stringent performance requirements [18], [28].

In the context of modern industrial growth, SCMs have gained prominence not only because of their technical benefits but also because they are widely available as by-products of several large-scale manufacturing processes. Coal-based power generation produces millions of tonnes of FA annually, the ferrosilicon industry releases SF in significant quantities, and calcined clays (including MK) are increasingly produced through thermal activation of naturally available kaolinitic clays. Many of these by-products have historically been disposed of through landfilling, which presents environmental challenges such as land occupation, dust emissions, and contamination of nearby ecosystems. Utilising these materials in concrete transforms industrial waste into a valuable engineering material, helping reduce disposal-related problems while promoting sustainable construction practices [24], [28]. This approach is well aligned with global goals of reducing the carbon footprint of construction materials, particularly since cement production alone contributes nearly one tonne of CO_2 per tonne of cement produced.

The technical value of SCMs becomes especially evident in the production of HSC. High-strength mixes generally have low w/b ratios and require a dense microstructure, characteristics that SCMs are particularly effective in achieving. SF, for instance, is known for its ultrafine particle size typically around 0.1 μm and its high amorphous silica content. Its addition enhances matrix densification, accelerates pozzolanic reactions, and strengthens the ITZ, resulting in markedly improved compressive and tensile strength of HSC mixes [16], [17], [18]. Its influence on matrix refinement also leads to improved resistance to microcracking, which is a critical aspect in maintaining prolonged structural integrity in high-strength applications.

MK, another widely studied SCM, also contributes significantly to HSC performance. Produced by calcining kaolinitic clay at temperatures typically between 650-800°C, MK is highly reactive and participates actively in pozzolanic reactions. Its inclusion has been shown to enhance early and long-term strength, reduce pore connectivity, and improve the overall compactness of the cementitious matrix [28], [29]. When used in conjunction with SF or other SCMs, MK helps improve workability, reduces the susceptibility to autogenous shrinkage, and enhances the composite performance of the concrete mixture [30]. Such synergistic effects are particularly beneficial in high-strength systems, where fine-tuning of rheology, setting characteristics, and strength development is essential.

Beyond improvements in strength, SCMs play a decisive role in enhancing durability, an equally important requirement for HSC used in aggressive environments. SCMs help reduce permeability by refining the pore structure and decreasing the volume of capillary pores, thereby lowering the risk of chloride ingress, sulfate attack, and internal microstructural deterioration. Studies have reported substantial improvements in resistance to chloride penetration and sulfate-induced degradation when SCMs such as SF, MK, and slag are incorporated in concrete [11], [15], [26]. Reduced permeability also limits moisture transport, which in turn enhances the freeze-thaw durability and long-term dimensional stability of HSC. Such qualities are crucial for huge infrastructure developments, such as skyscrapers, bridges, and offshore structures, where the concrete is often exposed to harsh conditions over extended service periods.

Overall, SCMs serve a dual function: they improve engineering performance while simultaneously supporting sustainability objectives by decreasing cement consumption and utilising industrial by-products. Their role in HSC is therefore integral, combining material efficiency with improved strength and enhanced long-term durability [34].

1.10 Significance of the Research

The accelerating pace of urbanisation and infrastructural development across the globe, especially in emerging and developing economies like India and many others, has led to an immense surge in demand for concrete, a material surpassed only by water in terms of global usage. With cities expanding vertically and horizontally to accommodate growing populations, industrial activities, long-span bridges, resilient and robust transportation infrastructure, and many other significant engineering developments across the nation and globe, there is an increasing requirement for concrete that can sustain higher loads and provide improved long-term performance during its service life. In this context, HSC has emerged as a key material due to its superior mechanical properties, making it highly suitable for high-rise skyscrapers, long-span bridges, precast segments, and heavy-duty industrial constructions.

However, this increased demand for HSC places a consistent pressure on raw material resources particularly natural coarse and fine aggregates, which are traditionally sourced from riverbeds. The extraction of natural river sand and gravel from the riverbeds on a large scale causes severe ecological imbalance, including depletion of river ecosystems, disruption of aquatic life habitats, erosion of riverbanks, alterations in natural flow regimes, and even the potential shifting of river courses. Such environmental and ecological disturbances pose a long-term threat not only to biodiversity but also to water security, agricultural productivity, and global climate conditions in long term.

Understanding these environmental and resource-related concerns, the scenario underscores the necessity of exploring alternative aggregates that are more abundant, regionally available, or industrial by-products the significance of this research lies in its timely response to the need for sustainable alternatives to conventional aggregates in HSC. Exploring materials like limestone and granite aggregates, which are either abundantly available, provides a viable route for conserving natural riverbed resources while meeting the functional requirements of modern construction. This research, therefore, aims not only to assess the mechanical performance of such alternative aggregates in HSC but also to contribute toward a broader goal of eco-efficient and resource-conscious concrete

production, thereby aligning civil engineering practices with the principles of sustainability, circular economy, and responsible urban development.

1.11 Gap in the Research Area

Although earlier studies have examined the effect of coarse aggregates on the behaviour of HSC, most investigations have treated these materials in isolation rather than comparatively. A very few studies have systematically examined the combined effect of different coarse and fine aggregates' mechanical and durability characteristics, specifically in HSC. This lack of a comprehensive, side-by-side evaluation creates a gap in understanding how different coarse-fine aggregate combinations influence long-term performance parameters, which are critical for HSC applications. Moreover, there was almost no study found, where different combinations of granite and limestone with silica sand and Quarry Sand, had been studied.in HSC

While numerous studies highlight the role of SCMs such as SF and MK in improving strength and long-term durability, the interaction between SCM rich concrete and alternative aggregate sources has been less explored.

1.12 Objectives of the Present Research

The proposed objectives of study are given as

- To study the effect of granite and limestone as coarse aggregates along with silica sand and Quarry sand as fine aggregates on the mechanical properties of high-strength concrete.
- To test the durability of high-strength concrete mix.
- To determine the cost of high-strength concrete mix thus arrived.

1.13 Thesis Organisation

The thesis is systematically organised into five chapters, which are given as below.

Chapter 1: Introduction

This chapter outlines the general introduction, HSC and its background, and the objectives of the study. It discusses the need for HSC in modern infrastructure, the composition of HSC, applications of HSC, the role of aggregates, Supplementary

Cementitious Materials (SCM) and their use, environmental implications of using conventional aggregate, and the need for the present research.

Chapter 2: Literature Review

This chapters showcases a detailed analysis of existing research, covering the review of the use of SCM in HSC. Furthermore, the effect of various parameters, including SCM, coarse aggregates, fine aggregates, water-cement ratio, and many other parameters, on the characteristics of concrete has discussed in depth.

Chapter 3: Materials and Methodology

This chapter provides an in-depth description of the various materials used in the present research, including cement, SF, MK, different fine aggregates, coarse aggregates and admixtures. It involves the discussion of the various physical and chemical properties of the different materials used in the experimental research. Moreover, the experimental methodology adopted, along with the test procedures of various mechanical and durability tests are also explained in this chapter in sufficient depth. Details of the mixes prepared and the various mix designations used are also discussed.

Chapter 4: Results and Discussion

This chapter reports the results obtained for the different concrete properties in the ongoing experimental program. A detailed discussion of the results of different mechanical and durability properties for understand the effect of different materials used, are the part of this chapter. The behaviour of HSC with different combinations and replacement levels of aggregates is compared and interpreted in this chapter.

Chapter 5: Conclusions and Recommendations

This final chapter sums up the decisive findings, provides conclusions drawn from the experimental study, and offers a few recommendations from the work. Moreover, suggestions for the future scope of work are also discussed in this specific chapter.

CHAPTER 2 LITERATURE REVIEW

2.1 General

Concrete continues to underpin modern infrastructure owing to its versatility, structural reliability, and adaptability to diverse construction demands. In the past decades, demand for infrastructural developments has shifted the attention for special concretes, performing better in different aspects of strength and durability. As with the advancements in materials and construction practices over time, the selection and understanding of the basic ingredients is a major concern of present time. This chapter reviews the major developments reported in literature, focusing on various aspects of the material behaviour, strength, performance, etc of the concreting systems.

2.2 Introduction to HSC

Caldarone et al.[53] provides one of the most comprehensive treatments of HSC, outlining the practical considerations involved in its production and performance. The book explains how mixture proportioning, aggregate quality, and curing regimes collectively influence the development of high compressive strengths. It emphasises the importance of low water-binder ratios and high-reactivity supplementary materials in achieving dense microstructures. The text also highlights construction-phase challenges associated with HSC, including workability control, heat generation, and quality assurance. Overall, the work serves as a foundational reference, demonstrating how material selection and proportioning strategies govern the reliable production of HSC in field applications.

Megat Johari et al. [54]investigated how different SCM modify the engineering behaviour of HSC. Using SF, FA, and slag at varying replacement levels, the authors demonstrated that these materials significantly refine the pore system and enhance both strength and durability. Their results showed notable improvements in compressive strength and elastic modulus, particularly when SF was incorporated. The study also reported reduced permeability and improved resistance to chloride ingress, attributes closely linked to the dense

microstructures developed in HSC systems. The work established that rational combinations of SCMs can produce high-strength mixes with superior long-term performance.

Amin and Abu El-Hassan [55]explored the effect of several nanomaterials nano-silica, nano-clay and nano-alumina on the mechanical behaviour of HSC. Their results indicated that nano-silica was most effective in enhancing early and later-age strength owing to its high pozzolanic reactivity and ability to accelerate CSH formation. Nano-clay improved cohesion and reduced segregation, while nano-alumina contributed modestly to strength gains. The overall findings showed that controlled nano-material dosages significantly improved compressive and tensile strength by densifying the matrix and refining microstructural packing. This study demonstrated that nanotechnology can be strategically employed to further elevate the performance of HSC.

Lee et al. [56] examined the applicability of NDT methods to evaluate the hardened-stage strength of HSC. By correlating UPV and rebound hammer readings with laboratory-measured compressive strength, the authors developed prediction models suitable for high-strength mixes, which typically present greater sensitivity to small variations in material quality. Their findings revealed that combined NDT approaches yield more reliable estimations compared to single-method assessments. The study demonstrated that calibrated NDT techniques can effectively track strength development in HSC structures, providing a practical tool for in-situ evaluation where direct sampling is limited.

Beushausen and Dittmer [38] investigated how different aggregate types affect the Strength in compression and elastic modulus of HSC. Their results showcased aggregate stiffness plays a decisive role in governing overall mechanical behaviour, with stronger and denser aggregates leading to higher modulus values and improved load-carrying capacity. The study also highlighted that in HSC, the aggregate paste interface becomes a critical determinant of performance due to the highly refined cement matrix. By demonstrating the strong link between aggregate

quality and HSC mechanical properties, the authors underscored the need for careful aggregate selection when designing high-strength mixes.

The reviewed studies indicate that the behaviour of High-Strength Concrete is strongly influenced by various factors such as low water-binder ratio, aggregate quality, and the incorporation of reactive supplementary cementitious materials. Many past studies have reported that materials such as silica fume, fly ash, and nanomaterials improve compressive strength and durability by refining the pore structure and producing a denser cement matrix. Microstructural investigations also revealed that improvement in the interfacial transition zone and additional C–S–H formation play an important role in enhancing the properties of HSC. At the same time, several studies observed reduced workability and increased sensitivity to curing and material proportions in high-strength mixes. Previous investigations mainly and primarily focused on binder modification and very limited aggregate variations, whereas fewer studies comparatively evaluated the role of different natural coarse aggregates and alternative fine aggregates. Hence, the present study was undertaken to understand the combined influence of granite, limestone, silica sand, and quarry sand on the behaviour of HSC.

2.3 Utilisation and role of SCM in Concrete mixes

SCM are used in different concretes with an aim to alter the properties of the cementitious mixes. There are many mineral admixtures which are used in concrete.

2.3.1 Influence of Metakaolin

Karoline and Arnaldo [57] in their study investigated the influence of MK fineness on the flowable and mechanical characterisation of SCC. Its is designated to flow freely under its self weight and pass through densely reinforced formwork while maintaining homogeneity, which necessitates a higher proportion of fine particles in the mix, along with chemical admixtures such as superplasticizers. To enhance the fines content, mineral admixtures like MK are often incorporated, typically replacing a portion of cement. In their study, the authors evaluated three different fineness levels of MK, substituting cement at replacement levels ranging from 5% to 35%.

The results indicated that increased fineness of MK led to higher superplasticizer demand due to the greater specific surface area requiring more water for dispersion. However, this demand could be mitigated by optimizing the paste volume. Mixes with paste contents of 0.45 and 0.50 demonstrated improved workability and required lower superplasticizer dosages to achieve target slump flow. Despite these advantages in fresh properties, these same mixes exhibited relatively lower strength performance, suggesting a trade-off between workability optimization and mechanical properties when using finer MK at these paste volumes.

Nikhalia et.al [58] partially replaced cement with MK at 0-30% to develop HSC and assessed fresh, mechanical, and durability characteristics. Workability significantly reduced with increasing MK content, attributed to its fine texture and water demand. Mechanical properties improved with MK, with optimum strength recorded at 15% replacement. Beyond ambient temperature, MK mixes displayed altered stress-strain behaviour at 200-500°C. Durability tests in HCl and H_2SO_4 showed enhanced resistance at 0.5% and 1% exposure, with HCl being less aggressive. Improvements were linked to MK's strong pozzolanic reaction and densification of the matrix.

Immanuel Dorai (2019) [59] investigated the enhancement of HSC properties using MK and fibres (hooked-end steel and PP fibres) using a hybridization technique. In their research work, they focused on enhancing the HSC performance by varying the proportions of the MK and fibers to achieve better strength and durability. In total, 15 mixes were formulated using different percentages of MK and fibres (hooked-end steel and PP fibres). Out of the mixes having MK percentage as 10%, 15% and 20%, the mix with 15% MK gives the highest strength. Other mixes prepared had steel fibres (0.25%, 0.5% and 1%), PP fibres (0.25%, 0.5% and 1%), and hybrid fibers (combination of steel and PP fibres). The resulting outcomes showcased that the incorporation of MK in concrete reduces workability owing to its fine particle size and higher use of water, with a replacement level of 15% by weight of cement providing the optimal

balancing between fresh and hardened qualities. At this dosage, HSC containing 15% MK and 1% hybrid fibers demonstrated enhanced mechanical properties when compared with ordinary concrete. Strength in compression improvised by 24%, splitting tensile strength by 12%, and strength in flexure by 15%, stressing the synergistic effect of MK's pozzolanic nature and fiber reinforcing on the load-carrying capacity of concrete. The RCPT test marks suggested substantially diminished chloride ion penetration, categorizing the concrete in the class of very least permeability in terms of durability. Furthermore, sorptivity and water absorption assessments validated a more compacted matrix with reduced interconnecting voids, leading to diminished capillary water absorption and enhanced durability. Their overall research study suggested that the combined use of 15% MK and hybrid fibers enhances the structural performance of HSC.

Younis Khaleel [60] studied HSC incorporating MK (5% and 10%) and PVA fibres (1-2%) with varying aspect ratios. MK refined the microstructure and improved particle packing, reducing porosity significantly, especially at 10% replacement. Compressive strength increased by about 16.5%. Tensile and flexural strengths were also enhanced with combined MK and fibre addition. PVA fibres induced deflection-hardening behaviour, with the mix containing 10% MK and 2% fibres showing the highest toughness and post-peak deformation (up to 6 mm). Findings demonstrated that MK-PVA systems can produce durable, ductile HSC suitable for advanced structural applications.

Nuruddin Muhammad Fadhil et.al.[61] in their experimental programme investigated the mechanical and ductile behavior of high-strength ductile concrete incorporating MK as a cement replacement and PVA fibers for enhanced toughness. studied high-strength ductile concrete incorporating MK (5% and 10%) and PVA fibres (1-2%) with varying aspect ratios. MK refined the microstructure and improved particle packing, reducing porosity significantly, especially at 10% replacement. Compressive strength increased by about 16.5%. Tensile and flexural strengths were also enhanced with combined MK and fibre addition. PVA fibres induced deflection-hardening behaviour, with the mix containing 10% MK and 2% fibres showing the highest toughness and post-peak deformation (up to 6

mm). Findings demonstrated that MK-PVA systems can produce durable, ductile HSC suitable for advanced structural applications.The study concludes that HSDC with 10% MK and 2% PVA fibers offers an optimal balance of strength, durability, and ductility, making it a promising solution for structural applications requiring high performance and sustainability.

Peiliang Shen et.al. [62] evaluated MK (0-15%) in HSC produced at a small w/b ratio of 0.23 and steam-cured at 80°C. Results showed the best performance at 10% MK, where strength increased due to MK's pozzolanic reactivity and its ability to reduce calcium hydroxide and limit ettringite formation under thermal curing. Porosity reduced from 14.4% to 11.3% as MK increased, and pore sizes decreased considerably. SEM analysis showed a dense matrix with no visible ITZ between aggregate and paste. MK's aluminium-rich composition modified the CSH structure, enhancing thermal and mechanical stability. The study identified MK as a valuable SCM for steam-cured high-performance concrete.

Jawad Ahmad et. al.[63] presented a assessment on the influence of MK on concrete's mechanical, durability, and microstructural properties. Their findings highlight that increasing MK content generally reduces fresh concrete workability, particularly beyond 15-20%, due to its fine particle size and high surface area. Strength parameters compressive, flexural, and tensile were consistently enhanced when MK was used within 10-20% replacement, with peak compressive strength gains of around 33% at 90 days for 20% MK. Durability improvements were also notable; MK significantly decreased permeability, chloride penetration, sorptivity, and water absorption owing to improved pore refinement and strong pozzolanic activity. The review concluded that 10-20% MK is the optimal range for improving both strength and durability while maintaining adequate workability.The study also revealed that benefits may plateau or reverse if the MK percentage becomes too high. Test results various strength's using different percentages of MK and at different days w.r.t experimental study are shiown in figures below.

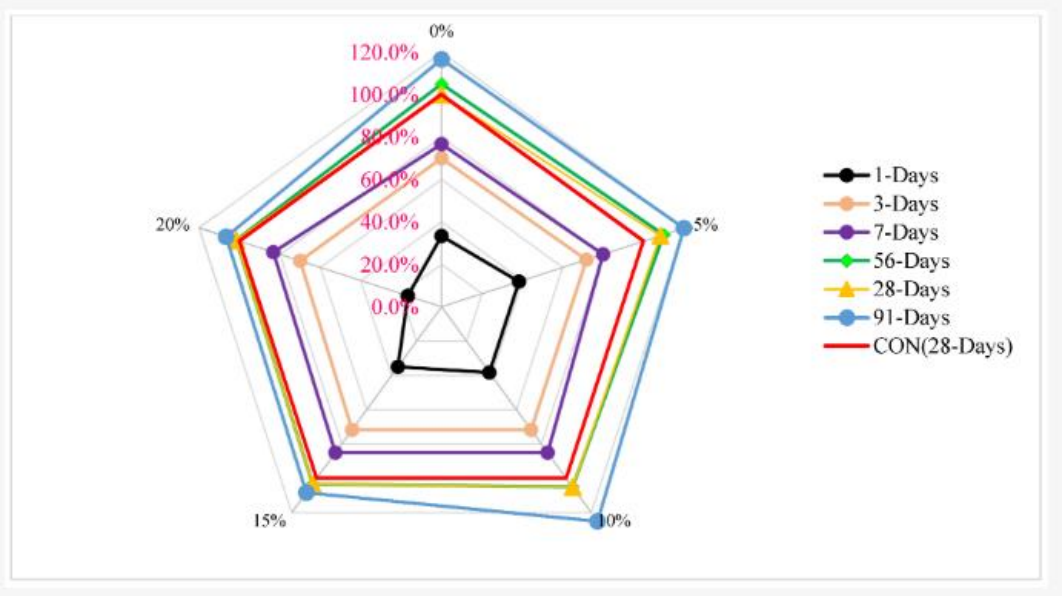

Figure 1 Variation of the compressive strength of concrete at different ages of concrete with different dosages of MK [63]

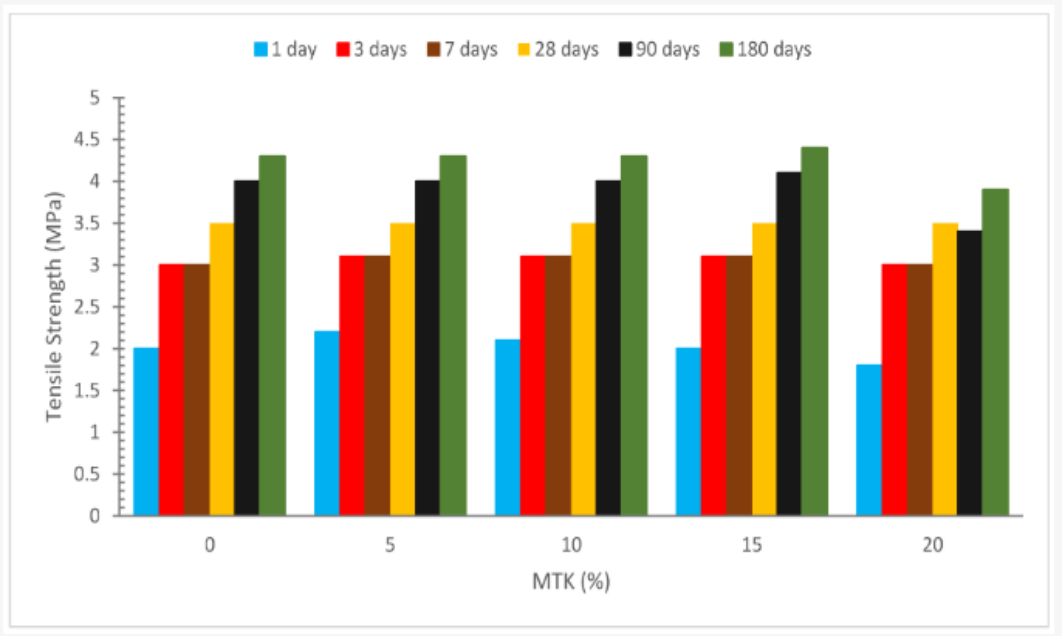

Figure 2: Tensile strength concrete at various MK percentages at different curing days [63]

Their review of the durability parameters included some key properties, including chloride ion penetration, water Absorption, water Sorptivity, and permeability. Their studies indicated that concrete with MK demonstrated better resistance when used in concrete. Their study of the diverse literature revealed that using

MK from 10-15% greatly boosted durability by reducing permeability and achieving denser microstructures. The use of MK for enhancing the strength and durability is attributed to the capabilities of MK to refine the pore structure and promote pozzolanic reactions which gave outcome by imparting denser microstructure, stronger matrices, and improved ion penetration resistance. The overall recommendation of their study confirmed that replacing cement with 10-20% MK in concrete provides optimal development in strength and enhancement in durability for resisting harsh environmental conditions.

Detailed literature review confirms that use of metakaolin significantly enhances the strength and durability properties of concrete because of its high pozzolanic reactivity and ultra-fine particle size. Most studies reported optimum performance at replacement levels between 10% and 15%, where improvements in compressive, tensile, and flexural strengths were achieved through matrix densification and pore refinement. Microstructural observations revealed that MK reduces calcium hydroxide content and improves the ITZ by forming additional C-S-H gel. Researchers also noted that MK-based mixes exhibit lower permeability and improved resistance against aggressive environments. However, excessive MK content often leads to reduced workability due to higher water demand and increased surface area. Existing research mainly concentrated on cement replacement and fibre-reinforced systems, while limited studies explored the interaction of MK with varying aggregate combinations. Hence, the present investigation extends this understanding by studying MK-based HSC prepared with granite and limestone aggregates together with silica sand and quarry sand.

2.3.2 Influence of Silica Fume

Mazloom et al. [64] investigated the impact of SF incorporation on the mechanical characterisation of HSC. The study showed that replacing a portion of cement with SF considerably improved compressive and tensile strength, primarily due to enhanced matrix densification and refinement of the ITZ. The authors highlighted that SF reduced porosity and contributed to a more cohesive microstructure, resulting in superior stiffness and reduced brittleness. Their work demonstrated

that the mechanical gains were strongly associated with the pozzolanic activity of SF and its ability to modify the micro-level packing characteristics

Srivastava et al. [30] examined concrete mixtures incorporating SF together with MK, focusing on how this combination alters strength development. Their results indicated that mixtures containing SF displayed notable improvements in early and prolonged compressive strength, attributed to accelerated pozzolonic reactions and better particle packing. The study also noted that SF supported the formation of a denser CSH gel network, particularly when used alongside MK. Overall, their work suggested that SF plays a central role in enhancing matrix refinement and contributes significantly to the synergistic performance of blended cementitious systems.

Park et al. [50] reviewed the contribution of SCM to UHPC, with SF being identified as a critical component. The authors emphasized that SF enhances the particle packing efficiency of UHPC and serves as a highly reactive pozzolan that strengthens the microstructure through secondary CSH formation. Their synthesis of existing studies showed that SF is essential for achieving the extremely low porosity and high strength typically associated with UHPC. The review concluded that SF remains irreplaceable for improving durability, strength, and the overall densification of UHPC matrices.

Sharif et al. explored pozzolanic concretes containing various mineral admixtures, with SF evaluated for its role in modifying mechanical performance. Their results demonstrated that SF contributed markedly to strength improvement, mainly through reduction of voids and enhancement of the ITZ. The study reported that SF produced more cohesive mixes and promoted superior long-term strength compared to other admixtures tested. The authors attributed these benefits to the fine particle size and strong pozzolanic reactivity of SF, reinforcing its effectiveness as a performance-enhancing material in blended concrete systems.

Piotr Smarzwski [65] examined the use of CSF as a partial substitute for cement in HPC, focusing on its effects on mechanical charactersics and microstructure. The

concrete mixtures prepared with a w/b ratio of 0.25, and five dissimilar mixes were developed by altering the CSF content at levels of 5%, 10%, 15%, 20%, and 25%. Several mechanical traits were evaluated, such as strength in compression, splitting tensile strength, modulus of elasticity, flexural strength, and fracture characteristics of HPC containing fluctuating percentages of CSF as cement replacement. The findings directed that replacing cement with up to 25% CSF had a constructive influence on the mechanical properties of HPC. The test results exhibited increase in compressive strength by up to 14%, flexural strength by up to 16%, and splitting tensile strength by as much as 26%, representing considerable improvements. However, at the 25% cement replacement level with CSF, the modulus of elasticity, flexural strength, and fracture properties displayed slight reductions of up to 2%. Test results of compressive strength and splittig tensile strength indicate the variation at different replacement percentages of CSF as shown in Figure 3 and 4

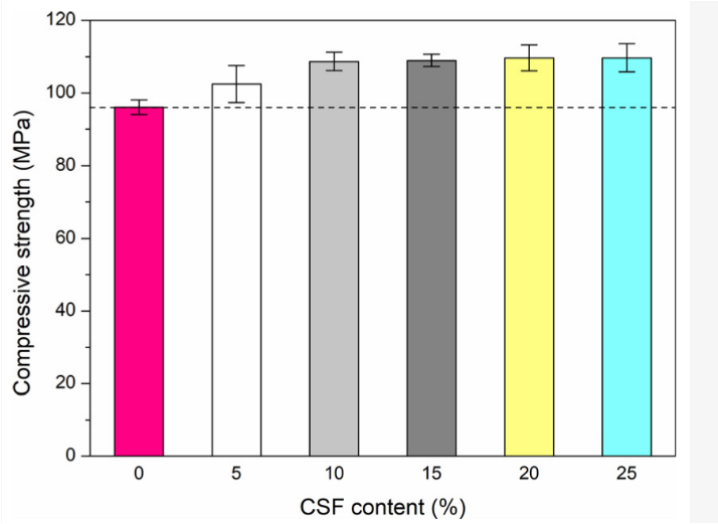

Figure 3: Compressive strength versus percentages of CSF [65]

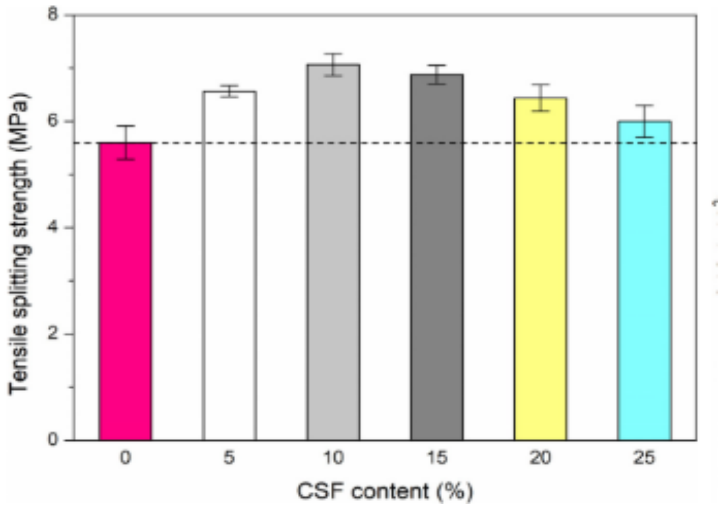

Figure 4: Splitting Tensile strength versus CSF [65]

HG Sahin et.al. [66] studied the effect of SF on rheology and structural build-up in 3D-printed concrete. Increasing SF content improved early structural build-up, enabling higher layer stability due to enhanced particle packing and increased inter-particle cohesion. Although beneficial for buildability, higher SF levels reduced workability and pumpability, which are critical for extrusion. The study emphasised the need for an optimal SF dosage balancing printability and shape retention. Their results contributed significantly to developing rheology-controlled mixes for 3D concrete printing.

Uma Reddy et al.[67] in their experimental work investigate the effects of SF, a synthetic pozzolan, when used as a replacement for cement in mix. Their research focused on the strength parameters of the SF concrete. Test results indicated that with 15% SF**,** it significantly enhances concrete strength parameters. Specifically, the bending strength upgraded by up to 15%, with recorded values increasing from 4.44 MPa at 7 days to 6.72 MPa at 28 days. Their test results indicated strength enhancement, which can be attributed to the pozzolanic Reaction, Micro-filler Effect, and improved microstructure of the concrete incorporating SF. Test results overall stated that optimal SF replacement (around 10-15%) provides the best balance of workability, strength, and durability. Excess SF may reduce workability and does not proportionally increase strength or durability, highlighting the amount of cementitious content plays a substantial part in the mix design after SF is added in the concrete for various concreting applications.

Amandeep Singh (2024) [68] reviewed SF's role as a cementitious replacement, concluding that 10-25% SF significantly increases compressive and flexural strengths while reducing permeability by 35-50%. These improvements arise from its high amorphous silica content reacting with CH to form additional CSH gel and its ultra-fine particles filling microvoids. The review stressed SF’s ability to produce highly durable and chemically resistant concrete suitable for aggressive environments, while also promoting sustainability by reducing cement use.

The reviewed literature highlights silica fume as one of the most effective supplementary cementitious materials for producing dense and durable HSC. Most researchers reported significant improvements in compressive, tensile, and flexural strengths due to the micro-filler effect and high pozzolanic activity of silica fume. Micro-level studies revealed that silica fume reduces pore connectivity, strengthens the ITZ, and enhances the formation of secondary C-S-H gel, resulting in lower permeability and better chloride resistance. Many studies also observed improved abrasion resistance and long-term durability with optimum silica fume incorporation. However, higher silica fume content reduced workability because of its very fine particle size and increased water demand. Although extensive work has been carried out on silica fume-based concrete,

comparatively fewer studies examined its behaviour with different natural coarse aggregates and alternative fine aggregates in HSC. Therefore, the present study attempts to evaluate the combined effect of silica fume with granite, limestone, silica sand, and quarry sand under similar mix conditions.

2.3.3 Use of blended SCM

Guneyisi et al.[69] conducted an extensive experimental investigation on SCC incorporating various mineral admixtures, both individually and in combination. Their study focused on FA, GGBFS, SF, and MK, evaluating their influence on mechanical performance and durability-related properties. A total of 65 different mix designs were developed to assess the impact of these SCM under varying replacement levels. To ensure adequate workability and compliance with SCC criteria, all mixes included superplasticisers to achieve the desired flow characteristics without segregation.

In the study, FA and GGBFS were employed as part replacements for cement at stages of 20%, 40%, and 60%, while SF and MK were incorporated at 5%, 10%, and 15%. Compressive strength outcomes exposed that upgrading the proportion of FA leads to a reduction in early- and mid-term strength, likely due to its slower pozzolanic reaction rate. In contrast, GGBFS showed a more neutral effect on strength development, maintaining acceptable performance even at higher substitution rates. On the other hand, both SF and MK significantly enhanced compressive strength across curing ages, attributed to their high reactivity and ability to refine the pore structure through secondary hydration reactions.

Among the multi-component blends, the combination of Portland cement with SF and MK demonstrated superior strength performance, outperforming binary and other ternary systems. This suggests a synergistic effect between these highly reactive pozzolans in densifying the cementitious matrix. With regard to volume stability, mixtures containing FA, GGBFS, and MK exhibited reduced drying shrinkage, indicating better dimensional stability over time. Conversely, the inclusion of SF was associated with increased drying shrinkage, likely due to

higher self-desiccation and finer microstructure leading to greater capillary stress development.

This comprehensive study highlights the importance of carefully selecting and combining mineral admixtures in SCC to balance fresh properties, strength development, and long-term durability. While certain materials like FA may compromise strength, they can improve shrinkage behavior, whereas highly reactive additives like SF and MK boost strength but require careful handling to mitigate potential cracking risks.

Tuan et al. [70] assessed RHA as a sustainable alternative to SF in UHPC. Fifteen mixes were prepared using OPC, fine silica sand, polycarboxylate superplasticizer, SF, and laboratory-processed RHA. Due to its high amorphous silica and fine surface texture, RHA exhibited significant pozzolanic activity, comparable to SF. Compressive strength results showed that RHA can partially replace SF without compromising UHPC performance, offering a cost-efficient and locally available solution for high-performance materials. The study demonstrated the viability of agricultural left-over as a alternative for premium SCMs in UHPC.

Prem et al. [71] in their experimental investigation studied the mechanical behaviour of UHPC designed to achieve high compressive strengths. Their study focused to prepare a mix having exceptional strength and durability, utilizing high-quality materials and steel fiber. Materials used included OPC of 53-grade, to ensuring high early strength development. SCM included SF and quartz, both contributing to micro-filling and pozzolanic reactions that densified the cement paste. Two different grades of sand were used, i.e Grade I having a particle size range of 0.6 to 2.36 m.m and Grade III ranging from 0.075 to 0.15 mm. Water-cement ratio of 0.22 and polycarboxylate-based superplasticizer ensured the required workability. designed UHPC using OPC, SF, quartz, fine sands, superplasticizer, and steel fibres of different lengths (S1 and S2). Five mixes were prepared by varying fibre volume fractions from 0% to 2.5%. designed UHPC using OPC, SF, quartz, fine sands, superplasticizer, and steel fibres of different lengths (S1 and S2). Five mixes were prepared by varying fibre volume fractions

from 0% to 2.5%. The R1 mix with 2.5% of longer S1 fibres recorded the highest compressive and flexural strengths. Fibre reinforcement significantly improved crack bridging and post-cracking behaviour, whereas the mix without fibres (R5) showed the lowest strength. The study confirmed that combining SF with fine powders and steel fibres leads to a dense microstructure and exceptional mechanical performance in UHPC.

Table 1: Details of the steel fibre type and percentage used in different mixess

Mix designation	Steel fibres Type	Steel fibres (%)
R1	S1	2.5
R2	S1	2
R3	S2	2.5
R4	S2	2
R5	NA	NA

Compressive and bending strength test results on the samples demonstrated that the mix designation R1, having 2.5% steel fibres, had the highest strength, and mix designation R5, with no fibres in it, demonstrated the least strength, as the fibres acted as the crack arresters in concrete and can take more load as compared to mix with no fibres.

Tarunbir et al. [72] in their research study investigated the effectiveness of using MK and FA as SCM in NFC to recompense for the inherent strength deficiencies due to the absence of fine aggregate. The study focused on evaluating mechanical charaters inclsuing compressive, split tensile, and bending strength as well as durability parameters such as water permeability, porosity, density, abrasion resistance, and water absorption. Researchers in their experimental study prepared various NFC mixes by varying the amount of the FA and MK as a percentage of cement in the mix design ratios. Various mixes used in the experimental study for further analysis of the technical attributes are mentioned in Table 2

Table 2: Design proportioning for the no fine concrete s

Mix	Cement (kg/m^3)	Aggregates (kg/m^3)		Fly ash (kg/m^3)	Metakaolin (kg/m^3)	Water-cementitious ratio (w/cm)	Cement-aggregate ratio (c/a)
		10 mm	20 mm				
NFC-0	403.2			0	0		
NFC-5FA	383			20.2	—		
NFC-10FA	362.8			40.2	—		
NFC-15FA	342.6			60.5	—		
NFC-20FA	322.6	740.88	1375.92	80.6	—	0.38	1:4.5
NFC-5MK	383.0			—	20.2		
NFC-10MK	362.8			—	40.2		
NFC-15MK	342.6			—	60.5		
NFC-20MK	322.6			—	80.6		

In the various mix proportions for the study, MK denotes MK, and 5MK denotes 5% MK (by weight of cement), and FA denotes FA, and 5FA denotes 5% FA (by weight of cement). In all the mixes, to understand the effect of other parameters, water-cementitious ratio of 0.38 was maintained in all NFC mixes.

Their findings exposed that fractional replacement of cement with MK improved the mechanical performance of NFC.

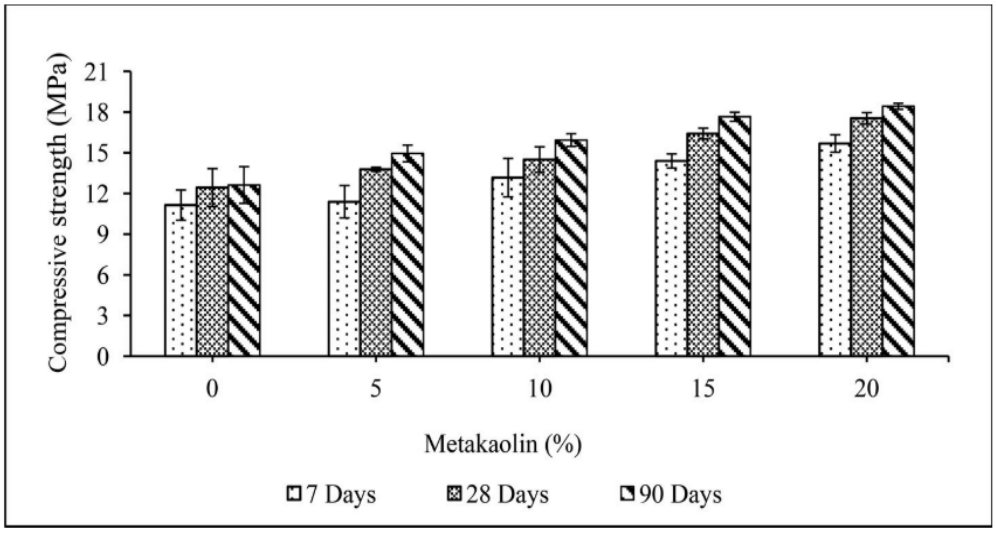

Figure 5: Compressive strength in NFC mixes with MK [72]

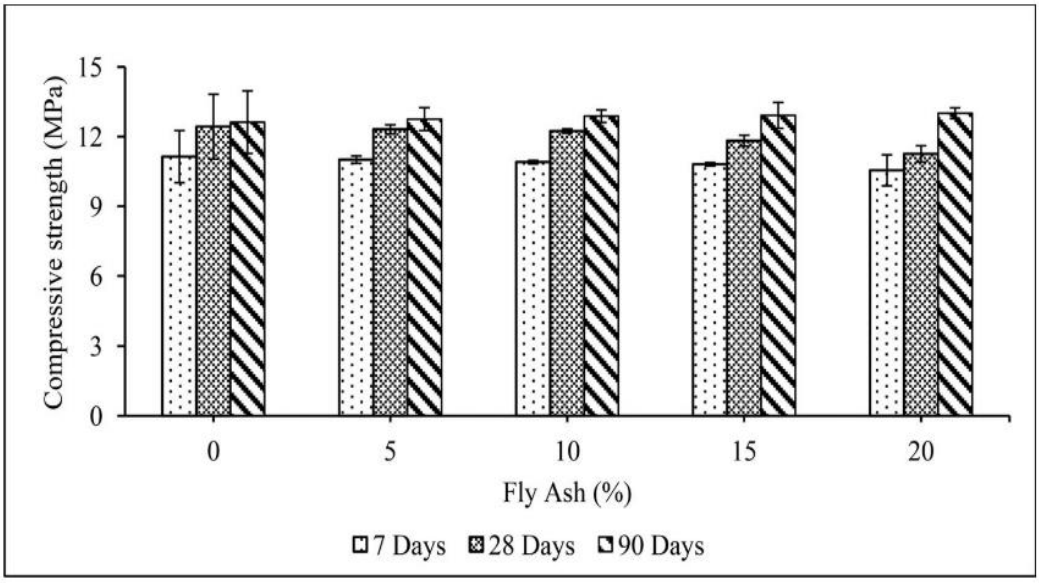

Figure 6: Compressive strength of NFC with FA [72]

Investigated FA and MK as SCMs in NFC to compensate for the lack of fine aggregates. Multiple mixes were made with constant w/b of 0.38. MK significantly enhanced strength, with 20% replacement improving compressive, tensile, and flexural strengths by 46%, 67.3%, and 25% at 90 days. SEM and XRD analyses confirmed dense microstructure and increased CSH formation. FA showed gradual strength improvement due to delayed pozzolanic action. Durability tests showed acceptable densities and improved abrasion resistance for

both MK and FA mixes. MK, in particular, reduced permeability and porosity, making it suitable for low- to medium-traffic pavement applications. Their study summarized that usage of MK and FA as SCM for improving strength and durability in NFC with no compromise to permeability, which makes them a suitable option for sustainable roadway applications for areas having low to medium traffic conditions.

Wang et.al. [46]evaluated the mechanical performance of concrete incorporating LD slag at 15%, 30%, and 45% cement replacement under two w/c ratios (0.50 and 0.35), targeting compressive strengths of 47 MPa and 73 MPa. Early-age compressive strength reduced on account of slower hydration and limited early slag reactivity. However, slag mixes showed faster long-term strength development, becoming comparable to control concrete at 90 days and exceeding it at 360 days, particularly at higher replacement levels. Mixes with lower w/c ratio exhibited smaller variations in strength retention. Overall, LD slag demonstrated favourable long-term performance and can be considered a viable substitute for cement in strength-focused applications.

Mohammad Zuaiter et al. [73] evaluated geopolymer concrete using GGBS and SF as combined binders. Incorporating SF up to 50% (binder basis) increased 28-day compressive strength by 50% at a solution ratio of 1.5. However, exceeding this level drastically reduced performance, with tensile strength decreasing by 79% and compressive strength by 56%, largely due to poor dispersion and lower workability. Optimal SF refined pore structure, enhanced packing density, and improved mechanical performance through improved geopolymerisation. The study confirmed that controlled amounts of SF significantly enhance geopolymer concrete but excessive replacement is detrimental.

The literature on blended supplementary cementitious materials suggests that combining reactive pozzolans can substantially improve the mechanical and durability performance of concrete. Studies involving silica fume, metakaolin, fly ash, slag, and rice husk ash reported improved compressive strength, reduced permeability, and enhanced long-term durability due to synergistic hydration

reactions and refined pore structure. Microstructural investigations confirmed that blended systems produce denser matrices with reduced voids and improved ITZ characteristics. However, researchers also observed that excessive incorporation of fine SCMs may increase shrinkage and reduce workability because of water demand. Most of the previous studies were focused on the effect of binders on cementitious mixes, and fewer studies focused on binder optimisation. Moreover, in the past studies less work has been reported on the use of blended Supplementary cementitious materials, along with the combined use of different coarse and fine aggregates in high-strength mixes. Hence, the present work aims to evaluate such

2.4 Effect of Coarse Aggregates

Yuli Wang et.al. [74] examined the influence of coarse aggregate size on concrete mechanical performance, focusing on compressive strength and elastic modulus, alongside microstructural changes within the ITZ. Their results showcased that keeping lower water-cement ratio (w/c equal to 0.3), increasing aggregate size led to a thicker and weaker ITZ, resulting in reduced strength and stiffness due to higher porosity and microcracking caused by inadequate hydration. In contrast, at a higher w/c ratio (0.4), an optimal aggregate size improved paste-aggregate bonding, reduced ITZ thickness, and enhanced overall mechanical performance.

J.K. Periasamy et.al. [75]investigated the partial replacement of natural coarse aggregates with RCA at substituting percentages between 0% to 100%. The test consequences showed that a 30% RCA replacement caused only a marginal reduction in strength capacity in compression (7-10%) contrsting to conventional concrete, demonstrating its practical feasibility. Increasing RCA content reduced workability and density due to higher porosity and water absorption. The study concluded that concrete incorporating up to 30% RCA can achieve mechanical and physical properties comparable to natural aggregate concrete, making it suitable for diverse usage.

K.P. Vishalakshi et.al. [36] evaluated the effect of different coarse aggregate types on normal and HSC, using Grey Granite, Anorthosite, Charnockite, Limestone,

and Gneiss across M30, M50, and M80 grades. The results showed that aggregate type significantly influenced strength, particularly in HSC, where aggregate mineralogy governed mechanical behavior. Grey Granite produced the highest strength in compresion, then Anorthosite and further Charnockite. Fracture energy and elastic modulus exhibited similar trends. The study emphasized that petrological and mineralogical characteristics of aggregates play a critical role in determining HSC performance.

Chenzhi Li [76] explored the performance of RCA as partial replacements for natural coarse aggregates at 30%, 60%, and 90%, using a w/b ratio of 0.35. The RA were prewetted to address their higher absorption capacity. Results revealed a progressive reduction in strength in compression with incremental in RCA content, credited to the presence of old and new ITZs and porous adhered mortar. Strength losses of 8.6%, 19.9%, and 33% were reported at respective replacement levels. The study demonstrated that incorporating limestone powder as a cement replacement effectively compensated for strength reductions.

Chunheng Zhou et.al. (2017) [77] inspected the mechanical behavior of concrete comprising different natural and RCA, including crushed rock, pebbles, and RA derived from both sources. Although RA exhibited more absorption of water and reduced density, RCA showed compressive and flexural strengths comparable to or exceeding those of conventional concrete. Improved bonding was attributed to enhanced moisture availability from RCA. However, the elastic modulus decreased with higher RCA content, with maximum reductions of 18% and 22% observed, primarily due to reduced stiffness and density of recycled aggregates.

Mohamed Elwi Mitwally et.al. [78] examined steel slag as a coarse aggregate replacement at levels up to 100%, keeping a fixed w/c ratio of 0.44. The inclusion of steel slag reduced workability due to its angular shape but significantly enhanced compressive strength owing to its pozzolanic nature and increased C-S-H formation. Split tensile strength improved up to 30% replacement, beyond which ITZ weakening led to crack propagation. In their study they have used steel slag as coarse aggregates replacement for 10%, 20%, 30%, 50%, 75% and 100%,

with mignations used as M10, M30, M50, M75 and M100, where M represent mix and 10 (number) represenet replacement percenatage.Test results of their slump test are shown in the figure below.

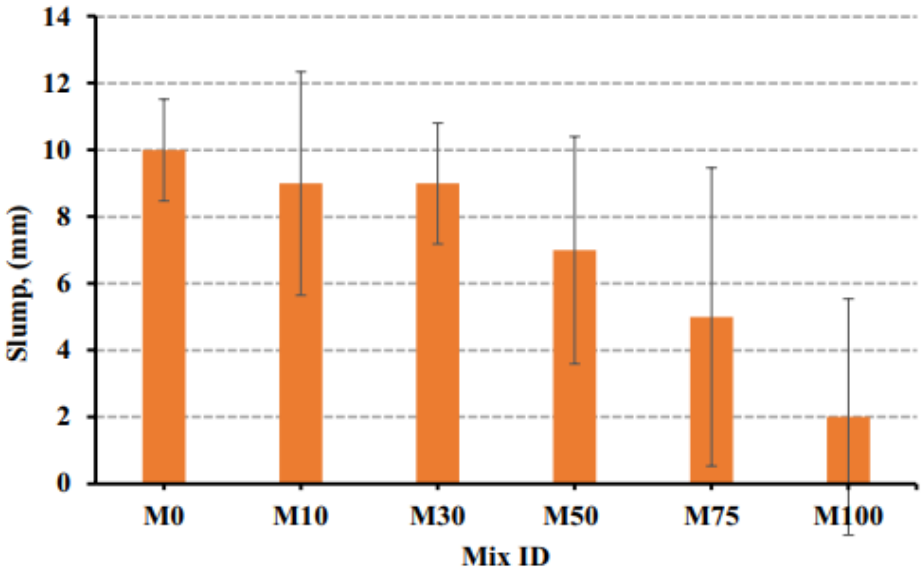

Figure 7: Variation of the slump in different slag mixes [78]

Also, the tensile strength test reults of concrete having steel slag during their work are shown in figure below.

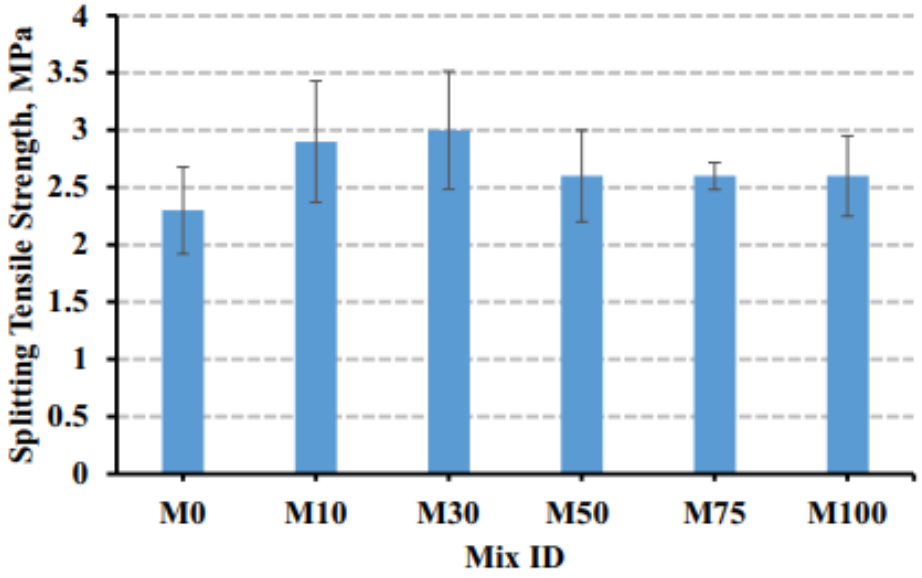

Figure 8: Splitting tensile strength versus different mixes [78]

The study concluded that a 30% steel slag replacement offers optimal mechanical performance, producing concrete with improved strength and durability characteristics.

Moustafa Abdulrahim Mohamedsalih et al. [79] assessed the usability of using plastic waste as fractional coarse aggregate replacement at levels up to 12.5%. Results indicated that replacements beyond 2.5% caused significant drops in bending, compressive and splitting tensile capacities due to poor bonding and the hydrophobic nature of plastics. While compressive strength decreased by less than 1% at 2.5% replacement, a sharp decline of 24% occurred at 5%. The study concluded that limited plastic waste incorporation of less than 2.5% can be safely adopted without compromising structural strength.

Ibrahim Y. Hakeem et.al. [80]developed sustainable HSC incorporating 100% RCA from construction debris, combined with industrial by-products replacing OPC at 50% and 75%. They tested 25 mixes control, binary, ternary, and quaternary blends with varying nano-silica (0-5%). Assessments covered fresh slump, mechanical strengths (compressive, splitting tensile, flexural, modulus), and transport properties (permeability, sorptivity, chloride penetration). The

quaternary blend at 75% with 3% nano-silica showed excellent long-term performance, while the 50% quaternary with 3% nano-silica delivered peak values: 80.7 MPa compressive, 6.46 MPa tensile, 10.09 MPa flexural at 28 days, low permeability, and reduced chloride ingress.

P.P. Li et.al. [81] investigated UHPC using coarse basalt aggregates, with fixed steel fibers (2% volume), microsilica (5%), lime powder (20%), and w/p=0.2. Varying basalt fractions altered mix designs. Results showed coarse basalt slightly lowered strengths, with larger particles reducing compressive (144 to 132 MPa) and splitting tensile (9.8 to 8.2 MPa) at 28 days due to packing changes.

Muhammad Aslam et.al. [82] produced lightweight HSC by partially replacing oil-palm-boiler clinker with oil palm shell (0-60% by volume). OPS addition decreased density and mechanical properties owing to its smoother, lighter nature versus OPBC. Yet, over 20% OPS yielded structural lightweight HSC, with 20-40% replacement optimal for balancing strength and absorption

Megha Kalraet et al. [83] reviewed coarse aggregate influences on HSC, noting direct impacts on compressive strength from aggregate type and stiffness unlike normal concrete. Elastic modulus is concerned to mortar-aggregate bonding and aggregate strength; tensile strength varied little but responded to surface texture. Strong interfaces proved vital for durability and overall mechanics, underscoring careful aggregate selection.

P.P. Li et.al. [81] examined basalt coarse aggregates with limestone powder and SF in UHPC, optimizing powder ratios (5% microsilica, 20% limestone). Larger basalt sizes adjusted optimal content, slightly diminishing strengths as particles grew (compressive 144-132 MPa, tensile 9.8-8.2 MPa at 28 days). Limestone boosted shrinkage 1.6 times by 91 days from capillary pores, mitigated 15% by microsilica.

Past literature clearly indicate that coarse aggregate type considerably affects the strength and durability behaviour of HSC. Researchers observed that stronger and denser aggregates generally provide higher compressive strength, elastic modulus,

and abrasion resistance because of improved stiffness and stronger aggregate–paste interaction. Studies further showed that aggregate mineralogy and surface texture influence the quality and bond of the ITZ, which becomes highly important in HSC. On the other hand, porous or recycled aggregates often resulted in reduced strength and durability because of weaker bonding. Although several investigations examined recycled and industrial aggregates, limited comparative studies are available on conventional natural aggregates such as granite and limestone, under identical HSC conditions. Furthermore, the effect of combined coarse aggregate and alternative fine aggregates has not been sufficiently explored. Hence, the present study evaluates different combinations of granite and limestone-based High strength concretes.

2.5 Effect of Fine Aggregates

Aymen J. Alsaad et.al. (2025) [84] examined the usability of employing PET as a fine aggregate substitute in mixes of concrete, with emphasis on surface modification. Direct replacement using untreated PET resulted in reduced capacity in compression due to feeble interfacial bonding with the cement matrix. To overcome this limitation, PET particles were coated with cement or SF and subjected to microwave treatment, which significantly enhanced adhesion and improved mechanical and durability performance. At lower replacement levels, treated PET demonstrated strength comparable to natural sand, while higher substitutions caused strength reduction due to PET's lower stiffness.

Md Nuruzzaman et.al. [85] examined the combined replacement of natural sand with quarry dust and ferronickel slag in mixes at varying proportions. Among the mixtures investigated, the blend containing 25% of quarry dust and 75% of ferronickel slag exhibited optimal performance, achieving compression and split tensile capacities of 62 MPa and 4.29 MPa. These values represented notable improvements over the control mix, along with reduced drying shrinkage. Enhanced mechanical interlocking arising from angular particle geometry and denser microstructure contributed to the observed strength gains.

Yao-Ming Hong et.al. [86] explored oyster shell powder as a waste-derived fine aggregate replacement in concrete at replacement levels up to 40%. The study reported reduced workability and density with increasing oyster shell content due to its high porosity and absorption capability.Strength in compression declined at all curing ages, with reductions ranging from 2.6% to over 26% as replacement increased. The strength loss was attributed to the lower specific gravity and porous nature of oyster shell powder, which adversely affected hydration and matrix densification.Test results of the variation of slump diameter with the level of replacemement of the OCP

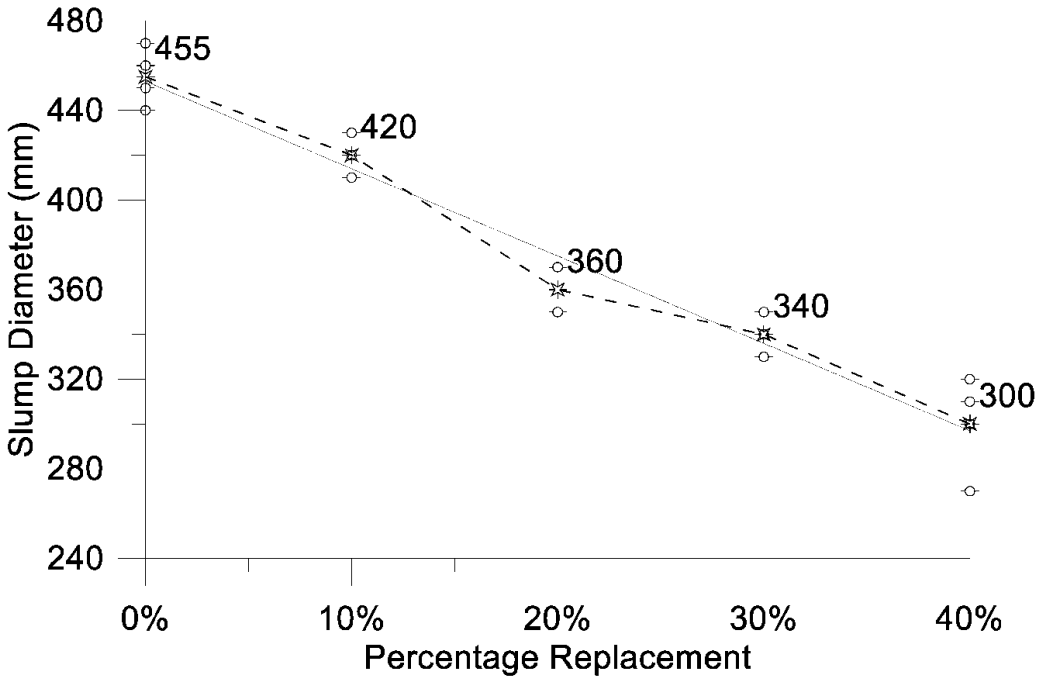

Figure 9 Variation of the slump diameter with the replacement level of OSP [86]

Ali Umara Shetima et.al. [87]evaluated iron ore tailings as an alternative fine aggregate in mixes at replacement levels from 25% to 100%. While workability decreased with higher tailings content, improvements were observed in compression, splitting tensile capabilities, and modulus of elasticity compared to conventional concrete. These enhancements were attributed to the dense packing of particles and improved interfacial bonding attributed by iron ore tailings. The

study concluded that iron ore tailings can effectively replace natural sand while offering economic and environmental advantages.

Zainab Z. Ismail et al. [88] investigated the utilisation of waste glass as a fractional fine aggregate replacement in concrete up to 20%. Increasing glass content led to reduced workability due to angular particle shape. Mechanical testing indicated that at twenty eight days, concrete containing 20% glass as waste exhibited increases of 4.23% in compressive strength and 10.99% in flexural strength. Mortar bar tests further showed significant reduction in expansion, demonstrating that finely ground glass can enhance long-term performance and durability.

Kirti Vardhan et al. [89] assessed marble waste as a alternate for natural river sand in concrete, with replacement levels up to 60%. Results indicated that marble waste improved compressive strength by up to 20% and reduced drying shrinkage by nearly 30%, with optimum performance observed at 40% replacement. Microstructural analysis revealed a denser cement matrix resulting from improved particle packing and filler effects. Beyond the optimum level, performance gains diminished, highlighting the importance of controlled replacement for effective utilization.

Geiser Cabanillas Hernandez [90] examined the consequence of using wood sawdust as option for partial alternative of fine aggregate at low dosages. While workability decreased and air content increased with higher sawdust content, mechanical properties improved up to an optimum replacement of 1%. At this level, compressive, tensile, and flexural strengths showed notable enhancement. Beyond 1%, strength reductions were observed due to excessive air entrainment. The study recommended limiting sawdust content to non-structural applications while emphasizing its sustainability benefits.

Navdeep Singh et al.[91] reviewed the application of CBA as a fine aggregate substitute in conventional along with SCC. The review highlighted that coal bottom ash exhibits comparable performance to natural sand owing to its rough

and porous texture, which promotes mechanical interlocking. Its ability to absorb and gradually release water during hydration was identified as beneficial for strength development. Overall, the study supported CBA as a viable fine aggregate alternative with favorable green and hardened concrete properties.

N. Jayasimha et al. [92] studied iron ore tailings as fine aggregate replacement in HSC at levels up to 50%. The results showed improved workability and enhanced compressive and tensile strengths up to a 40% replacement level. Although durability indicators such as water absorption increased beyond this limit, the adverse effects remained marginal. The findings confirmed that iron ore tailings can effectively replace natural sand in HSC while contributing to sustainable material management and reduced environmental impact.

Chinnadhurai et al. [93]investigated copper slag utilised as a viable option for fine aggregate replacement in concrete across a wide range of substitution levels. Mechanical testing revealed strength enhancement up to 40% replacement, with compressive strength gains of 10-15% due to improved particle packing and higher density. Tensile and flexural strengths followed similar trends. At higher replacement levels, strength declined due to poor paste-slag bonding. Durability tests confirmed reduced permeability at moderate replacements, supporting copper slag as an effective partial substitute.

Gurwinder Singh et al. [94] evaluated rubberized concrete incorporating crumb rubber as fine aggregate replacement, supplemented with SF and waste glass powder. Crumb rubber alone reduced strength and workability; however, the inclusion of supplementary materials significantly improved performance. The addition of 10% SF with 5% crumb rubber resulted in an 11% upgrading in compression capability compared to rubberized concrete without SCMs. The study concluded that SF was more effective than waste glass powder in mitigating strength loss.test results of the slump test in various specimens is presented in the below figure.

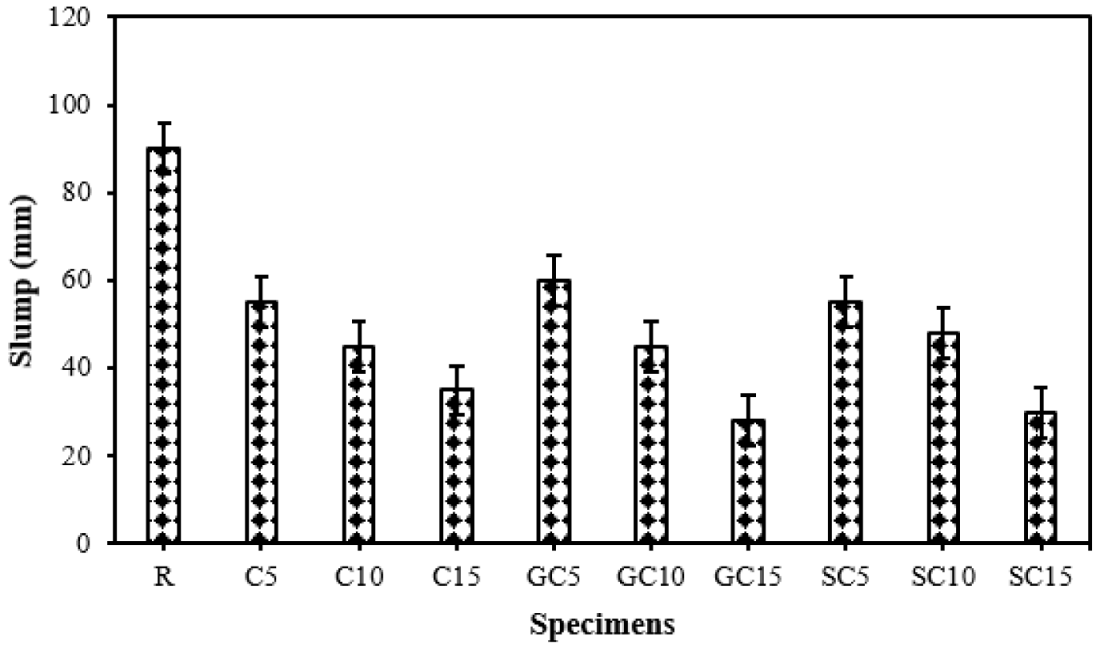

Figure 10 : Fluctuation of the workability of the various concrete mixes prepared [94]

Lilesh Gautam et al. [95] examined ceramic waste powder as a fine aggregate replacement in SCC. Replacement levels up to 50% were studied, with 20% substitution yielding the most favorable results. Improvements were observed in compressive strength and ultrasonic pulse velocity, while higher replacement levels led to strength reduction due to smooth ceramic surfaces and increased porosity. The study emphasized that controlled incorporation of ceramic waste can enhance SCC performance while offering sustainable waste management benefits.

Tarek Uddin Mohammed et al.[96] investigated various alternative fine aggregates, including recycled brick fines, stone fines, and furnace slag, as substitutes for natural sand. The study reported strength improvements at optimal replacement levels, particularly 30% for brick and stone fines and 20% for slag aggregates. Notably, recycled brick fine aggregates demonstrated increasing strength even at full replacement. These findings highpoint the probability of industrial end products to enhance mechanical performance while reducing reliance on natural sand resources.

Sanjay Mundra et al. [97] conducted an experimental study using sandstone cutting waste as a partial replacement for natural river sand in concrete. Mixes

were designed with water-cement ratios of 0.35, 0.40, and 0.45, following IS 10262:2009 guidelines. The effects on fresh concrete properties and hardened state properties was examined. Microstructural analysis was performed using SEM and optical microscopy. A control mix (0% replacement) was compared with mixes at 10%, 20%, 30%, 40%, 50%, and 100% substitution. Results indicated that sandstone cutting waste can effectively replace river sand up to 10% at w/c 0.35 and up to 30% at w/c 0.40 and 0.45 for structural concrete.

Areej Gamieldien et al.[98] studied the replacement of dune sand with fine RCA in concrete mixtures. Increasing replacement levels reduced workability; however, hardened properties, including compressive capacity, permeation capacity, and porosity remained comparable to control mixes. The results indicated that fine recycled concrete aggregates can serve as a partial substitute for natural sand without significantly compromising performance, supporting their application in sustainable concrete production using C&D waste.

Chin Mei Yun et al. [99] evaluated glass waste as a alternatuve replacement of fine aggregate in concrete at levels up to 25%. The results outcomed, improvised compressive strength at all levels of replacement compared to the control mix, with optimal performance observed at 20%. The addition of superplasticizer further enhanced strength development. Material characterization confirmed improved particle packing and matrix densification. The study concluded that glass waste, combined with chemical admixtures, can be effectively utilized as a sustainable sand replacement.

Dinesh Ganvir et al.[100] investigated jarosite as a partial fine aggregate alternative in pavement quality concrete. Replacement levels up to 30% were examined, with 20% substitution yielding the maximum compressive and bending capacities. Drying shrinkage decreased with increasing jarosite content, although abrasion resistance declined at higher replacement levels. The study demonstrated that jarosite can be effectively used at controlled proportions to enhance strength while maintaining acceptable durability characteristics in pavement concrete.

Soundararajan et al. (2023) [101] investigated high-performance concrete using ferro slag as partial replacement (0-40%) for natural coarse aggregates, alongside fixed FA (15%) and SF (10%) in the binder. The MF30 mix (30% ferro slag) achieved the highest compressive strength of 71.20 MPa, about 30% above the control, due to strong slag-matrix bonding and enhanced pozzolanic activity. Under acid, sulphate, chloride, and wet-dry exposures, MF30 retained superior residual strength and minimal mass loss, confirming excellent durability and sustainability potential for aggressive environments.

D Sau et al. [102] replaced natural fine and coarse aggregates alongside polyethene (PE) and PET plastic waste (0-40% by their volume). Strength in compression decreased with higher replacement, yet PE mixes remained viable up to 30%. Plastic aggregates weakened interfacial bonding due to smooth surfaces, but improved chloride resistance, reduced sorptivity, and enhanced impact toughness PE40 absorbed 83% more energy before cracking while showing better sulphate resistance.

Singh et al.[103] assessed granite cutting waste (GCW) as fine aggregate replacement (10-70%). Workability dropped due to angular particles, but compressive strength peaked at 40% GCW and remained near control even at 70%. Flexural strength stayed comparable, while water penetration and abrasion resistance improved markedly at 40-55% replacement, supporting GCW use for sustainable pavements and surface elements.

Patil et al.[85] fully replaced natural sand with quarry dust and FNS blends. The QD25-FNS75 combination yielded 62 MPa compressive strength (16% above control) and 4.29 MPa splitting tensile strength (20% higher), owing to angular textures improving interlocking and packing. This mix also showed lower drying shrinkage and denser microstructure, proving full sand substitution with industrial wastes viable for high-performance green concrete.

Aquino Carlos et al.[104] examined fine limestone replacement for natural sand (30-100%) at w/c ratios ranged between 0.45 to 0.65. Higher limestone content

increased compressive, flexural, and elastic modulus values through improved packing and filler effects that densified the ITZ. Drying shrinkage reduced substantially with greater limestone proportions, demonstrating fine limestone as an effective, environmentally beneficial full substitute for sand with enhanced mechanical and dimensional stability.

The literature reveals that fine aggregate characteristics such as shape, texture, etc., significantly influence the fresh and hardened properties of concrete. Many researchers reported that angular and finely graded materials improve particle packing and mechanical interlocking, resulting in higher compressive and tensile strengths at optimum replacement levels. Microstructural analysis in several studies showed reduced porosity and improved matrix densification due to filler effects and better packing characteristics. However, excessive replacement of natural sand often caused reduced workability and increased water demand because of higher fines content and angular particle shape. Studies of the past reveal that durability improvements, particularly in permeability and abrasion resistance, were also reported at moderate replacement levels. Although various waste-derived fine aggregates have been studied, limited research literature is available on the combined use of silica sand and quarry sand with different natural coarse aggregates in HSC. Therefore, the present work attempts to investigate these combinations systematically to determine replacement levels for achieving improved mechanical and durability performance.

2.6 Mechanical Properties

Various mechanical characteristics of concrete were studied using different materials in concrete, and past studies in the form of literature are discussed.

2.6.1 Effect on Compressive Strength

Murthy et al.[105] compared high-strength and UHSC mixes, showing that compressive strength increased markedly with reduced water-binder ratio and optimised particle packing. Ultrahigh-strength mixes achieved substantially higher 28-day compressive values when fine grading and low w/b were strictly controlled. The study attributed the gains to densified matrix and reduced ITZ

porosity, and stressed that ultrahigh compressive performance demands tighter control of materials and processing than conventional HSC.

Scheinherrova et al.[106]studied two novel HSCs (w/c = 0.24, SF and fine reactive powders) exposed to temperatures from ambient to 800 °C. Compressive strength fell progressively with temperature: moderate loss at 200 to 400 °C but severe reductions beyond 600 °C due to dehydration of CSH and thermal microcracking. While the mixes retained useful residual strength up to intermediate temperatures, the study documents large strength degradation at fire-range temperatures, underscoring the need to consider thermal performance when specifying HSC for fire-exposed structures.

Nirosha D et al. in their study evaluated silica-fume replacements (various dosages) in HSC and reported that a 15% SF substitution produced the largest compressive strength increase at 28 days. Moderate SF doses refined pore structure and boosted pozzolanic activity, whereas excessive SF reduced workability and produced marginal or reduced compressive gains. The paper concludes an optimum SF content (around 10-15%) yields the best compressive strength improvement in HSC, provided mix water and admixture are adjusted to maintain paste workability.

Zende et al. [107] produced high-strength SCC with target compressive strengths exceeding 70, 80 and 90 MPa for three mix families. By lowering w/b ratio and optimising powder content and superplasticiser, the mixes achieved compressive strengths in those ranges at 28 days, with higher binder packing producing steeper strength gains and stiffer stress-strain responses. The study underlined that rheological control (flowability without segregation) plus dense paste quality is crucial for attaining 70 to 90 MPa compressive capacity in self-compacting HSC.

2.6.2 Effect on Splitting Tensile Strength

Ibrahim et al.[108] investigated concrete incorporating lightweight bubble aggregates and evaluated its mechanical performance, including split tensile strength. The inclusion of bubble aggregates reduced density and compressive

strength; however, the split tensile strength showed comparatively lower reduction due to improved crack-bridging and stress redistribution around the lightweight pores. The authors observed that although tensile strength decreased with increasing lightweight aggregate content, the strength-to-weight efficiency improved. The study highlights that aggregate morphology and internal void structure significantly influence tensile resistance mechanisms in lightweight concrete systems

De Souza Castoldi et al. [109]compared PP and sisal fibre-reinforced concretes to assess their influence on mechanical properties, including split tensile strength. Both fibre types significantly enhanced tensile resistance relative to plain concrete, with sisal fibres providing higher strength gains due to improved fibre-matrix bonding. PP fibres contributed to better crack distribution but lower peak tensile strength. The findings confirm that fibre type, stiffness, and interfacial adhesion govern tensile performance, and that fibre-reinforced concretes are particularly effective in enhancing resistance to indirect tensile stresses.

Alabduljabbar et al. (2019) studied the combined influence of steel fibres and cement-replacement materials in SCC. The inclusion of steel fibres substantially increased split tensile strength due to enhanced crack arresting and load transfer across microcracks. Even with partial cement replacement, tensile strength gains were maintained when fibre volume fractions were optimized. The study highlighted that steel fibres are more influential on tensile strength than compressive strength and can compensate for strength losses associated with SCM’s in SCC systems.

Mansilla et al. [110] evaluated the mechanical performance of concrete reinforced with Eucalyptus globulus bark fibres, with particular emphasis on tensile behavior. The results demonstrated notable improvements in split tensile strength with fibre incorporation, attributed to fibre bridging across cracks and enhanced post-cracking resistance. Optimal fibre contents improved tensile strength without adversely affecting workability, while excessive dosages caused fibre clustering and strength reduction. The study concluded that natural fibres can effectively

enhance split tensile capacity and crack control when dosage and dispersion are properly controlled.

Wang and Yue[111] presented a comprehensive review on the time-dependent development of concrete strength, with attention to tensile behavior alongside compressive performance. The review emphasized that split tensile capability evolves extra slowly than strength in compression due to delayed microcrack stabilization and bond development at the paste aggregate interface. The authors noted that curing conditions, hydration kinetics, and supplementary materials significantly affect tensile strength growth rates. Their synthesis of experimental data confirms that tensile strength prediction models must explicitly account for time-dependent microstructural evolution rather than relying on compressive strength correlations alone.

The reviewed literature studies indicate that the mechanical behaviour of high-strength concrete is controlled by particle packing, water binder ratio, aggregate characteristics, and the use of supplementary cementitious materials. Most researchers observed that compressive strength improves considerably with lower porosity, denser microstructure, and stronger aggregate paste interaction. Microstructural observations from earlier studies revealed that refinement of the ITZ and formation of additional C-S-H gel contribute directly to higher compressive performance. At the same time, studies on tensile behaviour highlighted that crack propagation resistance depends strongly on matrix cohesion and ITZ bonding. Several researchers reported that optimum dosages of silica fume and other SCMs improve both compressive and tensile properties, whereas excessive fines may reduce workability and create dispersion-related issues. Although earlier work has separately examined compressive and splitting tensile behaviour, comparatively fewer studies have evaluated these properties together in HSC containing different coarse aggregates and alternative fine aggregates. Therefore, the present study attempts to examine the combined influence of granite, limestone, silica sand, and quarry sand on the overall mechanical performance of high-strength concrete.

2.7 Durability Properties

In concrete, different factors are responsible for affecting the different durability properties, which have a crucial effect on the longevity of the concrete. Various durability properties are discussed from the past literature and are discussed.

2.7.1 Water Absorption

Kwan et al. (2012) examined the impact of varying RCA proportions (0 to 100%) on concrete mix design and durability, emphasising absorption characteristics. Through systematic testing, they found that RCA's inherent porosity elevated water absorption rates progressively with higher replacement levels, reaching up to 20% more than natural aggregate mixes. This stemmed from the adhered mortar in RCA, which amplified capillary channels. Despite the rise, mixes with 50% RCA maintained acceptable absorption below 8%, suggesting moderated use could balance sustainability and performance without severe durability trade-offs.

Divsholi et al. [112] replaced Portland cement with 30 to 70% GGBS and assessed microstructural durability after 28 days. The incorporation notably curbed water absorption, dropping it by 15 to 25% across blends compared to plain cement, thanks to GGBS's pozzolanic refinement of pores and denser gel formation. Higher GGBS contents further minimized ingress pathways, enhancing long-term resistance to moisture-related degradation, though early-age absorption remained marginally elevated due to slower hydration.

Alexandridou et al.[113] assessed concrete made from RA sourced from Greek demolition plants, substituting natural ones at 25-100%. Durability evaluations highlighted a marked uptick in water absorption up to 12% higher in full-replacement mixes attributable to the recycled materials' rough texture and residual porosity. Even so, partial substitutions (less than 50%) kept absorption under 7%, comparable to controls, while mechanical integrity held firm. The work underscores RA's viability for non-critical elements, provided absorption thresholds guide application to mitigate potential corrosion risks.

Wang et al. [114] probed coarse aggregate types (gneiss, limestone, basalt, diabase) on cement concrete durability across w/b ratios of 0.22-0.45. Aggregates with elevated water absorption, like gneiss (highest at 2.5%), induced greater concrete porosity and thus amplified overall absorption by 10 to 15% versus low-absorption diabase. This correlation weakened at lower ratios, where matrix densification offset interfacial voids. Findings linked aggregate absorption directly to permeability proxies, advocating low-absorption options for harsh exposures to sustain moisture barrier efficacy.

Valenzuela-Leyva et al. (2025) [115] tested rhyolite aggregates paired with recycled (SCMs like 10% SF or 20% FA) in concrete at w/c equal to 0.57. SCMs drove down water absorption to 4.3% at 90 days for FA blends a 25% reduction over rhyolite-only mixes via pore refinement and ASR mitigation. This bolstered compressive gains and chloride barriers, affirming SCMs' role in taming rhyolite's silica-driven absorption while advancing circular practices for resilient structures.

2.7.2 Chloride permeability

Bravo et al. [116] assessed durability in concrete incorporating RA from C&D waste, replacing natural coarse aggregates at levels up to 100%. They employed rapid chloride penetration tests at 28 and 90 days to gauge ion ingress. Results revealed a notable escalation in chloride penetration for full-replacement mixes 53% higher at 28 days and 47% at 90 days stemming from the porous adhered mortar in recycled particles, which widened capillary pathways. Partial replacements mitigated this somewhat, but overall, the findings caution against high RCA use in chloride-exposed settings without compensatory measures like coatings.

Alexandridou et al. [113] evaluated mechanical and durability aspects of concrete using RA from Greek waste plants, with substitutions ranging from 25% to 100%. Chloride ion penetration was measured via rapid chloride permeability testing, showing elevated charge passage in recycled mixes compared to controls, particularly at higher replacement rates, due to increased porosity from demolition-derived mortar residues. Even at 50% substitution, permeability rose

by about 20 to 30%, though still within moderate risk thresholds. The work highlights recycled aggregates' potential but stresses preprocessing to curb ion diffusion for marine or de-icing applications.

Rao and Kumar (2019) investigated class-F FA role in enhancing concrete durability against chloride ingress, replacing cement at 0%, 20%, 30%, and 40% while maintaining a consistent mix design. RCPT at 28 days indicated substantial reductions: up to 60% lower charge passed at 30% FA, attributed to the pozzolanic filler effect that refined pore structure and blocked diffusion routes. Beyond 30%, gains plateaued slightly due to slower pozzolanic activation. These outcomes position FA as a cost-effective additive for extending service life in chloride-laden environments like bridges.

Rezaei et al. [117] explored recycled coarse aggregate (RCA) integration at 0-100% alongside nano-silica (NS) dosages of 0-5% in concrete, optimizing via experiments and modeling for mechanical and durability gains. Chloride permeability assessments via RCPT demonstrated RCA alone boosted ion penetration by 25-40% from inherent porosity, but 4.5% NS countered this, slashing charge passage by 35-50% through pore refinement and denser interfacial zones. Predictive models confirmed optimal 50% RCA with 4.5% NS yields low permeability akin to natural mixes, advocating NS for sustainable, corrosion-resistant designs.

Valenzuela-Leyva et al.[115] developed durable concrete using rhyolite aggregates prone to alkali-silica reaction, blended with recycled SCM like 10% SF or 20% FA at w/c=0.57. Rapid chloride permeability tests at 100 days showed rhyolite mixes with high charge (8164 Coulombs), but FA reduced it to 450 Coulombs a 95% drop via long-term pore occlusion, while SF achieved 88% reduction (1004 Coulombs) through early densification. Electrical resistivity corroborated these trends, underscoring SCMs' efficacy in fortifying chloride barriers for volcanic aggregate concretes in aggressive settings.

Jamil et al.[118] produced carbonated recycled aggregate concrete (CRAC) with 100% replacement, further modified by SCMs including 10% SF and 5% zeolite at w/b=0.42-0.55, assessing durability proxies like porosity. Though direct chloride tests were absent, carbonation lowered effective permeability indicators reducing water absorption by 20% and pore interconnectivity implying 15-25% less chloride ingress versus untreated recycled concrete, as calcite infills sealed pathways. SCM additions, however, slightly elevated diffusion risks at higher w/b due to alkalinity drops, suggesting balanced use for enhanced ion resistance in eco-friendly mixes.

2.7.3 Abrasion resistance

Faleschini et al.[119] examined the substitution of natural coarse aggregates with Electric Arc Furnace Slag (EAFS) in high-performance concrete (HPC) to assess mechanical and durability characteristics. The investigation confirmed that EAFS aggregate possesses superior physical properties, including intrinsic hardness and high resistance to fragmentation, evidenced by lower LA abrasion values compared to natural aggregates. Consequently, the concrete mixtures incorporating EAFS exhibited improved mechanical strength. This enhancement suggests a resulting increase in the concrete's operational abrasion resistance, making EAFS concrete particularly suitable for structures subjected to high surface wear.

Wang et al.[114] investigated how the source rock influences concrete performance by comparing gneiss, limestone, basalt, and diabase coarse aggregates. Although the study primarily focused on chloride penetration and mechanical strength, the outcomes of test showcased that the intrinsic material characteristics of the aggregates governed overall durability. Gneiss aggregate, which produced the highest compressive strength, is expected to yield the best abrasion resistance because of its greater hardness and superior bond with the cementitious matrix. Conversely, using lower-strength aggregates like diabase inherently leads to a notable decrease in resistance to surface wear.

Jamil et al.[118] employed an accelerated carbonation technique.This process densified the porous adhered mortar and strengthened the weak ITZ by forming calcium carbonate, leading to a notable 30% increase in compressive capability and reduced capacity of absorption of water. The refinement of the microstructure and the resultant material hardening significantly increased the concrete's resistance to abrasion and surface degradation by minimizing particle dislodgement under frictional loads. However, blending this optimized CRAC with SCMs surprisingly diminished the gains in mechanical properties.

Valenzuela-Leyva et al.[115]sought to improve concrete durability using ASR-prone Rhyolite aggregates mitigated by recycled SCM. The resulting mixtures demonstrated superior 90-day compressive strength and highly effective suppression of Alkali-Silica Reaction, particularly with FA additions, alongside superior chloride resistance. The angular morphology of the rhyolite provides an improved mechanical interlock with the paste, and SCM densification further refines the micro-structure, collectively resulting in an overall increase in resistance to surface wear and abrasion across all tested combinations.

The reviewed studies collectively indicate that durability performance of high-strength concrete is strongly governed by pore structure refinement, aggregate characteristics, and the quality of the interfacial transition zone. Researchers observed that the incorporation of SCMs such as silica fume, fly ash, and GGBS considerably reduced water absorption and chloride permeability due to secondary pozzolanic reactions and improved matrix densification. At the microstructural level, reduction in capillary pores and discontinuity of permeable channels were identified as the primary reasons for enhanced durability. Conversely, recycled and porous aggregates generally increased absorption and ion penetration because of adhered mortar and higher internal void content. Several investigations also highlighted that aggregate mineralogy and hardness significantly influence abrasion resistance, particularly in high-strength concrete. Dense and angular aggregates provided improved mechanical interlock and surface wear resistance. The literature further suggests that optimum replacement levels are essential, as excessive fines or highly porous constituents may create micro-voids and

adversely affect long-term durability. These observations establish that both coarse and fine aggregate selection play a decisive role in controlling transport properties and surface deterioration. The findings reported in previous studies provide the basis for the present investigation involving limestone and granite aggregates together with silica sand and quarry sand in order to evaluate their combined influence on water absorption, chloride permeability, and abrasion resistance of high-strength concrete.

2.8 Critical and Microstudy Analysis

2.8.1 Comparative Analysis of Literature

The reviewed literature indicates that the performance of high-strength concrete is strongly dependent on the combined influence of aggregate characteristics, supplementary cementitious materials, and particle packing efficiency. Most researchers reported that highly reactive mineral admixtures such as silica fume and metakaolin improve compressive strength, tensile strength, and durability by refining pore structure and strengthening the interfacial transition zone. Similarly, studies related to alternative aggregates highlighted that aggregate mineralogy, angularity, and surface texture considerably affect both mechanical and durability behaviour of HSC. Many factors of coarse aggregates, such as crushing strength, abrasion resistance, impact resistance, specific gravity, etc., play a significant role in deciding the performance of the high-strength. Fine aggregate replacements such as different sands, slag, and industrial by-products were also found effective in improving packing density and matrix compactness when used within optimum limits. However, excessive replacement levels often resulted in reduced workability and marginal decline in properties due to higher fines content and increased water demand. Overall, previous investigations consistently suggest that optimum replacement levels rather than complete substitution govern the balanced performance of High strength concrete mixtures.

2.8.2 Microstructural and Micro Study Reasoning

Microstructural observations reported in earlier studies confirmed that the improvement in concrete performance mainly originates from pore refinement,

densification of the cementitious matrix, and enhancement of the aggregate–paste interface. Pozzolanic materials such as silica fume and metakaolin react with calcium hydroxide to produce additional C-S-H gel, thereby reducing microvoids and capillary continuity. Studies involving strong, better and dense mineral aggregates demonstrated lower permeability and improved abrasion resistance due to reduced internal porosity and stronger bonding characteristics. On the other hand, porous or recycled aggregates increased water absorption and chloride penetration because of the presence of microcracks and old adhered mortar. The literature therefore establishes that concrete performance is directly linked with microstructural compactness, which is influenced by various aggregate quality parameters such as shape, strength, density, impact resistance, surface texture and optimum binder reactivity.

2.8.3 Limitations of Previous Studies

Although extensive research has been carried out on HSC, most studies have focused on isolated parameters such as either supplementary cementitious materials, recycled aggregates, or alternative fine aggregates, individually. Limited investigations examined the combined influence of different coarse aggregates together with alternative fine aggregates under a single experimental programme in high-strength concrete. Many researchers concentrated primarily on compressive strength, while comparatively fewer studies evaluated durability aspects such as water absorption, chloride permeability, and abrasion resistance simultaneously using different coarse and fine aggregate combinations. Past literature studies have rarely used different proportions of combined coarse (Granite and limestone aggregates) and fine aggregates (silica sand and Quarry sand) in high-strength concrete, indicating the need for more systematic comparative studies.

2.8.4 Research Gap for Present Study

From the reviewed literature, it is evident that limited work has been reported on the combined utilisation of granite and limestone aggregates with silica sand and quarry sand in high-strength concrete (HSC). Previous studies generally examined either coarse aggregate variation or fine aggregate replacement independently,

whereas their integrated effect on properties of high-strength concrete has not been explored adequately. Moreover, comparative assessment between granite-based and limestone-based high-strength mixes is limited. The available literature also lacks sufficient information regarding the effective replacement levels of silica sand and quarry sand in relation to durability parameters such as RCPT, water absorption, and abrasion resistance. Therefore, the present investigation was undertaken to develop high-strength concrete using granite and limestone aggregates in combination with different proportions of silica sand and quarry sand, and to evaluate their influence on strength and durability performance.

CHAPTER 3 MATERIALS AND METHODOLOGY

3.1 General

This chapter investigates the different materials used to formulate the HSC, including cement, Silica Fume, Metakaolin, different coarse and fine aggregates. This specific chapter reports the physical characteristics, chemical compositions, and other characterisations of the different materials used in this particular work. The proportion of materials used in the preparation of HSC is also provided in this chapter. Furthermore, this chapter also covers the laboratory methods and procedures for determining the fresh properties (workability), strength properties (including compressive strength, flexural strength, and split tensile strength), and durability properties (including water absorption, Rapid chloride penetration test and abrasion resistance) of the HSC.

3.2 Material

Various materials used in this experimental research work were tested before their usage in the concrete, and details of the materials are provided.

3.2.1 Cement

In this study, Ordinary Portland Cement (OPC) of 53 grade conforming to IS 12269:2013. The cement was procured from ACC Limited, Barmana, and was tested for its physical properties in accordance with standard procedures specified in IS codes. Test results are presented in Table 3, along with the permissible limits as per standards.

Table 3: Physical Properties of Cement

Property	Test value	Permissible limit
Standard consistency	31 %	-
Specific gravity	3.11	-
Fineness	8 %	< 10 %
Initial setting time	108 min	Min. 30 min
Final setting time	275 min	Max. 600 min
Soundness	4 mm	10 mm

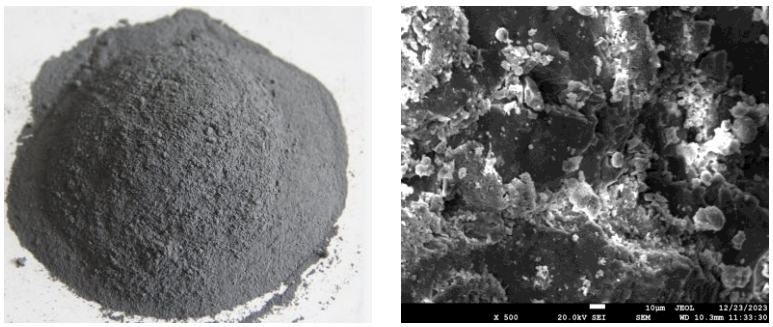

(a) (b)

Figure 11: a) Cement used in experimental work b)SEM image of cement used

Table 4:Chemical composition of cement

Compound	SiO_2	Al_2O_3	CaO	Fe_2O_3	MgO	Na_2O	Al_2O_3	$S0_3$
Composition (%)	19.35	4.57	68.64	1.21	1.39	0.47	4.57	3.14

3.2.2 Metakaolin

In the preparation of HSC, Metakaolin was incorporated as an SCM. Metakaolin used in this experimental study was in powdered form and was procured from Kaolin Techniques Private Limited, Gujarat. The physical properties and chemical composition of the metakaolin used are shown in Table 5 and Table 6, respectively. Figure 12 shows the metakaolin used and its SEM image.

Table 5: Physical properties of Metakaolin

Property	**Value obtained**
Specific gravity	2.60
Bulk density (kg/m^3)	350
Colur	Off white
Physical State	Powder

Table 6: Chemical Composition of Metakaolin

Compound	SiO_2	Al_2O_3	CaO	FeO	MgO	Na_2O	K_2O
Composition (%)	57.38	41.47	0.34	0.27	0.12	0.11	0.31

(a) (b)

Figure 12: a) Sample of metakaolin used b) SEM image of Metakaolin particles

3.2.3 Silica Fume

In the present work, SF was incorporated as an SCM for the production of HSC. The SF used was obtained from KGR Agro Fusion Ltd, Ludhiana. The SF used was in the form of powder with light greyish tone. The physical properties and chemical composition are shown in Tables 6 and 7. Silica Fume used along with its SEM image, is given below in Figure 13.

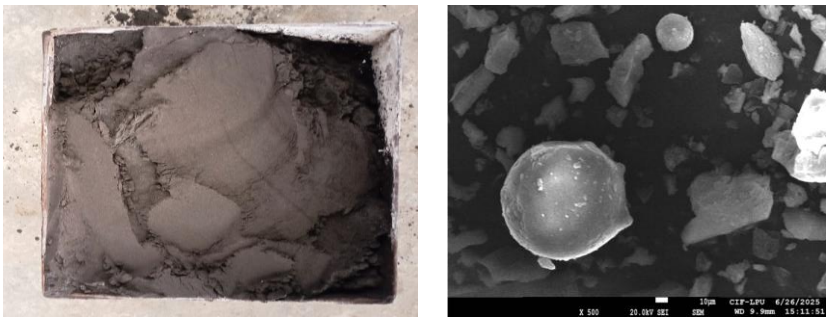

a) b)

Figure 13: a) Silica Fume used in the study b) SEM image of Silica Fume

Table 7: Physical properties of Silica Fume

Property	**Value obtained**
Specific gravity	2.20
Specific Surface Area	14000 m^2/ Kg
Bulk density (Kg/m^3)	386 Kg/m^3
Colur	Light greyish
Physical State	Powder

Table 8: Chemical Composition of Silica Fume

Compound	CaO	SiO_2	Al_2O_3	Fe_2O_3	MgO	K_2O	Na_2O	Others
Composition (%)	0.3	90.81	1.12	1.46	0.8	0.51	0.9	4.1

3.2.4 Natural Coarse Aggregates

Natural coarse aggregates used in the present experimental work for making the HSC were procured from the River Ravi, Punjab. Aggregates were dried prior to testing, and test results are tabulated in Table 9. Aggregates used are shown in Figure 14.

Figure 14: Natural Coarse Aggregates used in experimental work

Table 9: Properties of Natural Coarse aggregates and Standard limits of IS code

Property	**Test Results**
Bulk Density (kg/m^3)	1476
Specific Gravity	2.58
Water Absorption (%)	1.61
Aggregate Impact Value (%)	21.41
Aggregate Crushing Value (%)	25.7
Angularity Number	4
Fineness Modulus	7.10

3.2.5 Limestone and Granite coarse aggregates

Limestone aggregates used in the current experimental research work were obtained from M/s Sambal Crusher, Kotlu, Himachal Pradesh. Limestone aggregates were angular in shape and a specific gravity of 2.63.

Granite aggregates used in the present experimental study were sourced from Satpal Crusher's, Kathua and were used in the experimental program. These aggregates were characterised by a more angular shape (higher angularity) and rough texture. Test results of granite and limestone aggregate are presented in Table 10. Aggregates used are shown in Figure 15 (a) and Figure 15 (b)

a) b)

Figure 15 : a) Limestone Aggregates b) Granite coarse aggregates used in the experimental study

Table 10: Physical Test results of the Limestone and granite aggregates

Property	**Limestone aggregate**	**Granite aggregate**
Bulk Density (kg/m^3)	1559	1672
Specific Gravity	2.63	2.78
Water Absorption (%)	1.12	0.55
Aggregate Impact Value (%)	17.4	13.23
Aggregate Crushing Value (%)	22.4	18.6
Angularity Number	6	9
Fineness Modulus	7	6.80

3.2.6 Natural Fine Aggregates

In the experimental study, locally available river sand (RS) was used as the natural fine aggregate. The sand was procured locally, sieved through a 4.75 mm sieve to remove oversized particles. Natural fine aggregates used fell under grading Zone I, as per IS 383:2016. River sand was tested for various physical properties, and the test results are shown in Table 11

Table 11: Physical Characteristics of River Sand

Physical Property	Test results
Specific Gravity	2.62
Water Absorption	1.94%
Fineness Modulus	2.92
Bulk density (Kg/m^3)	1579
Zone	I

Figure 16: Natural river sand used in the study

3.2.7 Silica Sand and Quarry Sand

Silica sand used in this experimental work was obtained from Hum Khadd, Himachal Pradesh. Silica sand used in concrete was sieved through a 4.75 mm sieve and tested for other properties. Quarry sand used in the experimental work was procured from Narot Jaimal, Punjab. Quarry sand was obtained by mechanical crushing and contained a significant number of finer fractions, resembling dust-sized material. Sand samples were tested for determining various physical properties as per IS 2386, and the test results are tabulated in Table 12. Silica Sand and Quarry Sand used in the present experimental study are shown in Figure 17. Fig 18. shows the particle size distribution curve for natural fine aggregates, SS and QS used in study.

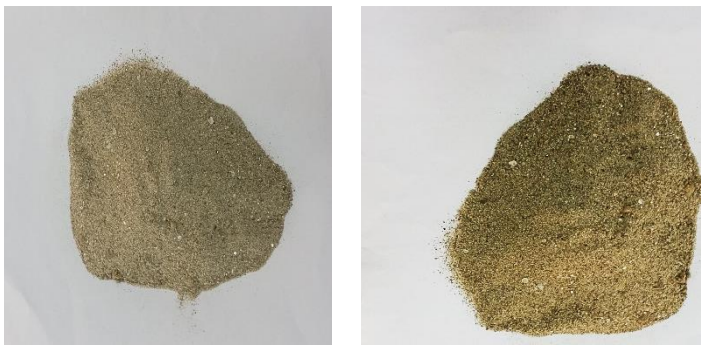

a) b)

Figure 17: a) Silica Sand b) Quarry Sand used in experimental study

Table 12: Characteristics of Silica sand and Quarry sand

Physical Property	Silica Sand (SS)	Quarry Sand (QS)
Specific Gravity	2.72	2.66
Water Absorption	1.14%	2.21%
Fineness Modulus	2.62	2.47
Bulk density	1637	1691
Zone	II	II

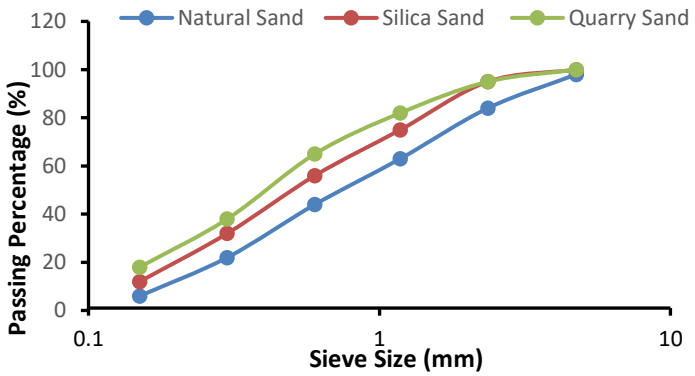

Figure 18: Particle size distribution curve for different sands used in study

3.2.8 Admixture

In the present experimental work, Polycarboxylate Ether (PCE) based superplasticizer, commercially available under the brand name Fairmate, Fairflo 160, was used current study. The basic physical properties of the superplasticizer used are noted in Table 13 and superplasticizer used in work is shown in Figure 19.

Figure 19 : Chemical Admixture

Table 13: Physical properties of the Admixture

Property	**Manufacturer Specification's**
Appearance	Brownish liquid
Base	Polycarboxylate Ether (PCE)
Specific gravity	1.05
pH Value	6-8
Chloride content (%)	< 0.2 %

3.3 Experimental Methodology

The research began with a detailed literature review to identify the gap in existing studies and address the challenges faced by the construction industry. The experimental programme was organised in sequential phases to evaluate the influence of aggregate on the HSC. In the first phase, control HSC mix was developed by iterative trials of water-binder ratio, superplasticiser and proportions of supplementary cementitious materials, including Taguchi optimisation until the final HSC is achieved, and this mixture was referred to as the control mix, i.e., CM. Using the Control mix as the baseline, two parallel series of mixes were produced to understand the effect of two different coarse aggregates, i.e., Limestone (L) and Granite (G), by replacing them (20, 40, 60, 80 and 100%) with the natural coarse aggregates. All obtained mixes of limestone and granite as coarse aggregates were evaluated for their mechanical strength at different ages,

and the best strength-performing mix of both series was further taken as the base for the second phase of work.

Following this, in the second phase of work, the selected limestone (L) and granite (G) concrete mixes served as a base to further understand the effect of Fine aggregates i.e Silica sand and Quarry sand. Now, for each selected base mix, the natural fine aggregate were replaced, one type at a time, by silica sand (SS) and quarry sand (QS) at different replacement percentages (i.e., 20, 40, 60, 80, and 100%), which further produced four different replacement series (G-SS, G-QS, L-SS and L-QS). Each of these series has five different concrete mixes falling under them. Now, these concrete mixes falling under different series were tested for their fresh (Workability), mechanical (compressive, split tensile, and flexural strengths) and durability tests (water absorption, RCPT and Abrasion resistance) to understand the effect of different aggregates on the concrete mixes. Furthermore, the best performing mixes from each series, the cost was calculated. The flow chart for the experimental methodology is shown in Figure 20.

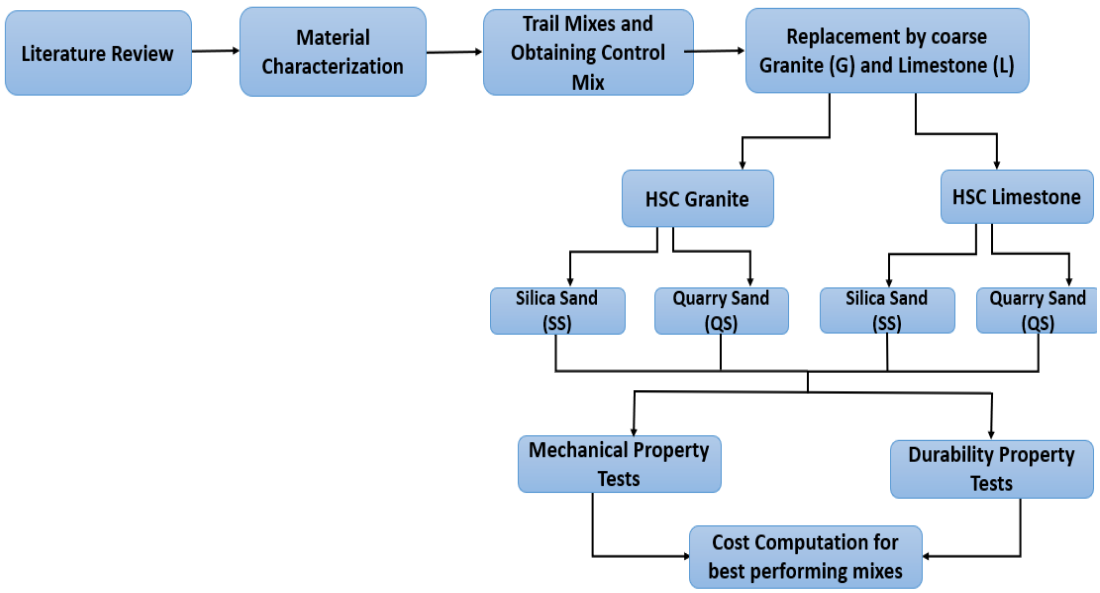

Figure 20: Flow chart of the experimental programme

3.4 Control Mix and Optimisation Process

The concrete mixes used in this investigation were proportioned in accordance with the provisions of IS 10262:2019. Ordinary Portland Cement (OPC) was used as the primary binder, while silica fume (SF) and metakaolin (MK) were

incorporated as supplementary cementitious materials for preparing the high-strength concrete mix. A polycarboxylate ether-based superplasticiser (under the brand name FairMate, Fairflo 160) was used to achieve the desired workability of mix.

To obtain an optimum high-strength control mix (CM), a systematic and structured mix optimisation process was adopted. In the first stage, a series of preliminary trial (PT) mixes were prepared by varying individual parameters, including superplasticiser dosage, silica fume content, metakaolin content and water binder ratio, while maintaining the remaining parameters constant with an objective of these trials to identify feasible ranges of the governing variables and to understand the behaviour of concrete w.r.t the influence on fresh and hardened concrete properties. Mixes exhibiting inadequate workability, excessive cohesiveness, segregation tendencies or unsatisfactory compressive strength were eliminated from further consideration.

In the second stage of the optimisation process, Taguchi design of experiments (DOE) approach was then employed to determine the optimum combination of the parameters. Three control factors (A, B and C), namely silica fume (SF), metakaolin (MK) and water binder (w/b) ratio respectively, each at three different levels (1, 2 and 3), were confirmed, considered and arranged using an L9 orthogonal array, where the strength was considered as the primary response parameter. The Taguchi method is widely employed in concrete research for optimisation with minimum experimental runs, providing statistically defensible optimal parameter combinations (Nair et al., 2020; Bhardwaj et al., 2019). Response analysis using signal-to-noise (S/N) ratio evaluation was performed to determine the optimum factor-level combination for the concrete mix optimisation.

The optimum parameter combination results obtained from the Taguchi analysis corresponded to A2, B2 and C1 (i.e., water binder ratio of 0.30). These optimised levels of orthogonal matrix produced the highest S/N ratio for all three factors. An experimental trial was conducted using the optimum levels given by the Taguchi design of experiments (DOE) approach. The final mix proportions of the control

mix (CM) are presented in Table 14. Annex A contains all relevant details and data of the mix design optimisation are process.

Table 14: Final optimised control mix after Taguchi analysis

Mix ID	w/b	Cement (kg/m^3)	SF (kg/m^3)	MK (kg/m^3)	NFA (kg/m^3)	NCA (kg/m^3)	Water (kg/m^3)	SP (kg/m^3)
CM	0.28	435	39.5	52.7	459	1236	148	6.32

To further assess the reliability of the results obtained from the Taguchi analysis, a confirmation trial was carried out using the optimum parameter combination. The performance of the resulting concrete mix was found to be satisfactory, indicating the confirmation of the optimisation process adopted. Complete details of preliminary trial mix data, Taguchi design tables, orthogonal matrix, factors, levels and optimisation process details are provided in Annexure A.

Further, as part of an experimental methodology, at the first level of replacement, natural coarse aggregates were replaced with limestone (L) and granite (G) at 20%, 40%, 60%, 80%, and 100%, considered individually for both aggregates. Details of the mix ID are shown in Table 15

Table 14: Mix designation of mixes formulated using limestone and granite coarse aggregates

Mix Series	Mix ID	Natural coarse aggregates (NCA) replacement with limestone and Granite aggregates
Granite (G)	G20	NCA replaced with 20% granite aggregates
	G40	NCA replaced with 40% granite aggregates
	G60	NCA replaced with 60% granite aggregates
	G80	NCA replaced with 80% granite aggregates
	G100	NCA replaced with 100% granite aggregates
Limestone (L)	L20	NCA replaced with 20% limestone aggregates
	L40	NCA replaced with 40% limestone aggregates
	L60	NCA replaced with 60% limestone aggregates
	L80	NCA replaced with 80% limestone aggregates
	L100	NCA replaced with 100% limestone aggregates

Where, L20 denotes Limestone coarse aggregates 20%

G20 denotes Limestone coarse aggregates 20%

Furthermore, each mix series of mix (limestone series and granite series), the mechanically best performing mixes obtained after experiment results (i.e L100 and G100), were taken for preparing further mixes for the study. Now, in this second level, to understand the effect of silica sand (SS) and quarry sand (QS) replacement, with natural fine aggregates i.e. river sand. The various mixes formulated with Silica Sand replacement for further study are tabulated in Table 16.

Table 15: Mix series and mix designation of mixes using Silica Sand (SS)

Mix Series	Mix ID	Natural Fine aggregates (NFA) replacement with Silica Sand (SS)
Granite Silica Sand (G100-SS)	G100SS20	NFA replaced with 20% Silica sand in granite mixes
	G100SS40	NFA replaced with 40% Silica sand in granite mixes
	G100SS60	NFA replaced with 60% Silica sand in granite mixes
	G100SS80	NFA replaced with 80% Silica sand in granite mixes
	G100SS100	NFA replaced with 100% Silica sand in granite mixes
Limestone Silica sand (L100-SS)	L100SS20	NFA replaced with 20% Silica sand in limestone mixes
	L100SS40	NFA replaced with 40% Silica sand in limestone mixes
	L100SS60	NFA replaced with 60% Silica sand in limestone mixes
	L100SS80	NFA replaced with 80% Silica sand in limestone mixes
	L100SS100	NFA replaced with 100% Silica sand in limestone mixes

Further, with the quarry sand (QS) replacement, various mixes were formulated and are presented in Table 17. Tables 18, 19 and 20 give the mix proportions of mixes.

Table 16: Mix series and mix designation of mixes using Quarry Sand

Mix Series	Mix ID	Natural Fine aggregates (NFA) replacement with Quarry Sand (QS)
Granite Silica Sand (G100-QS)	G100QS20	NFA replaced with 20% Quarry sand in granite mixes
	G100QS40	NFA replaced with 40% Quarry sand in granite mixes
	G100QS60	NFA replaced with 60% Quarry sand in granite mixes
	G100QS80	NFA replaced with 80% Quarry sand in granite mixes
	G100QS100	NFA replaced with 100% Quarry sand in granite mixes

Limestone Silica sand (L100-QS)	L100QS20	NFA replaced with 20% Quarry sand in limestone mixes
	L100QS40	NFA replaced with 40% Quarry sand in limestone mixes
	L100QS60	NFA replaced with 60% Quarry sand in limestone mixes
	L100QS80	NFA replaced with 80% Quarry sand in limestone mixes
	L100QS100	NFA replaced with 100% Quarry sand in limestone mixes

Where, G100SS20 denotes granite coarse aggregates 100% and Silica sand 20%

L100SS20 denotes limestone coarse aggregates 100% and Silica sand 20%

G100QS20 denotes granite coarse aggregates 100% and Quarry sand 20%

L100QS20 denotes limestone coarse aggregates 100% and Silica sand 20%

Table 17: Mix proportions of Limestone and Granite series mixes

Mix Designation	w/b	Cement (kg/m^3)	SF (kg/m^3)	MK (kg/m^3)	NFA (kg/m^3)	NCA (kg/m^3)	Limestone (L) (kg/m^3)	Water (kg/m^3)	SP (kg/m^3)
L20	0.28	435	39.5	52.7	459	988.8	247.2	147.6	6.32
L40	0.28	435	39.5	52.7	459	741.6	494.4	147.6	6.32
L60	0.28	435	39.5	52.7	459	494.4	741.6	147.6	6.32
L80	0.28	435	39.5	52.7	459	247.2	988.8	147.6	6.32
L100	0.28	435	39.5	52.7	459	0	1236	147.6	6.32
G20	0.28	435	39.5	52.7	459	988.8	247.2	147.6	6.32
G40	0.28	435	39.5	52.7	459	741.6	494.4	147.6	6.32
G60	0.28	435	39.5	52.7	459	494.4	741.6	147.6	6.32
G80	0.28	435	39.5	52.7	459	247.2	988.8	147.6	6.32
G100	0.28	435	39.5	52.7	459	0	1236	147.6	6.32

*w/b denotes water binder ratio

*SF- Silica Fume, MK- Metakaolin, NFA- Natural fine aggregates NCA- Natural Coarse aggregates, SP =Superplasticizer

Table 18: Mix proportions of Silica sand (SS) mixes

Mix ID	w/b	Cement (kg/m³)	SF (kg/m³)	MK (kg/m³)	NFA (kg/m³)	SS (kg/m³)	Limestone (L100) (kg/m³)	Water (kg/m³)	SP (kg/m³)
L100-SS20	0.28	435	39.5	52.7	367.2	91.8	1236	147.6	6.32
L100-SS40	0.28	435	39.5	52.7	275.4	183.6	1236	147.6	6.32
L100-SS60	0.28	435	39.5	52.7	183.6	275.4	1236	147.6	6.32
L100-SS80	0.28	435	39.5	52.7	91.8	367.2	1236	147.6	6.32
L100-SS100	0.28	435	39.5	52.7	0	459	1236	147.6	6.32
	w/b	**Cement (kg/m³)**	**SF (kg/m³)**	**MK (kg/m³)**	**NFA (kg/m³)**	**SS (kg/m³)**	**Granite (kg/m³)**	**Water (kg/m³)**	**SP (kg/m³)**
G100-SS20	0.28	435	39.5	52.7	367.2	91.8	1236	147.6	6.32
G100-SS40	0.28	435	39.5	52.7	275.4	183.6	1236	147.6	6.32
G100-SS60	0.28	435	39.5	52.7	183.6	275.4	1236	147.6	6.32
G100-SS80	0.28	435	39.5	52.7	91.8	367.2	1236	147.6	6.32
G100-SS100	0.28	435	39.5	52.7	0	459	1236	147.6	6.32

Table 19: Mix proportions of Quarry sand (QS) mixes

Mix ID	w/b	Cement (kg/m³)	SF (kg/m³)	MK (kg/m³)	FA (kg/m³)	QS (kg/m³)	Limestone (kg/m³)	Water (kg/m³)	SP (kg/m³)
L100-QS20	0.28	435	39.5	52.7	367.2	91.8	1236	147.56	6.32
L100-QS40	0.28	435	39.5	52.7	275.4	183.6	1236	147.56	6.32
L100-QS60	0.28	435	39.5	52.7	183.6	275.4	1236	147.56	6.32
L100-QS80	0.28	435	39.5	52.7	91.8	367.2	1236	147.56	6.32
L100-QS100	0.28	435	39.5	52.7	0	459	1236	147.56	6.32
Mix ID	**w/b**	**Cement (kg/m³)**	**SF (kg/m³)**	**MK (kg/m³)**	**FA (kg/m³)**	**QS (kg/m³)**	**Granite (kg/m³)**	**Water (kg/m³)**	**SP (kg/m³)**
G100-QS20	0.28	435	39.5	52.7	367.2	91.8	1236	147.56	6.32
G100-QS40	0.28	435	39.5	52.7	275.4	183.6	1236	147.56	6.32
G100-QS60	0.28	435	39.5	52.7	183.6	275.4	1236	147.56	6.32
G100-QS80	0.28	435	39.5	52.7	91.8	367.2	1236	147.56	6.32
G100-QS100	0.28	435	39.5	52.7	0	459	1236	147.56	6.32

3.5 Casting and Curing

For preparing of concrete mixes, a mixer machine was employed to ensure homogeneous blending of all constituents. Initially, the dry materials comprising cement, SCM, fine aggregates, and coarse aggregates were introduced into the mixer and blended for 2-3 minutes to ease the dry mixing, so as to uniformly disperse the binders and aggregates. Further, the required quantity of water, added with the measured dosage of superplasticiser, was constantly added.The process of mixing continuous until a uniform concrete was produced.

The fresh concrete was then poured into standard moulds for different specimen according to the different test, including cubes, cylinders , beams and other specimens as per the different tests.After the conceret was placed in steel moulds, they were vibrated on a vibrating table to expel entrapped air and achieve good compaction. The specimens were left undisturbed for 24 hours, and then were removed from moulds. Following the process of demoulding, all specimens were transferred to a curing tank, and were kept in water till the designated testing ages. Samples were cured for different ages as per the requirement of the strength and durability tests. Curing was done to ensure the proper hydration and strength developmeny of concrete mixes.

a) b)

Figure 21: a) Casting of concrete Specimen b) Curing of the specimens in the curing tank

3.6 Testing methodology

Various properties of the concrete were tested to understand and analyse the behaviour of concrete, by subjecting them to standard testing rpcedures , which are discuused below.

3.7 Fresh Properties

3.7.1 Workability

The workability of the fresh concrete was assessed through the slump cone test, following the guidelines of IS 1199. This test essentially evaluates how easily the concrete can be placed and compacted, serving as a practical measure of the mix consistency.The Slump cone appartus, consisting of a slump cone, which has 300 mm height, top dia meter equals to 200 mm and a bottom dia equals to 100 mm, along with a rod whose diameter is 16 mm and 600 mm long to tamp concrete.

Prior to conducting the test, the inner surface of the slump cone and the base plate were thoroughly cleaned. The cone was positioned on a rigid, non-absorbent surface. The freshly prepared concrete was filled into the slump cone in three approximately equal layers, with each layer being compacted using 25 uniform strokes of the tamping rod, evenly distributed over the cross-sectional area.Once the top layer got compacted properly, extra concrete is struck off to top level of cone. Now, the cone is carefully lifted in a vertical upward direction without lateral or torsional movement, letting the concrete to subside freely.

The reduction in height of the concrete mass, measured in form of the difference between the height of the cone and the average height of the subsidance, was recorded as the slump value. The slump measurement was reported in mm. The experiential slump values were used as a measure of the workability and consistency of the concrete mixes.

Figure 22: Slump cone for workability

3.8 Mechanical Properties

3.8.1 Compressive Strength

The compressive strength of hardened concrete was evaluated following the procedures specified in IS 516. This test provides the principal indication of the concrete's load-bearing capacity.

To assess the compressive strength, standard cube specimens measuring 150 mm × 150 mm × 150 mm were prepared and cured for varying periods, namely 14, 28, and 90 days. Prior to testing, the specimens were wiped dry with a cloth and then positioned centrally on the compression testing machine (CTM) with a capacity of 3000 kN.

The load was applied gradually at the specified rate of 14 MPa/min, until failure occurred in the cube specimen. The maximum load taken by the cube when it failed was noted down. Compressive strength, was then calculated using the given relationship

$$f_{ck} = \frac{P}{A}$$

Where,

f_{ck} signifies the strength in compression (MPa)

P is the max load at failure (N)

A is the cross-sectional area of the specimen (mm²)

The compressive strength at each testing age was determined by calculating the mean value of the compressive strengths obtained from the three specimens tested.

Figure 23: Compression Testing Machine (CTM)

3.8.2 Split Tensile Strength

It was performed as per the procedure specified in IS 5816:1999. This test is basically an indirect way to measure tensile strength of concrete, which is difficult to assess directly due to the brittle nature of concrete.

In this test, specimens cylindrical in shape, with dia of 150 mm and height 300 mm were cast and cured, as per the specified testing ages of 7, 28 and 90 days. Before testing, the specimens made dry using cloth and were carefully aligned on the CTM between loading strips. The cylindrical specimen placed diametrically along the central axis in the CTM, so as to apply load along the vertical diametral plane of the cylinder.

This load on cylinder was applied gradually at a uniform rate and the highest load carried by the specimen at failure point was noted. The split tensile strength was calculated using given this expression.

$$f_{ct} = \frac{2P}{\pi D l}$$

Where,

f_{ct} =Split tensile strength (N/mm^2 or MPa)

P = Maximum load at failure stage (N)

l = cylindrical specimen length (mm)

d = cylindrical specimen diameter (mm)

a)

b)

Figure 24: a) Catsted cylindrical specimens b) Specimen placed dismetrically in CTM

3.8.3 Flexural Strength

The flexural strength of concrete was evaluated in accordance with the procedure specified in IS 516. This test provides a degree of the concrete resistance to bending and cracking.

For this test procedure, prismatic beam specimens measuring 100 mm × 100 mm × 500 mm were cast and cured until they reached the specified testing ages. Before testing, the specimens were wiped to remove surface moisture and placed centrally on the supporting rollers of the flexural testing machine.

The test was conducted under two-point loading, with a clear span of 400 mm between supports and equal loading points placed symmetrically at one-third of the span length. This loading arrangement ensured the development of a pure bending zone in the middle third of the specimen.

The load was applied without shock and at a uniform rate until failure occurred. The maximum load carried by the specimen was recorded. The flexural strength, expressed as the modulus of rupture, was calculated using the following expression:

$$f_r = \frac{P * L}{bd^2}$$

where,

f_r = flexural strength (N/mm^2)

P = Maximum load at failure

l = length of specimen between supports

b = Width of specimens

d = depth of specimen

a) b)

Figure 25: a) Beam specimen casted for flexural test b) Flexural testing of specimens

3.9 DURABILITY TESTS

3.9.1 Water absorption

The water absorption capacity of concrete was determined in accordance with the standard provisions of ASTM C642 This test of durability also gives an idea about the pore structure and permeability.

In this test, cubical specimens of 100 mm size were prepared and cured for different days before testing. The specimensremoved from the curing tank are initially dried, and then placed in an oven maintained at 100 to 110 degree celcius, until they maintain a constant mass, recorded as W_1.

After oven drying, the specimens are cooled to room temperature and then dipped in water for the next 24 hours. At the end of this time, the specimens were taken out, and their surfaces were rubbed with a dry cloth to make them surface dry. the saturated mass was then recorded as W_2

The water absorption in form of percentage of the specimen was calculated as given

$$Water\ absorption(\%) = \frac{W_2 - W_1}{W_1} * 100$$

The average value of at least three specimens was reported as the representative water absorption of the concrete mix.

3.9.2 Rapid Chloride Permeability Test

The resistance of concrete to chloride ion penetration was determined by RCPT as per the procedure of ASTM C1202. This test gives an impression of concrete permeability in chloride environments. The method is grounded on gauging the electrical charge passed through a concrete specimen over six hours when a constant potential difference is applied across it.

The specimen used in this test is a cylindrical disc of 100 mm dia and 50 mm thickness. The specimens were dried initially and then subjected to vacuum for 3 hrs, followed by keeping in de-aired water under vacuum for an additional 1 hour. The specimen is placed between two cells of RCPT set up, one having 3% NaCl solution and another having 0.3 N sodium hydroxide (NaOH) solution.The test set up is turned on, and the current flowing through specimen was recorded at constant intervals of 30 minutes over a duration of 6 hours.The test set of RCPT used for the experimental work is shown in Figure 20.

The total charge passed (Q), expressed in coulombs, was calculated using the given formula.

$$Q = 900(I_0 + 2I_{30} + 2I_{60} + 2I_{90} + 2I_{120} \dots\dots\dots\dots 2I_{330} + I_{360})$$

Where,

Q denoted current flow through one cell

I_0 denoted current in amperes immediately after the voltage is applied

I_t denoted the current in amperes at t minutes after the voltage is applied

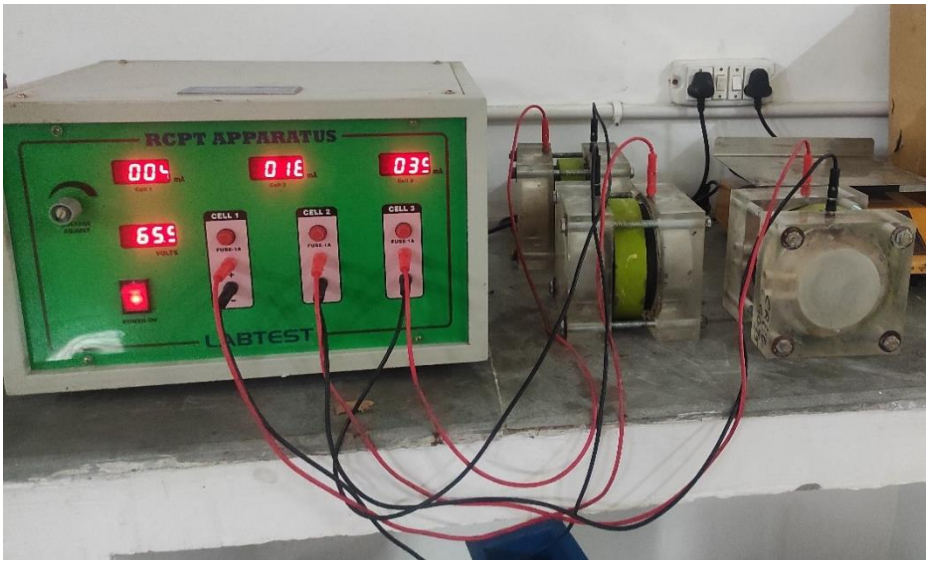

Figure 26: Specimens for chloride penetration in RCPT Apparatus

3.9.3 Abrasion Resistance

To evaluate the ability of concrete to withstand frictional wear, an abrasion resistance test was performed in accordance with IS 1237:2012. This test provides insight into the concrete's resistance to abrasion, particularly under repeated traffic loads or mechanical rubbing from any cause.

Concrete cube specimens measuring 70.6 mm were prepared and cured in water for durations of 28, 90, and 180 days. The specimens were then oven-dried at a temperature of 110 ± 5 °C for 24 hours. The mass of each specimen was recorded with high precision to the nearest 0.1 gram. Additionally, the thickness of the specimens was measured at four different corners as well as at the center of the cube.Then, the specimen was placed on the rotating disc of the abrasion testing machine, and it was held in firm position by holding device, with the testing surface placed in contact with the abrasive rotating disc. A central load of 300N was applied during the test procedure. The disc was rotated at 30 ± 1 rpm, ensuring uniform abrasion throughout the surface, and during the process, abrasive charge (aluminium oxide) was evenly placed on the rotating disc. At the end of the specified revolutions, Readings, i.e., the thickness and weight of the specimens, were taken at intervals of one and a half minutes, and the specimen was rotated at 90 degrees in a clockwise direction about its vertical axis. Once the rotations are completed, the final thickness and weight of the cube were noted.

The amount of wear was calculated by finding the difference in thickness between the specimen before and after the abrasion test, using the formula given

$$T = [(X-Y) \times V] / (X \times A)$$

where,

T = average thickness loss of specimen

X = initial weight of specimen

Y = final weight of specimen

V = volume of specimen before testing

A = surface area of specimen

Abrasion resistance was reported in terms of the average wear in millimetres, where a lower wear value corresponds to higher abrasion resistance of concrete.

a) b)

Figure 27: a) Abrasion testing machine b) Cube sample placed in machine

CHAPTER 4 : RESULTS AND DISCUSSIONS

4.1 General

This chapter presents the experimental results and their discussion on the behaviour of HSC incorporating different types of aggregates. The study initially investigates the effect of replacing natural coarse aggregates with limestone and granite aggregates at different replacement levels on the fresh and mechanical properties of HSC. Based on test results, in the next phase, further replacement of natural fine aggregates with silica sand and quarry sand was carried out to understand their influence on various properties of concrete. The results obtained cover workability characteristics in the fresh state, compressive strength, split tensile, and flexural strength in the hardened state, and durability indicators such as water absorption, RCPT and abrasion resistance. The findings are comprehensively analysed to understand the effect of the coarse and fine aggregate types and replacement levels on the performance of HSC.

4.2 Workability

4.2.1 Workability of Limestone and Granite Mixes

The workability of the HSC mixes was determined for the various mixes. In the first phase of replacement of natural coarse aggregates with limestone and granite aggregates, the workability determined for the various mixes is shown in Figure. 28.

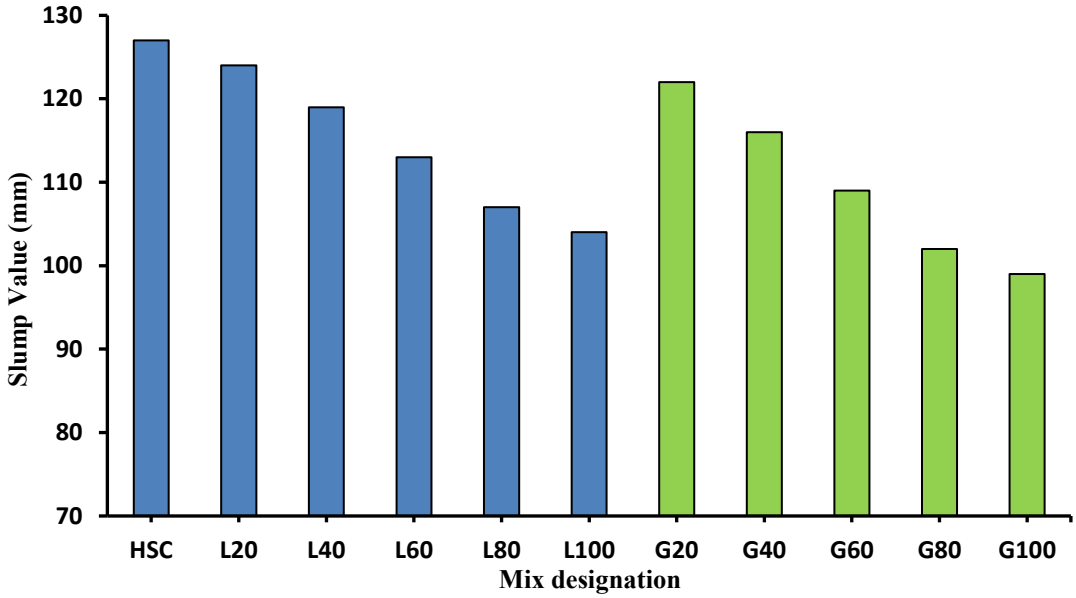

Figure 28: Variation of workability in various limestone and granite mixes

Test results shown in Figure 28 reveal that there is a general decrease in slump with an increase in the percentage replacement of natural coarse aggregates by both limestone and granite aggregates. In the case of various limestone series of mixes**,** a gradual reduction in slump was observed from 124 mm for L20 mix to 104 mm at complete replacement, i.e, in mix L100.In the case of limestone mixes, the workability decreased by 2.36 %, 6.2%, 11%, 15.7% and 18.11% in L20, L40, L60, L80, and L100 mixes, respectively, as compared to the control HSC mix. A similar trend in workability of granite mixes was seen, with a more pronounced reduction in slump, decreasing from 122 mm in G20 mix to 99 mm in G100 mix.. For granite mixes, the workability decreased by 3.93%, 8.66%, 14.1%, 19.6% and 22.04%, in G20, G40, G60, G80, and G100 mixes, respectively, in contrast to the control HSC. The reduction in the workability of both granite and limestone mix series as compared to the control HSC mixes is attributed to rough surface texture of the granite and limestone aggregates as compared to the natural coarse aggregates, thus restricting the slump flow of the concrete.

On comparison of various mixes of the limestone and granite series, it was recorded workability of mixes decreased for both limestone and granite mix series as compared to the control HPC, but the reduction in workability for the granite aggregate concrete was more when compared with the limestone aggregate

concrete at the same replacement level of the aggregates. For instance, at the complete replacement, mix L100 demonstrated a Slump value of 104 mm, while mix G100 demonstrated a slump value of 99 mm; and a similar trend of reduced workability in granite mixes was observed at other replacement percentages, when compared with the limestone mixes. Comparatively, it can be stated that at identical replacement percentages, concrete mixes with limestone aggregates exhibited higher workability than those with granite aggregates, which may be primarily attributed to the lower angularity number and relatively smooth surface texture of limestone aggregates as compared to the granite aggregates, whose particles facilitated better particle rearrangement and lesser interparticle friction, thus imparting more workability. In case of granite aggregate concrete mixes, angular and rough surface textured granite aggregates may restrict the flow of the concrete mix, thus contributing to the greater loss of workability. Also, the higher specific gravity of granite aggregates may have contributed towards the increased overall aggregate mass for a given volume, thereby effectively reducing the available paste film thickness surrounding the aggregate surfaces. This condition hindered the mobility of aggregates within the mix, making granite concrete mixes less workable in contrast to limestone aggregate mixes.

Practically, in spite of the observed minor reduction in slump, the mixes remained cohesive and showed no signs of segregation and bleeding. Moreover, all the mixes exhibited satisfactory workability within the medium-to-high range, which is considered suitable for HSC produced with polycarboxylate-based superplasticizer at a low water-binder ratio.

4.2.2 Effect of Silica sand on workability of Limestone and grante mixes

In this phase, silica sand was used at various replacement percentages in limestone and granite mixes to understand its effect on the limestone and granite mixes.Test results are discussed below in Fig 29.

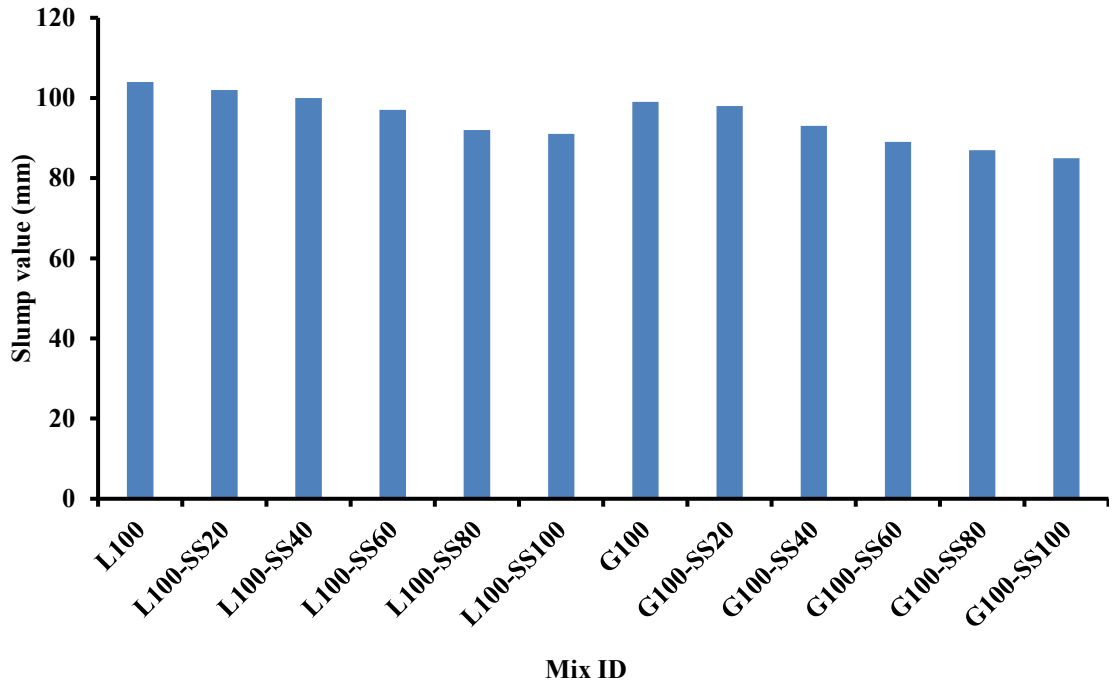

Figure 29: Variation in workability due to SS mixes in limestone and granite mixes

The workability of the high-strength concrete mixes incorporating silica sand (SS), measured in terms of slump value, is presented in Figure X. The results indicate a gradual reduction in workability with increasing levels of silica sand replacement in both limestone- and granite-based mixes. This trend is consistent across all replacement levels, suggesting a systematic influence of silica sand characteristics on fresh concrete behaviour.

In the limestone series, the slump value decreased from 104 mm for the L100 mix to 97 mm at 60% SS replacement, followed by a further reduction to 91 mm at full replacement. Similarly, granite-based mixes exhibited a decline from 99 mm for G100 to 89 mm at 60% SS replacement and reached a minimum of 85 mm at 100% SS. The observed reduction in slump can be primarily attributed to the angular and sub-angular morphology of silica sand particles, which increases internal friction and inter-particle resistance compared to the rounded nature of natural river sand. Additionally, the relatively finer grading of silica sand contributes to a higher specific surface area, thereby increasing water demand at a constant water-binder ratio.

Despite the reduction in workability, the mixes maintained adequate slump values suitable for high-strength concrete applications. The presence of silica fume and metakaolin, along with the use of a high-range water-reducing admixture, helped offset excessive loss in workability by improving paste cohesion and particle dispersion. It is also observed that granite-based mixes consistently exhibited slightly lower slump values than corresponding limestone mixes at similar replacement levels. This behaviour can be linked to the higher angularity and rougher surface texture of granite aggregates, which intensify aggregate interlock and further restrict fresh concrete flow.

4.2.3 Effect of Quarry sand on workability of Limestone and grante mixes

In this phase, Quarry sand (QS) was used at various replacement percentages in limestone and granite mixes to understand its effect on the limestone and granite mixes. Test results are discussed below in Fig 30.

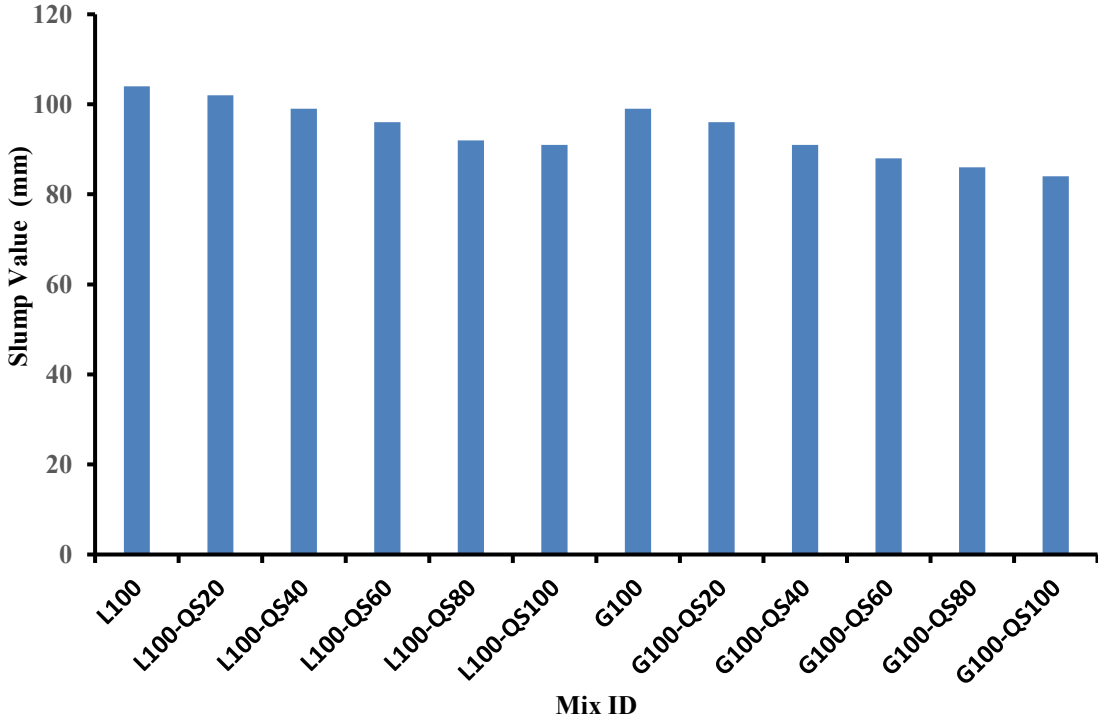

Figure 30 : Variation in workability due to QS mixes in limestone and granite mixes

The workability behaviour of high-strength concrete mixes incorporating quarry sand (QS), evaluated using the slump cone test, is illustrated in Figure 30. A consistent reduction in slump value is observed with increasing levels of quarry

sand replacement in both limestone- and granite-based concrete mixes. This reduction indicates the pronounced influence of quarry sand characteristics on the rheology of fresh concrete.

In the limestone series, the slump value decreased progressively from 104 mm for the L100 mix to 99 mm at 40% QS replacement, followed by a further reduction to 91 mm at full replacement. A similar but more pronounced trend was noted in granite-based mixes, where slump reduced from 99 mm for G100 to 91 mm at 40% QS replacement and reached a minimum of 84 mm at 100% QS. The steeper decline in workability for granite mixes can be attributed to the combined effect of angular granite aggregates and the highly angular, rough-textured quarry sand particles.

The reduction in workability with increasing QS content is primarily associated with the angular shape, rough surface texture, and higher fines content of quarry sand compared to natural river sand. These characteristics increase inter-particle friction and internal resistance to flow, leading to lower slump values at a constant water–binder ratio. Additionally, the presence of microfines in quarry sand contributes to increased water absorption, effectively reducing the free water available for lubrication in the fresh mix.

4.3 Compressive Strength

4.3.1 Compressive strength of limestone and granite aggregates

In the first phase of the experimental work, using limestone and granite aggregates in the concrete, the compressive strength of the concrete mixes at 7, 28, and 90 days is presented in Figure 29.

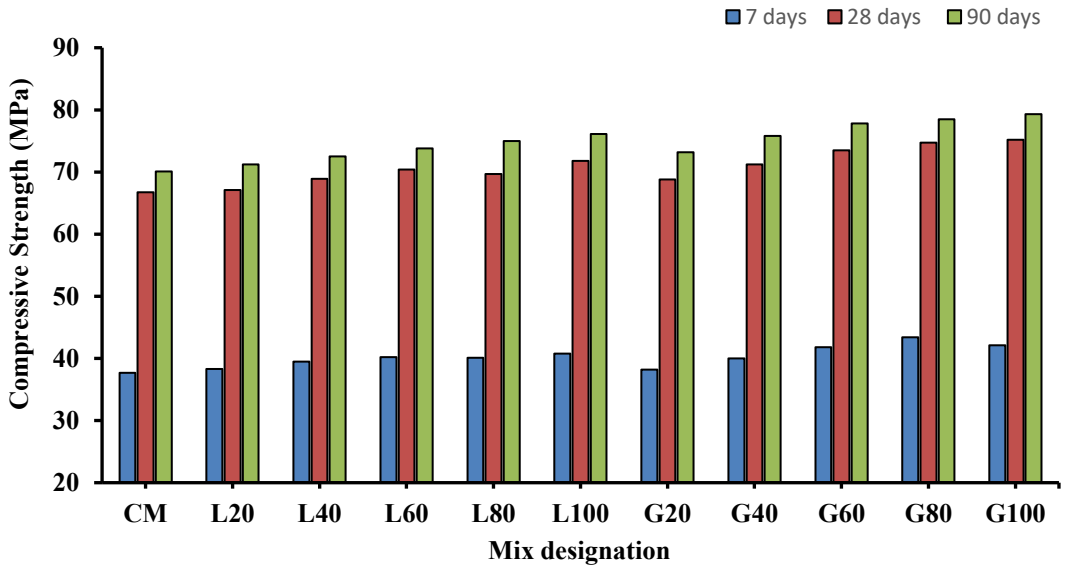

Figure 31: Compressive Strength of limestone and granite aggregate concrete at different ages of curing

Test results of compressive strength as shown in Figure 29 for different series of limestone and granite aggregates, demonstrate an increase in strength with curing age, i.e, 7, 28, and 90 days across all mixes, reflecting the effect of progressive hydration of SCM (SF and MK) with age, leading to the increased compressive strength. For instance, mix designation L20 demonstrated a compressive strength of 38.3 MPa at 7 days,67.1 MPa at 28 days, and 71.2 MPa at 90 days, which may be attributed to the enhanced curing effect of hydration products of concrete with the passing days.

In case of limestone series, i.e, from L20 to L100 mixes, the compressive strength of the concrete increased with the increase in the replacement percentage of natural aggregates with the limestone aggregates as shown in Fig.30. At 7 days strength increased with the increase in the replacement percentage of limestone aggregates with 38.3 Mpa at 20% replacement as compared to 40.8 Mpa strength at 100% replacement by limetsone aggregates. But over time, at 28 days of curing, compressive strength increased by 0.53%, 3.2%, 5.48%, 4.43% and 7.58% in L20, L40, L60, L80, and L100 mixes, respectively, as compared to control HPC. Such a strength increment with the increasing content of coarse limestone aggregates is attributed to the higher strength, more angularity, and rough surface texture of

these aggregates in contrast to natural coarse aggregates, thus forming a robust concrete mix. Similar trend of strength results were observed at 90 days of curing, where L100 mix demonstrated a strength increment of 8.55% at 90 days of testing.

Test results of the various granite mixes also demonstrated a consistent rise in compressive strength up to the full 100% replacement level. The 28-day strength increased from 68.8 MPa for mix G20 to 75.2 MPa for mix G100, while the 90-day strength reached 79.3 MPa, indicating a 12-13% improvement over the control HPC mix. To be specific, compressive strength at 28 days increased by 3.08%, 6.68%, 10.1%, 11.9% and 13.12% in G20, G40, G60, G80, and G100 mix, respectively. The increase in the compressive strength can be ascribed to the high crushing strength and more angularity of granite aggregates, which enhanced the mechanical interlock, thus contributing to better load transfer capacity, leading to higher compressive strength of the concrete mix. Also, the rough surface texture of granite contributes to improved adhesion with the cementitious matrix and leading to higher strength under compression. So, at all curing ages of the granite mixes, the mix designation G100 gave the maximum compressive strength.

When comparing both aggregate type mix series, granite-based mixes consistently exhibited higher compressive strength than limestone aggregate mixes when compared at the same replacement levels at all curing ages of 7, 28, and 90 days. In the case of granite concrete, the granite aggregates, due to their higher angularity, lower crushing strength, and rougher surface texture, in contrast to the limestone aggregates, contribute to the strength primarily due to effective mechanical interlocking, which resist higher loading, thereby enhancing the compressive strength of the granite concrete mixes.

Among all the mixes, the granite aggregates concrete at 100% replacement, i.e, G100 mix, exhibited the highest strength, and in the case of limestone mixes, L100 demonstrated the highest strength at all curing ages.

4.3.2 Compressive strength of mixes incorporating Silica sand and Quarry Sand

In the second phase of the experimental work, which was extended to understanding the effect of the Silica sand (SS) and Quarry Sand (QS) on the properties of the HSC. Various mix combinations of the concrete were made using the best mixes of limestone L100 and granite G100 series obtained from phase 1 of the experimental work.

4.2.2.1 Effect of Silica Sand on the Compressive Strength

In this Second phase, the effect of silica sand (SS) as a fine aggregate on various concrete mixes with limestone and granite coarse aggregates is studied. Test results for the various concrete mixes containing limestone and granite aggregates are shown in Fig. 30.

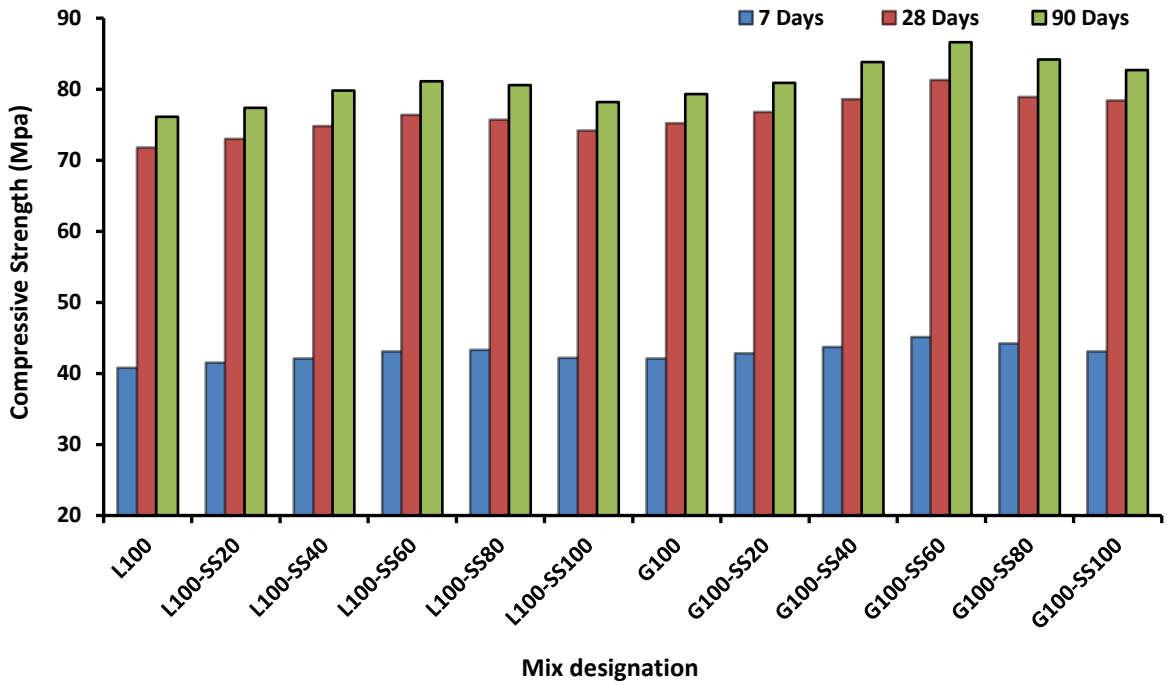

Figure 32: Variation in compressive strength of granite and Limestone mixes due to Silica sand (SS)

Compressive strength results obtained for the silica sand mixes as shown in Fig. 30 demonstrate a consistent enhancement in strength for both limestone based (L100-SS) and granite based (G100-SS) concrete up to a replacement level of

about 60%, beyond which a marginal decline is observed. In depth analysis of the test results also indicate that the magnitude of strength enhancement is slightly higher in case of granite blend mixes, which may be due to the inherently superior mechanical properties of granite aggregates.

For the Linestone Silica Sand (L100-SS) series, there is an increase in compressive strength from L100-SS20 to L100-SS60 across all curing ages, i.e, 7, 28, and 90 days. For instance, at 28 days of testing, strength enhancement ranged from 1.67% to 6.4%, with the highest rise seen at 60% replacement. Similarly, the trend of an increase in compressive strength was also recorded at 90 days of curing age, where strength increased from 79.3MPa to 86.6MPa. Such behaviour of strength can be attributed to the uniform particle size, high silica content, and angular morphology of the silica sand, which collectively contributed to efficient packing, densifying the microstructure and strengthening, due to the formation of CSH gel. As the replacement approaches the 80-100 % level, however, a slight reduction in compressive strength occurs. This may be due to the reason that at higher replacement levels, fineness of the silica sand begins to increase the overall surface area of the fine aggregate system, demanding slightly more paste for hydration. When this demand is unmet, localised paste deficiency and micro-porosity formation can weaken the cementitious, resulting in the observed strength drop.

In the case of Granite Silica sand mixes, an almost similar trend up to 60% replacement, but with higher compressive strength values than corresponding L100-SS mixes. For instance, at 28 days, in the case of granite mixes, strength at a 60% replacement level was 81.3 MPa, whereas, at the same replacement percentage, the strength observed was 76.4 MPa, which was nearly 6.41% higher than limestone mixes. Such an improvement may be attributed to the higher crushing strength, lower water absorption, and a sharper angular geometry of granite aggregates compared to limestone, which enhances mechanical interlock and reduces the likelihood micro-cracking. In the case of granite mixes, the highest strength was noticed in the G100-SS60 mix at all curing ages, with the highest strength reaching 81.3 MPa and 86.6 MPa at 28 and 90 days of curing.

Overall, the strength enhancement ranged from 2.12% to 8.11% at 90 days till 60% replacement, which may be the outcome of SS, which, due to their fine size and presence of higher silicon dioxide, occupy smaller voids and promote hydration, by generating additional CSH, thus contributes by strengthening the concrete. Beyond 60% replacement, the G-SS80 and G-SS100 mixes display a mild reduction in strength. Similar to the behaviour in the limestone mixes, the high volume of fine silica particles can disrupt the optimum aggregate grading, leading to excessive fines, reduced internal friction between particles, and higher water or paste demand.

A comparison between the two series demonstrates that the influence of SS in terms of strength is more pronounced when paired with stronger coarse aggregates. At 28 days, in case of limestone mixes, the strength increased by 1.67%, 4.5%, 8.11%, 4.92% and 4.2%, whereas in case of granite mixes strength increased by 2.12%, 4.52%, 8.11%, 5.91% and 2.75%, at 20%, 40%, 60%, 80% and 100% replacement level. Such strength trends clearly indicate in the case of, SS acts as a strength contributor by enhancing efficient packing and microstructural densification of the matrix.

Overall, in the case of granite and limestone mixes, G100-S60 and L100-SS60 gave the highest compressive strength at various replacement levels of the SS, which suggests that SS benefits the strength enhancement when used with granite and limestone aggregates.

4.4 Effect of Quarry Sand on the Compressive Strength

The variation in compressive strength for the QS modified concrete mixes at 7, 28, and 90 days is presented in Fig.31 for both limestone and granite-based concretes. Figure 32 shows the test results for different mix designations.

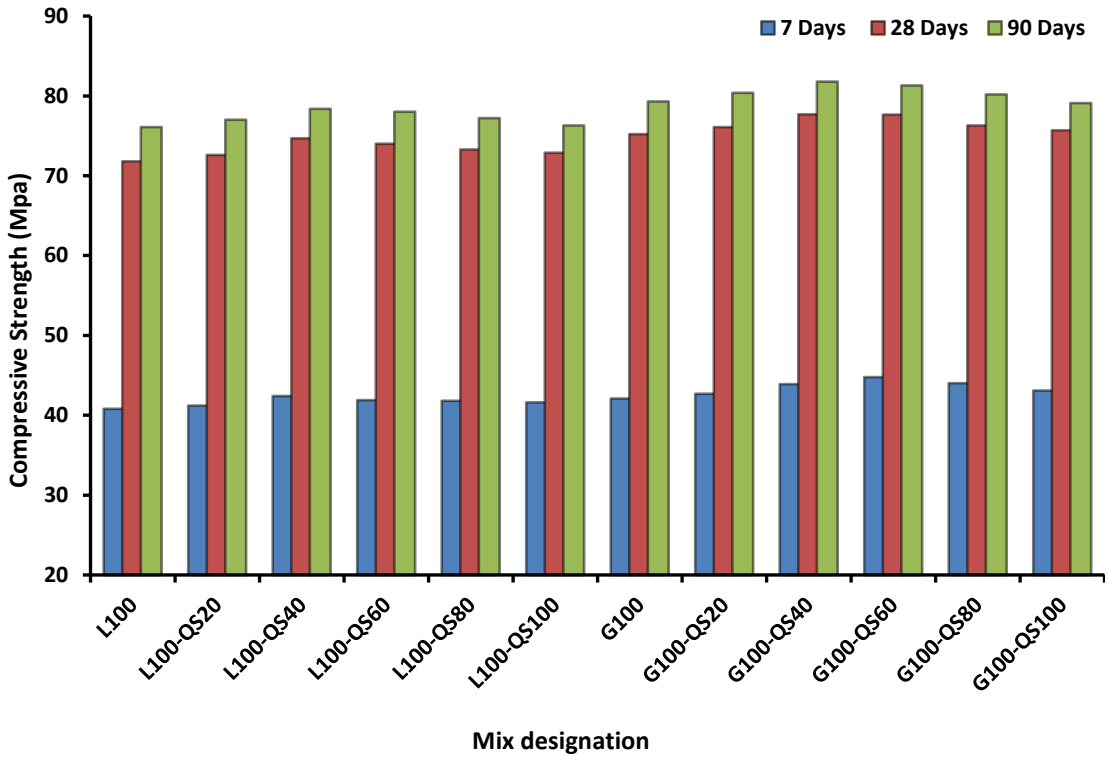

Figure 33: Variation in compressive strength of granite and Limestone mixes due to Quarry sand (QS)

In the limestone-based mixes, with the increase in replacement percentage of QS, the compressive strength of the mixes increases, and this strength increment goes up to about 40% replacement, with the highest peak value of strength demonstrated by the L100-QS40 mix (i.e, 74.7MPa at 28 days and 78.4MPa at 90 days), which marks the maximum strength improvement at 40% QS level by 4.03%. Such an improvement due to QS may be due to the micro-filler effect of quarry dust, wherein the presence of ultra-fine particles helps to refine the pore structure and reduce capillary voids within the cementitious matrix. Several previous studies also highlight that high fines improve packing density of the mix[120].Moreover, the higher angularity of the QS particles enhances mechanical interlocking within the matrix, thereby contributing to the strength of concrete, even at the early days, as mix L100-QS40 (strength 42.4 MPa) relative to the control mix L100 (strength 40.8 MPa), suggests improved early hydration, which may be due to the extra nucleation sites provided by fine QS. However,

beyond the mix L100-QS40, strength decreased with the increase in the replacement of QS, the compressive strength trend shows a slight decline in strength, which may be due to the presence of excess fines of QS, which increases the overall water demand, under a constant w/b ratio, leading to a decline in strength. As a result, mixes such as L100-QS80 and L100-QS100 display only marginal improvements over the control and show no further strength gain beyond the mix L100-QS40.

In granite mixes, the increment in the QS proportion enhanced the strength of the mixes up to a replacement percentage of 40% QS, and afterwards, replacement with the QS diminished the strength. but the magnitude of strength is consistently higher than their limestone counterparts. For instance, the 28-day strength increases from 75.2 MPa (G100-QS0) to a peak of 77.7 MPa at G100-QS40, with the 90-day strength also maximising to 81.8 MPa.The improvement in G100-QS mixes up to 40% can again be attributed to the filler effect and improved packing due to the finer particles of QS, but the gains are more pronounced than in L-QS because the mechanically stronger and rougher textures of granite aggregates provide superior confinement to the fine and angular particles of QS, leading to the stronger cementitious matrix, which contributes to the incremented strength in case of G100-QS mixes in comparison to the L100-QS concrete mixes. At higher replacement levels of QS in Granite mixes, i.e, beyond 60%, L-QS60 to L-QS100, the strength begins to slightly decline with the increasing replacement percentage. For instance, at 28 days of curing, the strength magnitude reduced from 77.6 MPa to 75.7 MPa, leading to a slight loss of 2.54%, which restricts the use of QS beyond a 40% replacement level. Such a reduction can be attributed to the presence of excessive microfines in QS, leading to marginal loss. Although the decline is modest, the reduction at G100-QS60 to G100-QS100 reflects the limit beyond which QS no longer contributes positively to the matrix structure of concrete. Thus, in a series of granite mixes with QS, mix G100-QS40 gives the highest compressive strength.

4.5 Split Tensile Strength

The split tensile strength results provide an understanding of the behaviour of the concrete under indirect tensile loading. Use of different types of coarse and fine aggregates affects the splitting tensile strength of the HSC, and the results have been discussed in detail.

4.5.1 Split Tensile Strength using Limestone and Granite coarse aggregates

Test results of the Splitting tensile strength of the HSC using various percentages of limestone and granite aggregates are shown in Figure 32.

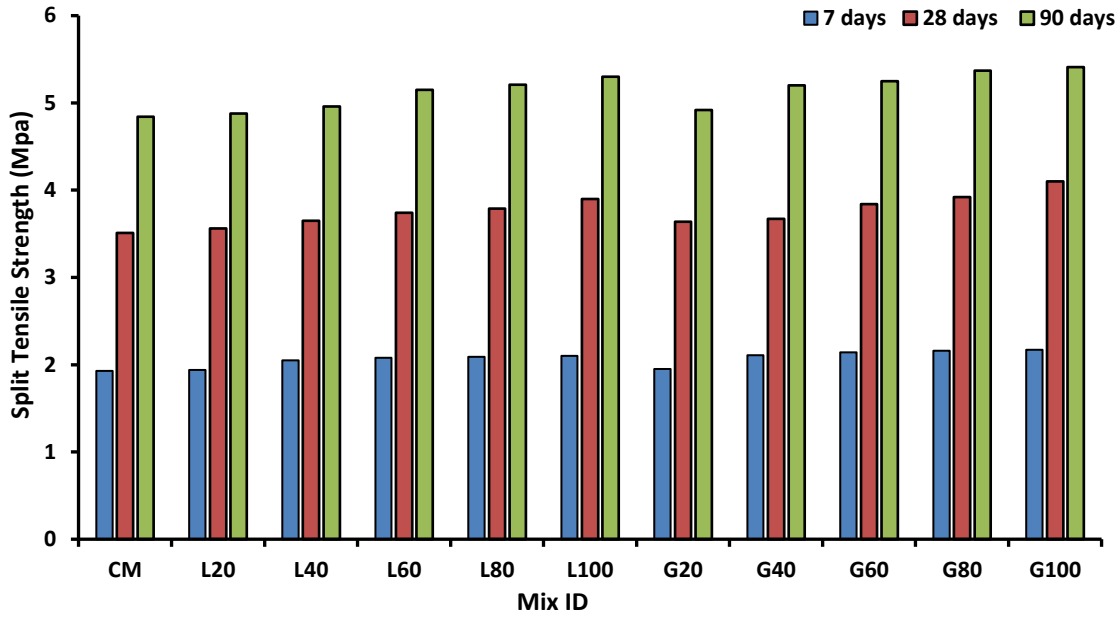

Figure 34: Split Tensile Strength of concrete mixes using limestone and granite aggregates

Test results of Fig. 32 demonstrate that L-series mixes show a progressive rise in split-tensile strength as the proportion of limestone coarse aggregate increases from 20% to 100%. For instance, at 28 days, the values increase from 3.56 MPa (L20) to 3.87 MPa (L100), while the 90-day strength ranges from 4.88 MPa to 5.30 MPa. Increment in the splitting tensile strength using limestone aggregates can be attributed to the higher angularity and lower crushing strength, which contributed towards the stronger comentitius matrix, as when tensile loads are applied in concrete, the aggregates attempted to separate from one another; under

such circumstances interfacial transition zone must bear tension stresses to maintain the integrity of the concrete mixes.Test results of the splitting tensile strength also indicated that the strength increment at 7 days of curing was less, which ranged from 0.55% to 8.8%, which was a bit less in contrast to the strength increment at 28 days, whose value lies in the range of 1.4% to 11.1%, which may be due to the fact that early-age tensile capacity is ruled by the cement paste matrix, with only a limited contribution from the aggregate paste interface. Also, at higher ages of curing, the matrix forms a better bond with the rough-textured limestone aggregates, thus significantly contributing towards the strength enhancement at 28 days as compared to 7 days of curing.

Test outcomes of the G-series of concrete mixes show an enhancement in the splitting tensile strength with the increment in the replacement percentage of the natural coarse aggregates. Specifically, at 7 days of testing, the tensile strength increased by 1.03%, 9.32%, 10.8%, 11.95 and 12.4% at 20%, 40%, 60%, 80% and 100% replacement by natural aggregates, respectively. Similarly, at 28 days of curing strength enlarged by 3.70 %, 4.55 %, 9.40 %, 11.68 %, and 16.80 % at 20%, 40%,60%, 80% and 100% replacement, respectively. Such a strength increase in the split-tensile strength with rising granite content can be attributed to the better physico-mechanical properties of the granite aggregates, which, due to their higher anulairty and more surface roughness, provided better mechanical interlocking, imparting more mechanical strength to the granite concrete mixes. Additionally, the another factor responsible for uplifting the split tensile strength is the angularity and rough surface texture of the granite aggregates, which made effective bond with the matrix of cementitious materials, thus provoking strength.

On the comparison of various mixes made using limestone and granite aggregates, it is clear from Figure 33 that the granite series mixes have higher split-tensile strength than their Limestone counterparts at all ages. The strength difference is more at higher replacement percentages, i.e from 60% to 100%, where the tensile strength is enhanced in the range of 6 to 10% for granite mixes as compared to limestone mixes. Such a trend of strength is due to the established understanding that in mixes prepared using a low water binder ratio, the benefits are more specifically from the aggregates, which play a vital role in strength contribution.

Granite aggregates used in the concrete mixes possess low crushing strength, abrasion value, rough surface texture and higher angularity, in contrast to the limestone aggregates, which may promote higher frictional resistance at the aggregate paste interface and better mechanical interlocking, resulting in higher tensile strength.

4.5.2 Split Tensile strength using Quarry Sand

To understand the effect of the QS on the Splitting tensile concrete, various granite and limestone-based concrete mixes were tested at different curing ages of 7, 28 and 90 days. Results of the split tensile strength for various mixes are presented in Fig.33.

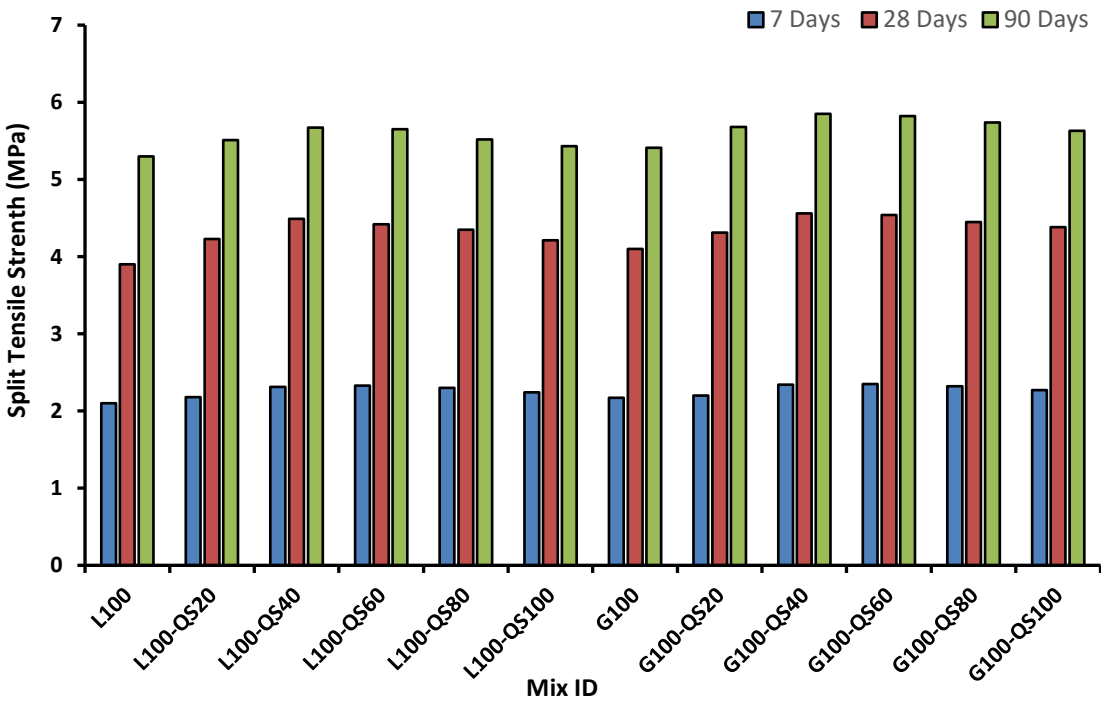

Figure 35: Variation of Split tensile strength in limestone and granite mixes due to quarry sand (QS)

Test results of the split tensile strength indicated that an improvement can be seen in Limestone quarry sand (L100-QS) series up to a replacement level of 40%. At 7 days of curing age, tensile strength increased from 2.10 MPa (L100-QS0) to 2.31 MPa (L100-QS40), representing an enhancement of 10%. Similarly, at the age of 28 days, tensile strength was enhanced from 3.90 MPa to 4.49 MPa, denoting an

increase of nearly 15.1%. Such an increase in the tensile strength can be primarily attributed to the higher angularity and rough surface texture of quarry sand, which promotes the development of better particle interlocking and friction within the mortar matrix. Literature reports also confirm that the sharper edged and irregular geometry of QS promotes better mechanical interlocking, thus resisting the tensile stresses up to a higher limit as compared to natural river aggregates.[121], [122] Test results beyond 40% replacement level by QS indicated a marginal reduction in tensile strength, specifically at 80 to 100% QS replacement. Such a reduction may be linked to the higher fines content and increased water demand associated with QS, which hinders the uniform dispersion and hydration of the cementitious material, thereby minimising the bond strength. Overall, the mix designation L100-QS40 demonstrated the maximum splitting tensile strength across all the curing ages in the limestone series of mixes.

Granite based mixes with the quarry sand (QS) demonstrated a similar trend in strength enhancement, with the strength incrementing up to 40% QS replacement level. Precisely, test results at 28 days demonstrated that splitting tensile strength increased from 4.10 MPa (G100-QS0) to 4.56 MPa (G100-QS40), and the 90-day strength went up from 5.41 MPa to 5.85 MPa, which may be due to the sharp, angular and rough texture of the QS particles, enhancing the tensile strength of concrete by better interlocking. Further, observations indicated that till 40% level of replacement, the tensile strength improvement is more evident in the granite series of mixes, when compared with the limestone series of mixes, which may be linked to the higher crushing strength, hardness, and lower porosity of granite coarse aggregates. Furthermore, replacement by the quarry sand (QS) beyond 40% indicated a decline in the splitting tensile strength of the granite-based QS mixes. Reduction in the strength beyond 40% can be attributed to the overpresence of fine particles of QS, which may remain unhydrated, leading to a diminishing in the strength of mixes. Insights of the test results indicated that even with the reduction of the strength at higher replacement levels of QS, granite mixes still retained higher tensile strength than limestone mixes.

On comparing the limestone and granite series of mixes, the test results of the splitting tensile strength indicated that granite concrete mixes resulted in higher

split tensile strength at corresponding QS replacement levels. This behaviour reflects the difference in the mechanical properties of the two aggregates, as Granite aggregates used have higher specific gravity, greater hardness, and superior crushing strength, leading to better strength of the high-strength mixes. Overall, both series show a highest strength around 40% QS replacement, demonstrating the tensile strength improvement, whereas excessive QS levels diminished the strength of mixes.

4.5.3 Split Tensile Strength using Silica Sand (SS)

In this section, the test results of the splitting tensile strength of various mixes of limestone and granite, to understand the effect of Silica sand (SS) on these mixes, are explained below.

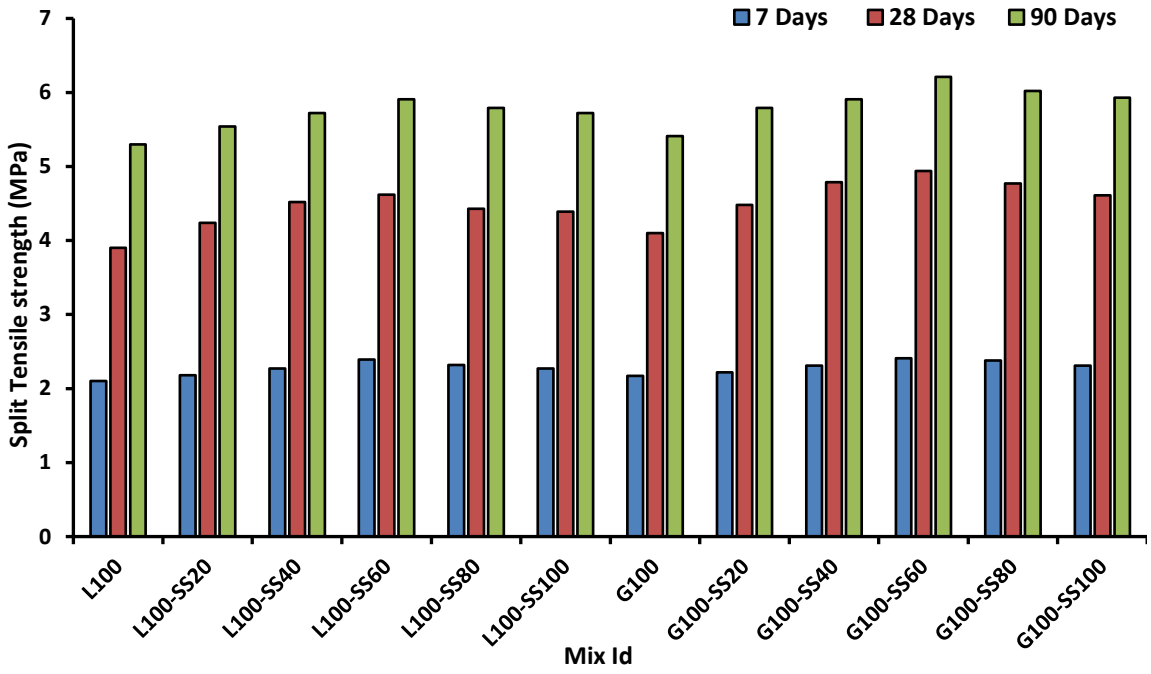

Figure 36: Variation of split-tensile strength with Silica sand (SS) replacement in limestone and granite mixes at 7, 28, and 90 days

Test results shown in Fig.34 indicate that the splitting tensile strength of the concrete increases with the increment in the replacement percentage of the natural sand with the Silica sand (SS) up to a replacement percentage of 60% in both granite and limestone-based concrete mixes. In case of limestone-based concrete mixes having different percentages of Silica sand (SS), tensile strength gains up

by 4.52% ,7.92% and 11.5 % at 20%, 40% and 60% replacement by Silica sand (SS). Similarly, strength increment can be seen at 90 days of curing age, which may be primarily due to the improvised particle packing by the fine silica sand particles. SS due to its fineness and high silica content, improves the better packing by densification of the matrix, which contributes to the strength of the concrete mixes.Test results indicate that the tensile strength reduced beyond 60% replacement, as test values clarify that the strength dropped down from 5.91 Mpa (L100-SS60) to 5.81 Mpa (L100-SS80) and 5.72 Mpa (L-SS100), which may be attributed to the increased surface area (due to increased SS content), raising the localised demand for water for hydration, leading to paste starvation and weaker matrix, which contributed negatively by diminishing strength at higher replacement levels.

In case of granite series of mixes, with the different replacement percentages of SS, outcomes of the test reflect that tensile strength of the concrete mixes enhances due to the use of SS up to 60% replacement level in high-strength mixes. Specifically at 28 days, the strength incremented by 9%, 16.8% and 20.4% at 20%, 40% and 60% replacement by the SS. Similar, trend of strength enhancement was seen at 90 days of curing age. Such enhancement by silica sand is due to the refined packing, due to the small particle size, as compared to the natural fine aggregates, and providing additional nucleation sites, which supported increased pozzolanic reaction, leading to increased tensile strength. Another, observation of the test results denotes that the pronounced strength gains are observed at 9a days, which may be attributed to the synergic effect of the SS and the continued binder hydration[50][123].Test results also indicated that the benefits due to SS are effective up to a replacement level of 60%, where the positive packing and matrix refinement outweigh the negatives of increased surface area, leading to incomplete hydration, decreasing the strength of concrete mixes beyond 60% replacement level.

Strength results using silica sand with the granite and limestone series of mixes also depict that the strength enhancement due to SS is more in the case of granite mixes in contrast to all counter mixes of the limestone series. This can be ascribed to the granite aggregates higher strength, angularity, rough texture and better

physico-mechanical properties in contrast with the limestone aggregates, which provide a stronger skeleton for the HSC, thereby contributing to the higher tensile strength. Out of the limestone series of mixes with SS, the mix L100-SS60 gave the highest strength, and a comparative analysis of the different mixes of the limestone and granite with the SS outcome that mix G100-SS60 outperformed all the mixes in terms of tensile strength.

4.6 Flexural Strength

Various concrete mixes formulated using limestone and granite aggregates as coarse aggregates and SS and QS as fine aggregates were tested for the Flexural strength, and test results obtained are discussed in the following sections.

4.6.1 Flexural strength using Limestone and granite aggregates

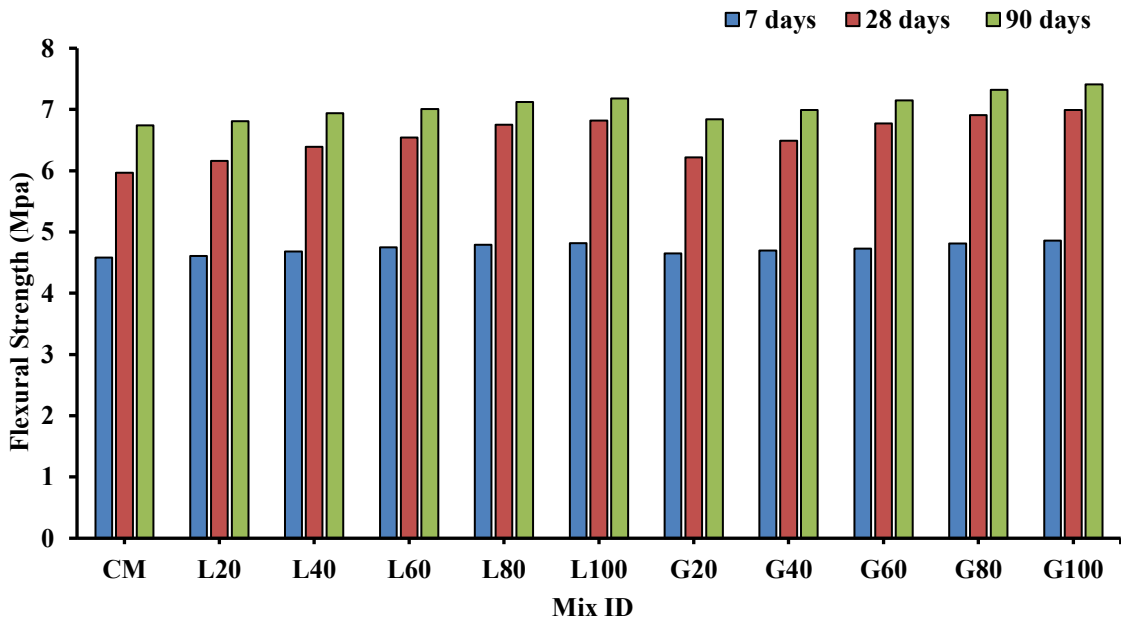

Figure 37: Variation of the flexural strength of the high-strength concrete using limestone and granite aggregates at 7, 28 and 90 days.

Flexural strength results, as demonstrated in Figure 35, indicate steady but consistent improvement as the quantity of limestone aggregates increased. On comparison with the control mix, the overall improvement in the limestone mixes ranged between 3.1% to 14.2% with the increase in the replacement level from

20% to 100%. More specifically, the flexural strength was boosted by 3.18%, 7.03%, 9.54%, 13.0% and 14.2% at 20%, 40%, 60%, 80% and 100% replacement, respectively by limestone aggregates. Similar, trend of strength enhancement was observed at 90 days, with the strength increment range lying between 2% to 6% as compared to the control concrete made using natural aggregates. Such surge in the strength of the HSC mixes by the enhanced physico mechanical limestone aggregates as compared to the natural coarse aggregates. In the limestone series of mixes, strength increased up to complete replacement, with the highest strength demonstrated by the L100 mix, out of the limestone series.

In case of granite-based mixes, flexural strength also exhibited better response, as the strength increased gradually from G20 to G100 mix, with the G100 mix showing a heightening of nearly 16.9% at 28 days and approximately 9.1% at 90 days comparative to the control HSC. More precisely, at the curing age of 28 days, flexural strength incremented by 4.18%, 8.7%, 13.4%, 15.7% and 16.9% at 20%, 40%, 60%, 80% and 100% replacement, respectively, by granite aggregates. Likewise, trend of strength was seen at 90 days, with the strength boosted by 1.58%, 3.7%, 6.08%, 8.16% and 9.19% at 20%, 40%, 60%, 80% and 100% replacement, respectively, by granite aggregates. Such an strength enhancement due to the granite aggregates may be attributed to their angular shape, rough texture and more toughness, which enhanced the mechanical interlocking, thereby improving the crack binding capabilities, especially in HSC, as a result bending initiated cracks absorb higher stress to propagate, leading to superior flexural strength.

Test results clearly distinct that though both limestone and granite aggregates upgraded flexural strength with increasing replacement levels, the percentage of improvement was higher for the granite mixes, due to strong and hard granite aggregates when compared with the limestone coarse aggregates. Results indicated that flexural strength of G100 (7.41 MPa) was a bit higher than that of L100 (7.18 MPa), supporting the role of coarse aggregate in better mechanical performance of the HSC.

4.6.2 Flexural strength incorporating Quarry Sand

In this stage of the work, the flexural strength of the various concrete mixes was examined after replacing natural river sand with diverse proportions of QS. Since the L100 and G100 concrete mixes resulted in the highest flexural capacity in the first phase, these were selected further for understanding the effect of QS. Test results of the mixes using QS are discussed below.

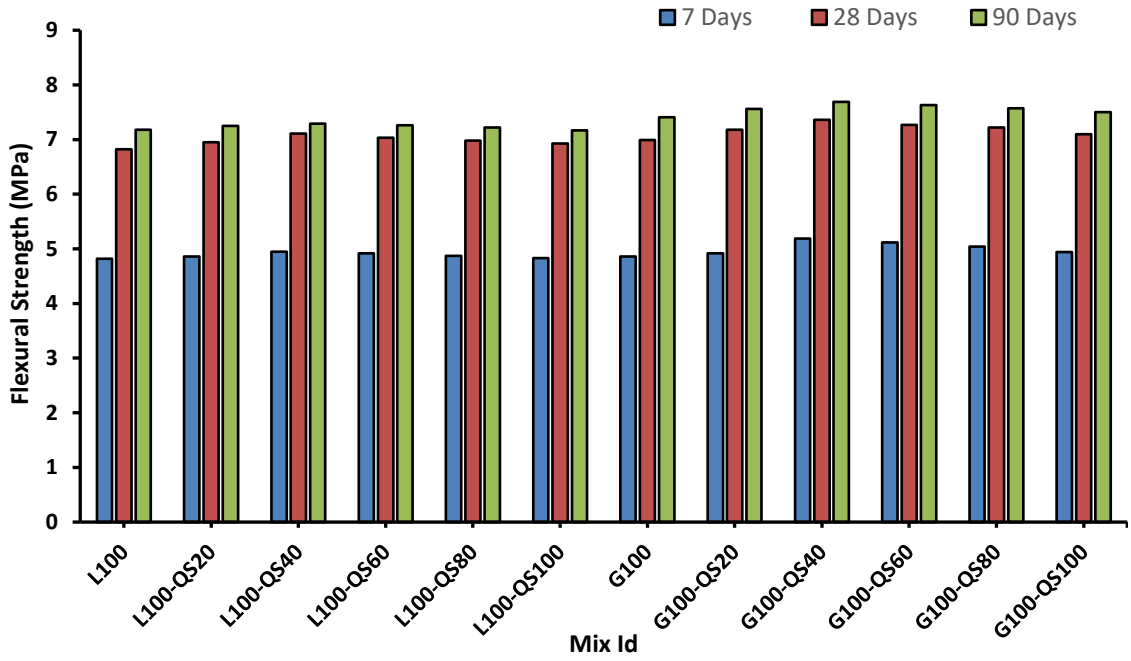

Figure 38: Variation of Flexural Strength at 7,28, and 56 days using different proportions of QS

Flexural behaviour of the mixes containing QS presented a clear and gradual improvement at lower percentages of replacement, and followed by reductions as the QS content incremented towards 100% replacement level. In case of mixes made using limestone-based concretes, flexural strength at the age of 28 days augmented from 6.82 MPa (L100-QS0) to 7.11 MPa (L100-QS40), corresponding to an improvement ranging from nearly 1.9% to 4.25 % over the control mix. A similar, pattern was recorded at a later age, i.e 90 days of curing, where the strength increased from 7.18 MPa to 7.29 MPa at the same replacement level of QS. Such improvements in the flexural strength by the QS can be ascribed to the angularity and rough surface texture of QS particles, which supported better anchorage within the cement matrix. Beyond, replacement of 40% the L100-QS

mixes exhibited a marginal reduction in flexural strength which may likely due to the excessive fines content present in QS, which tends to increase the water demand. Reduced availability of water in HSC due to a low water binder ratio in mix, creates weak zones, which lead to a reduction in the strength of mixes at higher replacement level by the QS. So, higher replacement percentages of QS do not outcome the strength gains as achieved at the intermediate levels.

Various granite-based mixes followed a similar trend, with the strength incrementing up to a replacement percentage of 40%. At 28 days, the mix G100-QS40 marked an approximate improvement of 5.3 % over the reference mix G100-QS0. The 90-day strength peaked by nearly 4% for the same mix, again representing the benefit at 40% QS level. The enhanced strength of such mixes due to QS can be attributed to the angular particles of QS, which, due to their finer sizes, contribute by pore refinement and densification of the matrix, leading to enhanced strength at 40% QS. In other mixes of Limestone, further increasing the QS content beyond 40% led to a reduction in the strength. At 100% replacement, flexural strength at 28 days (7.10 MPa) was still comparable but no longer higher than the peak value (7.69 Mpa). Similar, strength trend of decreasing strength was observed at 90 days, for mixes beyond G100-QS40 (i.e 40% QS level). This reduction is likely to be due to the augmented fines fraction creating localised paste deficient regions, thus reducing the flexural strength of HSC.

At all curing ages, the granite QS (G100-QS) mixes consistently presented higher flexural strength values than the limestone counterparts at identical QS levels. Such pattern line up with the mechanical superior granite aggregates specifically due to their higher crushing strength and toughness, which allows them to contribute to resist flexural stress.

Test results also confirm that QS replacement up to 40% is generally beneficial for flexural performance with both granite and limestone aggregates, while higher replacement provides diminishing returns. Overall, test results represent that out of Limestone mixes, L100-QS40 and out of granite mixes, G100-QS40 gave the highest flexural strength. Also, in all mixes, G-QS40 resulted in the highest flexural strength.

4.6.3 Flexural strength incorporating Silica Sand (SS)

Various mixes of limestone and granite as coarse aggregates were prepared using silica sand (SS) and tested for the flexural strength to understand the effect of the silica sand on various mixes.Test results of the various mixes are presented below.

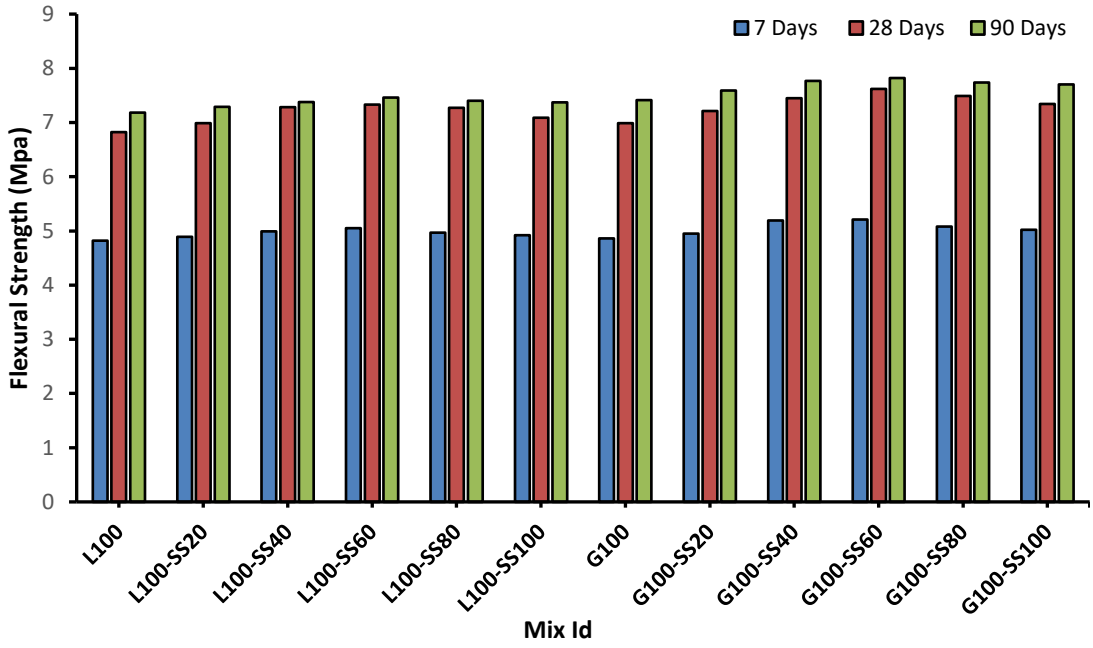

Figure 39: Variation of Flexural Strength at 7,28, and 56 days using different proportions of SS

Test results presented in Figure 37, indicate that replacing river sand with SS increased the flexural resistance up to about 60% level of replacement, after which the gains in strength reduce with further replacement. For the limestone matrix, L100-SS60 recorded the maximum 28 day flexural strength, representing an increase of about **7.5%** over the mix L-SS0.A similar behaviour was seen in the granite series with the G100-SS60 gave the highest peak 28 day value nearly 9% higher than G100-SS0. Test results at 90 day results follow similar pattern of results, signifying that the SS-induced improvements are also develop further with time. This strength increment SS can be ascribed to the efficient micro-filler effect of the finer and predominantly siliceous particles that fill micro-voids in the mortar, thus not only refining the matrix, but also improving the quality of matrix (due to more enhanced hydration), thus contributing to better stress transfer. Use of SS beyond 60% minimises the further benefit to flexural strength of mixes, as

this may be due to the increasing cumulative the fraction of fine silica particles, which incremented the specific surface area of the fine fraction and thereby the paste required to coat particles or promote hydration. Now, with a fixed water binder ratio and increased surface area, there tends to loss in the development of an effective binding matrix, thus leading to which reduces the incremental flexural gains at a replacement level of 80 to 100% SS.

Overall, SS meaningfully enhances flexural capacity when used up to an intermediate replacement 60%, with the effective increment in strength observed when SS is used with a rigid, tough and stronger coarse skeleton, i.e with the granite aggregates. On comparison of the various mixes made using SS with the limestone and granites aggregates, the strength is always seen to be higher in granite aggregate mixes (as same replacement percentage of SS), as compared to the limestone mixes, due to the enhanced physico-mechanical properties of the granite aggregates when compared with the limestone aggregates. . In the series of granite series, the mix designation G100-SS60 gave the highest flexural strength at all ages of curing.

4.7 Durability testing

Durability is a very significant aspect of HSC, as the long-term performance depends not only on the mechanical characteristics but also on its resistance to adverse environmental conditions. The use of different coarse (granite and limestone) and fine aggregates (SS and QS) in the HSC, will modify its durability concerns, which are significant to understand. Therefore, the various mixes are tested for different durability properties, and the test results are discussed as follows.

4.7.1 Water absorption of Silica Sand mixes

Water absorption test, as a part of determining the durability, was tested on various prepared mixes to understand the effect of the aggregates. The test results of the water absorption are discussed as below in Fig 38.

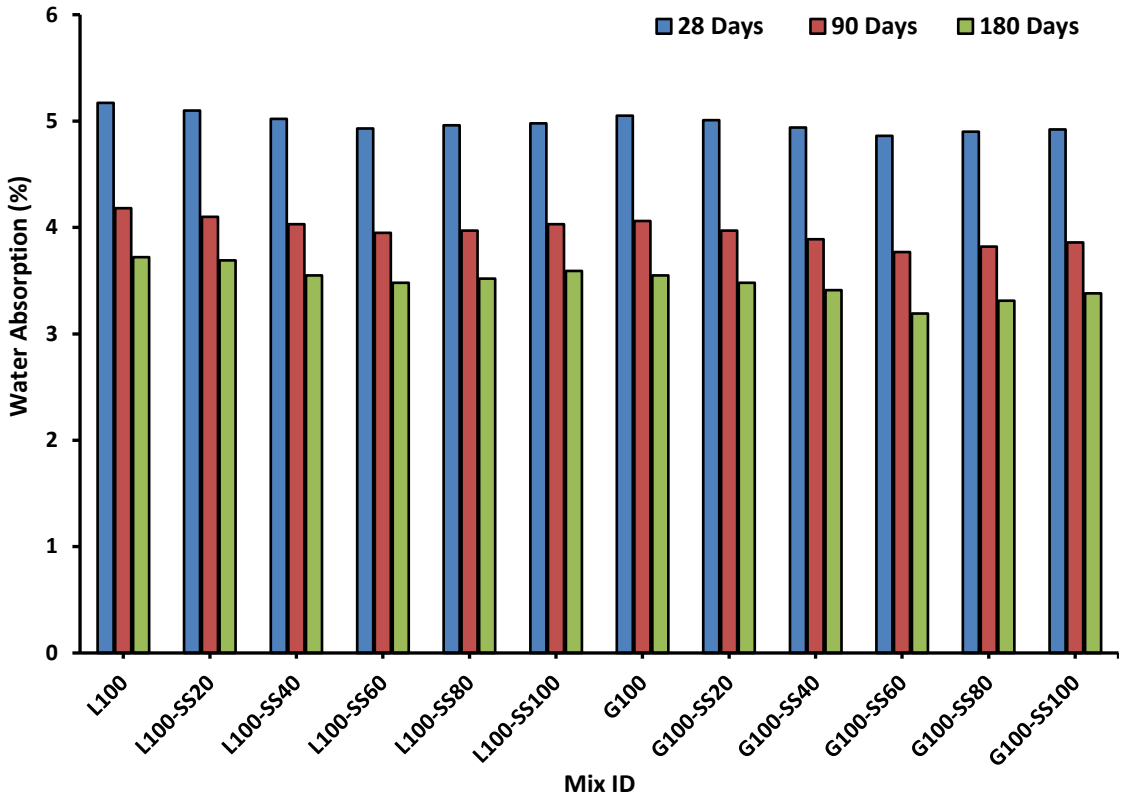

Figure 40: Variation of the water absorption in SS at 28, 90 and 180 days

The water absorption results for Limestone Silica Sand (L100-SS) and Granite Silica Sand (G100-SS) mixes show a reduction both with increasing age and with replacement level of natural river sand by SS. At 7 days, absorption ranges from about 5.17 to 4.86%, while by 90 days it falls to 3.72 to 3.19%, reflecting the increasing pore refinement as with the progression in hydration.

In the series of limestone mixes, absorption of water decreases from L100-SS0 to L100-SS60 at all ages of testing i.e 28, 90 and 180 days. The water absorption values decreased with the increasing age, specifically 180 days of testing of water absorption, value drops to around 3.48 to 3.55%, roughly 6 to 7% lower than their control mix. The granite mixes show an even more distinct and steep decline, with 180-day absorption of water reducing from G100-SS0 to G100-SS60, by a drop of nearly 10.14%. This superior absorption performance may be attributed to the consistent with the denser, stronger and less porous nature of granite aggregates, which helps limit moisture penetration. The enhancement with increasing silica sand content can be linked to its finer, more angular, and particle structure, which

enables better packing and reduces capillary pore connectivity. Studies in previous literature have also noted that silica-rich sands enhance the micro-filling effect and pozzolonic effect to help develop a denser microstructural matrix, thereby reducing the permeable voids. In contrast, natural river sand with its rounded particles cannot achieve the same level of compactness.

Between the two series of coarse aggregates, the granite-based mixes consistently exhibit lower water absorption compared to their limestone counterparts at similar replacement levels. This behaviour may be attributed to the higher density, lower porosity, and stronger aggregate paste interlock associated with rough surfaced granite aggregates. In both series of the mixes, silica sand gave its best performance at 60% replacement and in overall, the mix G100-SS60 gave the lowest water absorption of all the mixes.

4.7.2 Water absorption of Quarry Sand mixes

Various mixes prepared using the different replacement percentages of the QS were tested for the absorption of water and test results are presented as below.

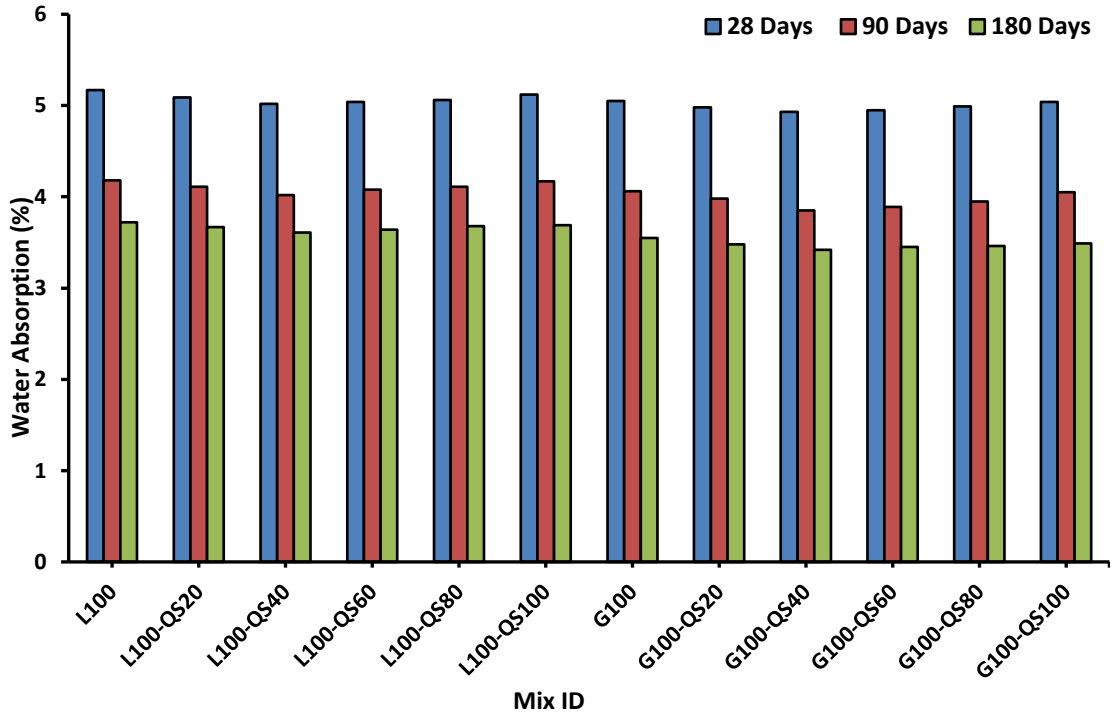

Figure 41:Variation of the water absorption by the QS in different mixes at 28, 90 and 180

The water absorption values for the QS mix show a decrease in the values, with the passing age i.e for a particular mix at any particular replacement percentage, the water absorption was highest at 28 days, decreases at 90 days, and the least value was observed at 180 days. Also, the use of QS presents a noticeable improvement in the water absorption when used up to a moderate replacement percentage, i.e 40%.

In the limestone series, the 28-day values fall from about 5.17% (L100-QS0) to 5.02% (L100-QS40), and the same trend lasts at later ages also, reaching 3.61 to 3.64% at 180 days. The granite mixes follow a similar pattern but with slightly lower values overall; for instance, G100-QS40 records around 4.93% at 28 days and reduces to 3.42% at 180 days. This improvement in water absorption till 40% replacement by the QS can be attributed to the physical nature, i.e., and crushed QS particles, which not only enhance better interlocking, but also minimise the unfilled voids and support enhanced packing, due to the presence of finer fraction in QS, thus leading to a decrease in the absorption capacity. Higher replacement percentages, i.e beyond 40 %, rise in water absorption was noticed due to the increased fines demanding more paste, and allowing very small voids to remain within the matrix, creating space for the capillary water, leading to increased water absorption. The effect is minor but consistent in both aggregate types. Overall, the granite mixes show marginally lower absorption in comparison to the limestone mixes and the best performance is generally observed around the 40% QS level. In both the series of limestone and granite with the Quarry sand, G100-QS40 demonstrated the lower water absorption.

4.8 Rapid Chloride Permeability Test (RCPT)

This test was conducted to evaluate the durability of high strength concrete by measuring its resistance to penetration of the chloride ions, which plays an significant role in initiating the reinforcement corrosion. Such an test gives an indication of the concrete to withstand aggressive chloride environments.

4.8.1 Effect of Silica Sand on Chloride Permeability

In this section, various mixes made using Silica sand (SS) using granite and limestone coarse aggregates were tested for the permeability of the ingress of chloride ions.

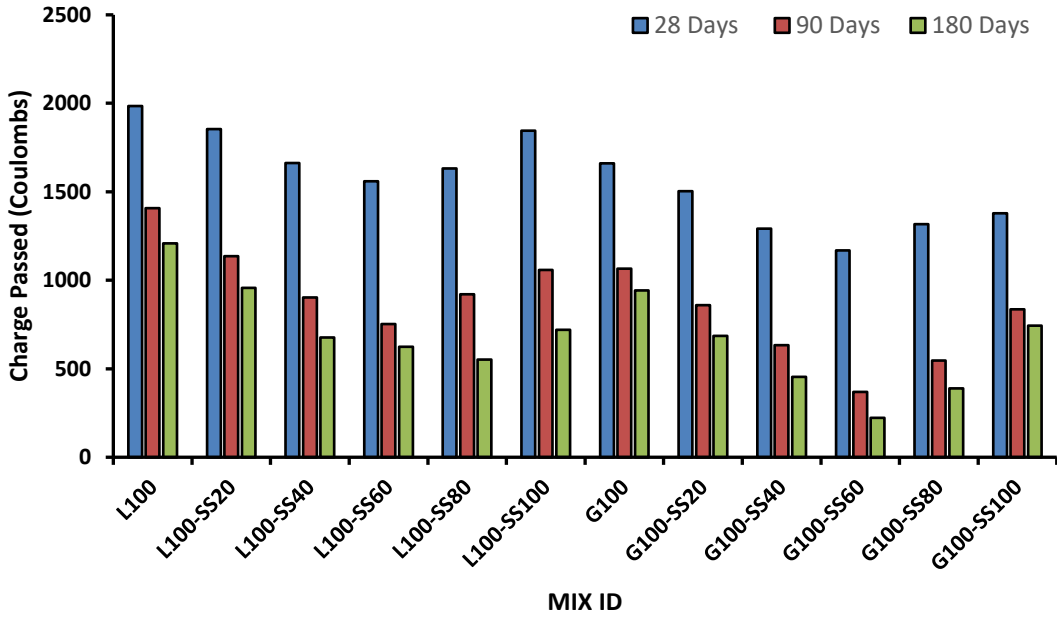

Figure 42: Test results of the charge passed in coulombs in SS mixes at 28, 90 and 180 days

RCPT results presented in Fig. 40 show that there is a constant reduction in charge passed (in Coulombs) as the percentage of SS increases, up to the 60% replacement level of SS. In the limestone series of mixes, for instance, the 28-day charge drops from about 1985 Coulombs (L100) to nearly 1560 Coulombs (L100-SS60), while the 180-day charge falls from 1208 Coulombs to 624 Coulombs over the same range of mixes. An almost similar pattern was noticed in the granite mixes, where G100 reduces from approximately 1660 Coulombs to 1168 Coulombs at 28 days, and the charge passed reaches as low as 222 C for G100-SS60 at 180 days. Such a reduction in the charge passed can be accounted for by the finer and highly angular SS particles, which fill the voids more effectively as compared to the natural river sand, thus lowering the connectivity of capillary pores. Also, the denser packing, due to the finer SS, may have restricted the movement of chloride ions, thus reflected in the form of reduced charge passed.

Test results also indicate that beyond the 60% level of replacement, a rise in charge passed is observed in both granite and limestone mix series. This mild increase may have occurred when the proportion of very fine SS particles becomes high enough to increase the water demand, thus leaving a few micro voids in the matrix, thereby increasing the charge passed.

On comparing the two aggregate types of mix series, i.e., granite and limestone series, the granite mixes consistently show lower permeability at comparable SS levels. This aligns with the less porous and denser structure of granite aggregates in comparison to limestone aggregates, which restricted the ease of ion penetration, thus lowering the charge passed. Overall, out of the limestone and granite series of mixes, the highest resistance to chloride penetration was demonstrated by G100-SS60.

4.8.2 Effect of Quarry Sand (QS) on Chloride Permeability

In this section, various mixes made using Quarry sand (QS) using granite and limestone coarse aggregates were tested for the permeability of the ingress of chloride ions.

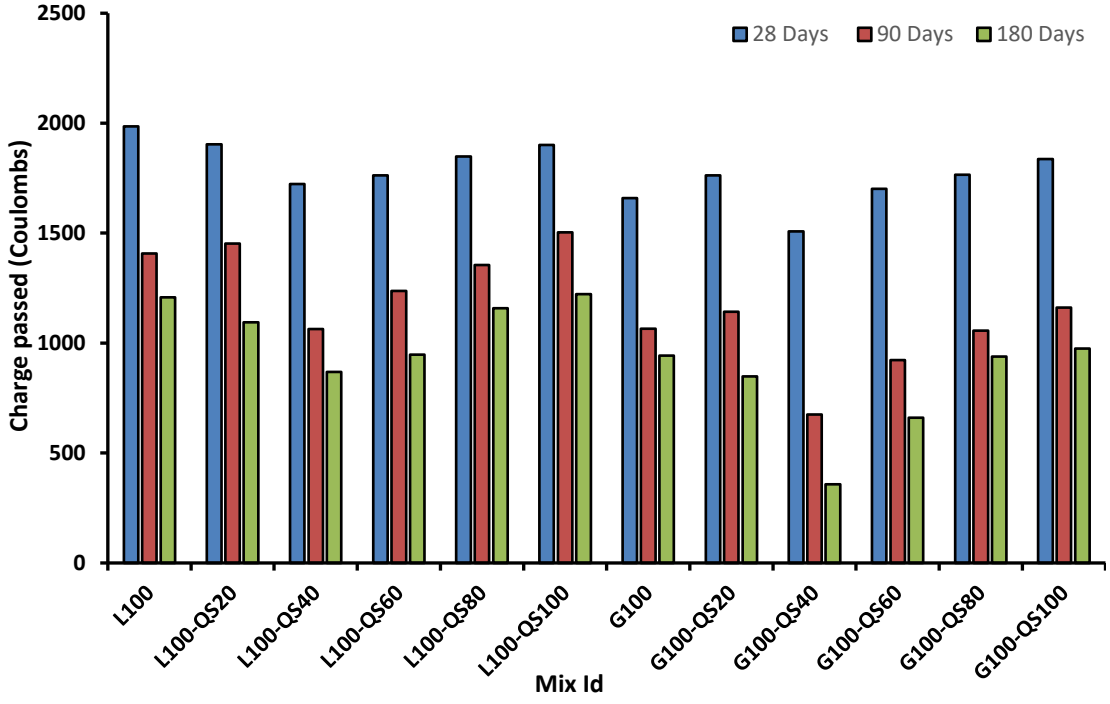

Figure 43: Test results of the Charge passed in coulombs for QS mixes at 28, 90 and 180 days

Test results presented in Figure 41 indicate a clear improvement, i.e., a reduction in charge passed up to a replacement level of 40% QS at all curing ages for both limestone- and granite-based mixes. For instance, in limestone mixes, the 28-day charge passed decreases from 1985 Coulombs in L100-QS0 to 1724 Coulombs in L100-QS40, while at 90 days the value reduces from 1408 Coulombs to 1064 Coulombs, representing a reduction of approximately 24.4%. A similar trend is observed at 180 days, where the charge passed decreases from 1208 Coulombs to 869 Coulombs for the same replacement level.

On comparison with granite-based mixes, a more pronounced improvement is observed, particularly at later ages. For the mix G100-QS40, the charge passed reduces from 1660 Coulombs to 1508 Coulombs at 28 days, while the 90-day value declines from 1065 Coulombs to 675 Coulombs, indicating a substantial reduction of about 36.6%. At 180 days, the reduction is even more significant, with charge passed decreasing from 943 Coulombs to 358 Coulombs, reflecting a marked improvement in resistance to chloride ion penetration.

Such reductions in charge passed can be attributed to the angular and fractured nature of quarry sand particles, which enhance particle interlocking and disrupt continuous pore channels within the concrete matrix. In addition, the micro-fine fraction of QS acts as a filler material, reducing capillary pore connectivity and thereby limiting the movement of chloride ions through the concrete.

However, at higher QS replacement levels beyond 40%, a gradual increase in charge passed is observed at all curing ages for both limestone and granite mixes. This behaviour is associated with the excessive fine content and higher specific surface area of QS, which, under a fixed water-binder ratio, can lead to localized paste deficiency and the formation of micro-voids. These micro-voids increase pore connectivity, facilitating greater chloride ion migration.

It is also evident from the results that granite-based mixes consistently exhibit lower charge passed values than limestone-based mixes at corresponding QS replacement levels. This can be attributed to the lower intrinsic porosity and denser skeletal structure of granite aggregates, which reduce overall transport paths and allow the micro-filler effect of quarry sand to be more effective in improving chloride resistance.

4.9 Abrasion Resistance

Abrasion Resistance of the concrete is a property of concrete giving an idea about the concrete's ability to withstand surface wear caused by the repeated frictional or mechanical action. Resistance to abrasion of concrete was measured in terms of the loss in thickness of specimen.

4.9.1 Effect of Silica Sand on Abrasion Resistance

For understanding the effect of the SS as fine aggregates on the various HSC mixes made using granite and limestone aggregates as coarse aggregates. Various concrete mixes were tested for their abrasion resistance, and the test results are discussed below.

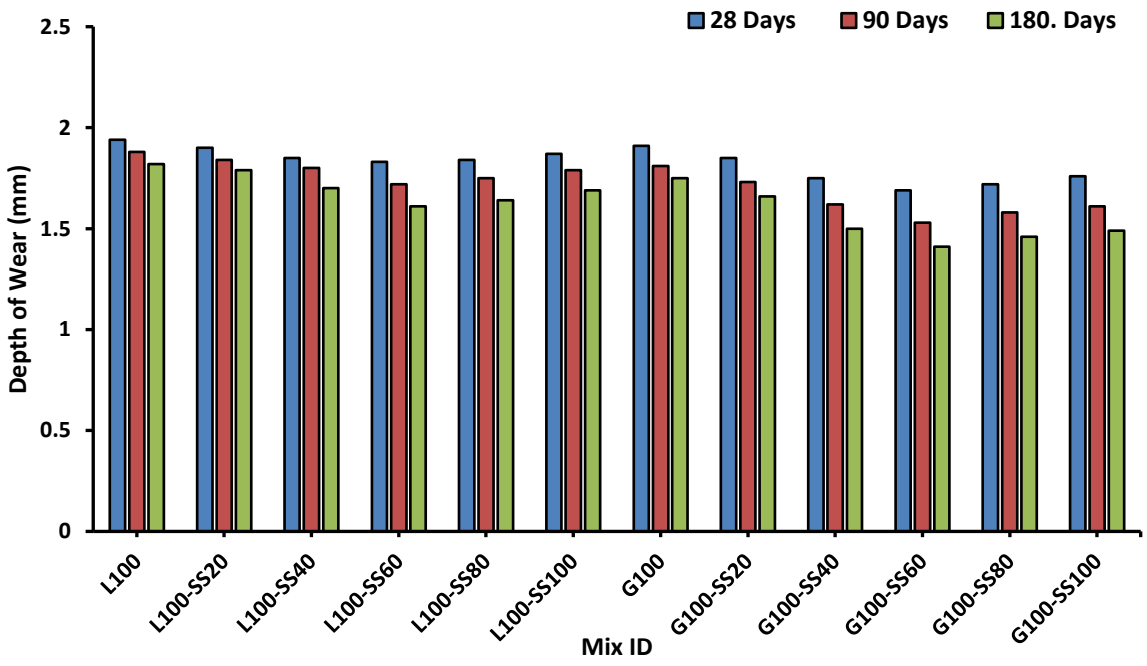

Figure 44: Variation in abrasion resistance (depth of wear) of mixes incorporating SS at 28, 90, and 180 days

The variation in abrasion resistance for different proportions of SS is presented in Figure 42. The depth of wear consistently decreased with age for all mixes, i.e., 28, 90 and 180 days, reflecting the strength gain and densification of the cementitious matrix over time.

For the limestone-based concretes (L100-SS series), the depth of wear reduced as the SS content increased up to 60%. For instance, at 28 days, the wear depth

dropped from 1.94 mm (L100-SS0) to 1.83 mm (L100-SS60), demonstrating a reduction of nearly 6%. This improvement can be linked to the finer particle size and angularity of SS particles, which helps fill microvoids around the limestone aggregates and improves the packing density of the mortar phase .For the granite series i.e G100-SS mixes, similar trend was observed but was more pronounced as granite aggregates, being harder with more rougher surface texture, allow the fine and angular SS particles to make a mechanically stronger layer of ITZ, which is harder to undergo wear, thus increasing the abrasion resistance of Granite mixes using SS. At 90 days, the wear depth reduced from 1.81 mm for G100-SS0 to 1.53 mm for G100-SS60, demonstrating the effectiveness of SS, which reduces the wear depth by nearly 15% lower, indicating a more compact and mechanically stronger surface layer, which resists abrasion. This aligns with literature reporting that high-strength mixes comprising hard aggregates having better physico-mechanical properties and finer particles produce denser abrasion-resistant surfaces[114], [124]. In both the series of mixes, replacement by SS above 60% tends to reduce the abrasion resistance of the concrete i.e depth of surface wear increases, which is consistent with the increment in the finer particles, leading to the imbalance in the paste required for hydration, thus causing an increment in the wear depth at higher replacement levels of SS. Overall, on comparison of all the mixes of limestone and granite aggregates, the mix G100-SS60 demonstrated the highest resistance to abrasion with the least value of depth of wear.

4.10 Effect of Quarry Sand on the Abrasion Resistance

For understanding the effect of the QS as fine aggregates on the various HSC mixes made using granite and limestone aggregates as coarse aggregates. Various concrete mixes were tested for their abrasion resistance, and the test results are discussed below.

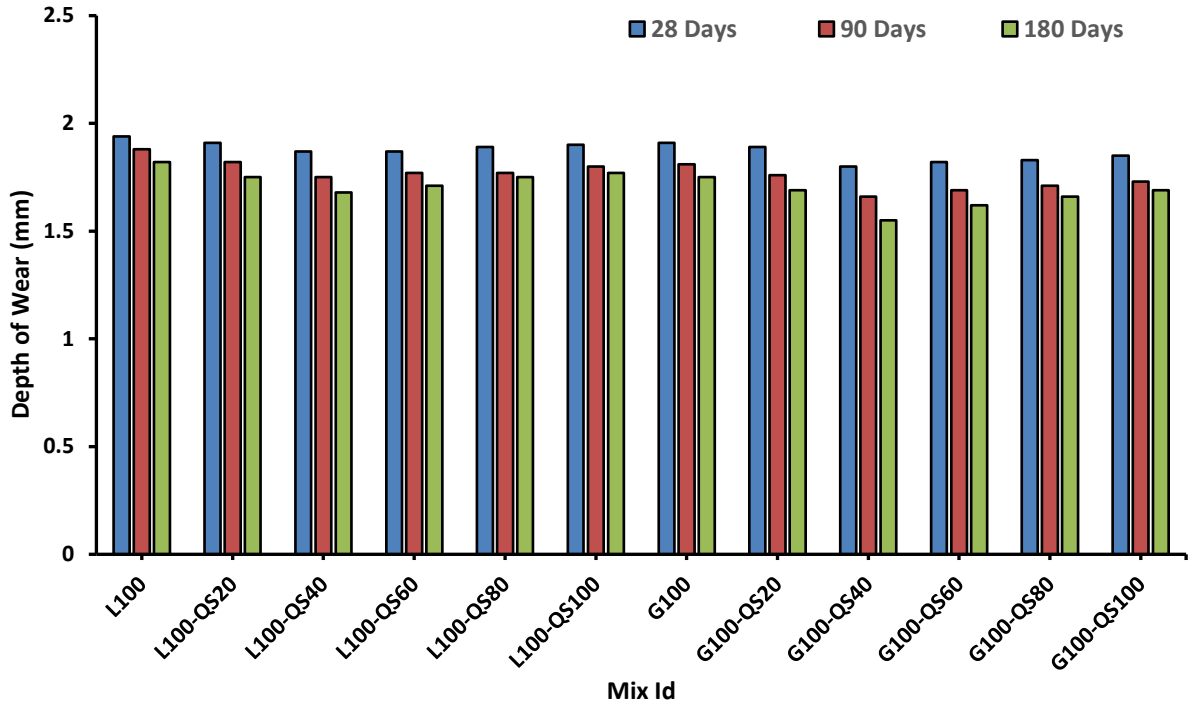

Figure 45: Variation in abrasion resistance (depth of wear) of mixes incorporating QS at 28, 90, and 180 days

From the given Figure 43, a clear trend of reduced depth of wear is noticed with the incorporation of QS, and the improvement becomes more noticeable at later ages. For instance, mix L100-QS40 shows nearly 3.6% to 6.91% lower abrasion loss than L100-QS0 at 28 and 90 days, while G-QS40 records nearly a 5.75% and 8.28 % reduction relative to its control, i.e G-QS0. These improvements align with the denser matrix developed due to the angular and finely graded quarry Sand particles, which tend to pack more efficiently and thus limit the micro voids along the wearing surface.

In the granite mixes, the effect of abrasion resistance seems to be more pronounced up to 40% replacement level of QS at all ages of curing. For instance, at 90 days of curing, the improvement in abrasion resistance at 40% replacement, i.e. for mix G100-QS40, was 8.28 %, while at the same replacement at 180 days, abrasion resistance improved by 11.24%, demonstrating the improvement in abrasion resistance with the curing age.

At higher replacement levels beyond 40%, the improvement in the abrasion resistance decreases due to the excessive fines may slightly increase water

demand and reduce cohesiveness of the surface layer, countering the benefits of formation of stronger layer. Ageing also plays a significant role in both the mixes i.e limestone and granite, as most of the mixes exhibit nearly 6 to 11.24% reduction in depth of wear, indicating the gain in surface hardness due to continuous hydration and gradual refinement of the matrix with the passing time.

Overall, in granite and limestone mixes with different proportions of SS indicate that 40% replacement by QS, provides a best abrasion resistance, specifically in granite mixes, where the synergy between the SS particles and granite aggregates, produced a mix i.e G100-SS40 with the least depth of wear, out of all tested mixes.

4.11 Cost of High Strength Concrete Mixes

The cost study of various mixes was undertaken after completing the mechanical and durability assessment of all the concrete mixes developed using different combinations of coarse (granite and limestone) and fine aggregates (silica sand and quarry sand). In the complete experimental programme, each mix was proportioned by varying either the coarse aggregate type or the fine aggregate replacement, and was further evaluated for compressive, tensile and flexural strengths, accompanied by water absorption, abrasion resistance, and chloride ion permeability.

To maintain clarity throughout the experimental investigation, different types of mixes were grouped into four distinct series based on the coarse and fine aggregate combination adopted.

Series 1 (Limestone Silica Sand): L100-SS20, L100-SS40, L100-SS60, L100-SS80, L100-SS100

Series 2 (Granite Silica Sand): G100-SS20, G100-SS40, G100-SS60, G100-SS80, G100-SS100

Series 3 (Limestone Quarry Sand): L100-QS20, L100-QS40, L100-QS60, L100-QS80, L100-QS100

Series 4 (Granite Quarry Sand): G100-QS20, G100-QS40, G100-QS60, G100-QS80, G100-QS100

The assessment of these series enabled a clear understanding that how different aggregate effects the overall strength and durability performance of concrete. Following the detailed analysis of both mechanical and durability results, one mix from each series was identified as the most efficient performer in its respective category. These selected mixtures **L100-SS60, G100-SS60, L100-QS40, and G100-QS40** represent best HSC options derived from the experimental study.

In accordance with the third objective of the work, the cost assessment was carried out exclusively for these four finalised mixes. This approach ensures that the economic comparison is meaningful and directly aligned with the most technically sound and durable concrete compositions obtained in the study.

For further study of the cost calculation of the selected HSC mixes, the costs of the materials used in the experimental study are recorded. The source rates adopted for each ingredient are presented in Table 21, and these values serve as the basis for determining the total material cost of the selected mixes.

Table 20: Cost of the ingredients at the source

S.No	Material	Material Cost (INR) per unit
1	Ordinary Portland Cement	550 per bag (50 kg)
2	Natural River Sand	Rs 27/cft
3	Natural Coarse Aggregates	Rs 44 /cft
4	Silica Fume	Rs 12/ Kg
5	Metakaolin	Rs 22/ Kg
6	Silica Sand	Rs 46 /cft
7	Quarry Sand	Rs 40 /cft
8	Granite Coarse Aggregates	Rs 53 /cft
9	Limestone coarse aggregates	Rs 49 /cft

To calculate the total cost of the HSC mixes, the material cost, along with the labour charges, was also considered from the practical point of view, so as to get the total cost of the concrete mix.

Table 21: Calculation of Cost of Control Mix (CM)

Item No	Quantity	Unit Cost of Material	Cost of Material (per kg)	Quantity Required	Cost per m^3 (INR)
1	Ordinary Portland Cement	550 per bag (50 kg)	10.4	435	4524
2	Natural River Sand	Rs 27/cft	0.60	459	275.40
3	Natural Coarse Aggregates	Rs 44 /cft	1.02	1236	1260.72
4	Silica Fume	Rs 12/ Kg	12	39.5	474
5	Metakaolin	Rs 22/ Kg	22	52.7	1159.40
6	Silica Sand (SS)	Rs 46 /cft	0.99		0
7	Quarry Sand (QS)	Rs 40 /cft	0.83	0	0
8	Granite Coarse Aggregates	Rs 53 /cft	1.24	0	0
9	Limestone coarse aggregates	Rs 49 /cft	1.09	0	0
Cost of Control Mix (CM)					**Rs 7693.52**

Table 22: Calculation of Cost of mix G100-SS60

Item No	Quantity	Unit Cost of Material	Cost of Material (per kg)	Quantity Required	Cost per m^3 (INR)
1	Ordinary Portland Cement	550 per bag (50 kg)	10.4	435	4524
2	Natural River Sand	Rs 27/cft	0.603	183.6	110.16
3	Natural Coarse Aggregates	Rs 44 /cft	1.02	0	0
4	Silica Fume	Rs 12/ Kg	12	39.5	474
5	Metakaolin	Rs 22/ Kg	22	52.7	1159.4
6	Silica Sand (SS)	Rs 46 /cft	0.99	275.4	272.65
7	Quarry Sand (QS)	Rs 40 /cft	0.83		0
8	Granite Coarse Aggregates	Rs 53 /cft	1.24	1236	1532.64
9	Limestone coarse aggregates	Rs 49 /cft	1.09	0	0
Cost of Mix G100-SS60					**Rs 8072.85**

Table 23: Calculation of Cost of mix G100-QS40

Item No	Quantity	Unit Cost of Material	Cost of Material (per kg)	Quantity Required	Cost per m^3 (INR)
1	Ordinary Portland Cement	550 per bag (50 kg)	10.4	435	4524
2	Natural River Sand	Rs 27/cft	0.603	275.4	165.24
3	Natural Coarse Aggregates	Rs 44 /cft	1.02		0
4	Silica Fume	Rs 12/ Kg	12	39.5	474
5	Metakaolin	Rs 22/ Kg	22	52.7	1159.4
6	Silica Sand (SS)	Rs 46 /cft	0.99		0
7	Quarry Sand (QS)	Rs 40 /cft	0.83	183.6	152.39
8	Granite Coarse Aggregates	Rs 53 /cft	1.24	1236	1532.64
9	Limestone coarse aggregates	Rs 49 /cft	1.09	0	0
Cost of Mix G100-QS40					**Rs 8007.67**

Table 24: Calculation of the Cost of mix L100-SS60

Item No	Quantity	Unit Cost of Material	Cost of Material (per kg)	Quantity Required	Cost per m^3 (INR)
1	Ordinary Portland Cement	550 per bag (50 kg)	10.4	435	4524
2	Natural River Sand	Rs 27/cft	0.603	183.6	110.16
3	Natural Coarse Aggregates	Rs 44 /cft	1.02	0	0
4	Silica Fume	Rs 12/ Kg	12	39.5	474
5	Metakaolin	Rs 22/ Kg	22	52.7	1159.4
6	Silica Sand (SS)	Rs 46 /cft	0.99	275.4	272.64
7	Quarry Sand (QS)	Rs 40 /cft	0.83		0
8	Granite Coarse Aggregates	Rs 53 /cft	1.24	0	0
9	Limestone coarse aggregates	Rs 49 /cft	1.09	1236	1347.24
Cost of Mix L100-SS60					**Rs 7887.44**

Table 25: Calculation of the Cost of Mix L100-QS40

Item No	Quantity	Unit Cost of Material	Cost of Material (per kg)	Quantity Required	Cost per m^3 (INR)
1	Ordinary Portland Cement	550 per bag (50 kg)	10.4	435	4524
2	Natural River Sand	Rs 27/cft	0.603	275.4	166.24
3	Natural Coarse Aggregates	Rs 44 /cft	1.02	0	0
4	Silica Fume	Rs 12/ Kg	12	39.5	474
5	Metakaolin	Rs 22/ Kg	22	52.7	1159.4
6	Silica Sand (SS)	Rs 46 /cft	0.99		0
7	Quarry Sand (QS)	Rs 40 /cft	0.83	183.6	152.39
8	Granite Coarse Aggregates	Rs 53 /cft	1.24	0	0
9	Limestone coarse aggregates	Rs 49 /cft	1.09	1236	1347.24
Cost of Mix L100-QS40					**Rs 7823.27**

The Cost of various mixes taken from each series is calculated is given as

S.No	Mix designation	Cost in INR (per m^3)
1	Control Mix	7693.52
2	G100-SS60	8072.85
3	G100-QS40	8007.67
4	L100-SS60	7887.44
5	L100-QS40	7823.27

4.12 Microstructural Analysis

Scanning Electron Microscopy (SEM) was carried out to examine the internal morphology of selected concrete specimens and to correlate the observed microstructural features with the mechanical and durability performance obtained during the experimental investigation. The SEM images were analysed mainly with respect to the presence of pores, voids, cracks, hydration products etc. Since the strength and durability characteristics of concrete are strongly influenced by its internal structure, SEM analysis provides supporting evidence for the trends observed in experimental results.

The SEM image of the control concrete specimen as shown in Figure 46 reveals the presence of visible pores and voids distributed within the matrix. Certain discontinuities and unfilled spaces can also be observed in the microstructure. These features indicate a comparatively less compact internal arrangement of the hydration products. The existence of such pores may facilitate the movement of water and aggressive ions through the concrete, thereby affecting its durability performance. In addition, the presence of voids reduces the effective load-carrying area of the matrix, which can contribute to comparatively lower mechanical strength. These observations are consistent with the compressive strength, split tensile strength, water absorption and chloride permeability results obtained for the control mix.

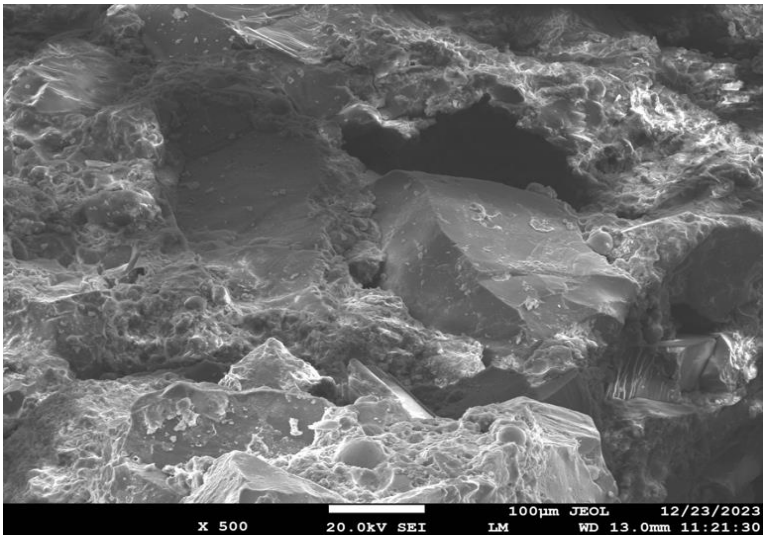

Figure 46: SEM image of control concrete showing pores, voids and discontinuities within the cementitious matrix

The SEM image of the concrete mix G100-SS60, as shown in Figure 47, exhibits a comparatively denser and more uniform microstructure. The matrix appears compact with fewer visible pores, and large voids are considerably reduced; the overall structure appears more closely packed than that observed in the control specimen. Such a compact microstructure generally indicates improved resistance to the penetration of water and harmful substances, while also providing better stress distribution within the matrix during loading.

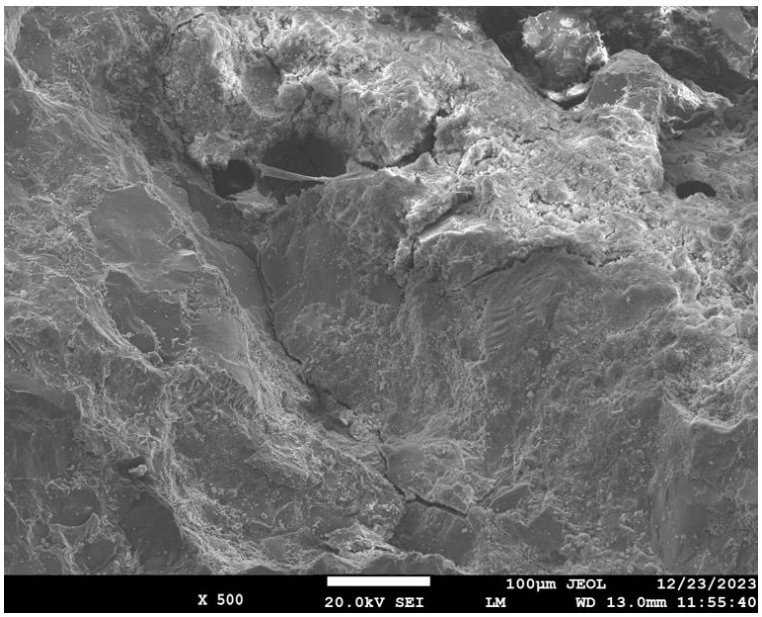

Figure 47: SEM image of G100-SS60 concrete showing a dense and compact microstructure with reduced pore spaces

A comparison of the two SEM images clearly indicates that the G100-SS60 mix possesses a more refined internal structure than the control concrete. The reduction in pore spaces and the increased compactness of the matrix is likely responsible for the improved mechanical and durability properties observed experimentally. The denser microstructure supports the higher compressive and split tensile strengths obtained for this mix, while the reduced pore network explains the lower water absorption and chloride permeability values. Therefore, the SEM observations provide microstructural support to the experimental findings and help explain the superior overall performance of the concrete mix.

CHAPTER 5 SUMMARY AND CONCLUSIONS

5.1 Overview

The present investigation examines the performance of HSC incorporating natural aggregates, with particular emphasis of using alternate coarse aggregate and the fine aggregates. Limestone and granite were employed as coarse aggregates, while silica sand and quarry sand were used as partial replacements for natural river sand to study their influence on strength, durability, and economy.

An experimental programme was undertaken involving four different series of concrete mixes developed using different combinations of coarse and fine aggregates. All these mixes were evaluated for compressive, split tensile, and flexural strengths at various curing ages. Durability behaviour was assessed through water absorption, abrasion resistance, and RCPT to capture both short-term and long-term performance. Based on overall performance, selected mixes were further analysed for cost to evaluate their practical feasibility.

5.2 Summary of Key Findings

The experimental study using different coarse and fine aggregates in HSC revealed certain insights on the performance of the different HSC developed.

1. Compressive strength increased with curing age for all mixes due to continued hydration and matrix densification. Replacement of natural coarse aggregates with limestone and granite aggregates resulted in notable strength enhancement, with granite-based mixes consistently outperforming limestone mixes.
2. At 28 days, complete replacement with granite aggregates (G100) resulted in an increase of approximately 13% in compressive strength compared to the control HSC mix, while limestone replacement (L100) showed an improvement of about 7-8%.

   Incorporation of silica sand further enhanced strength, with an optimum at 60% replacement, beyond which strength marginally declined. The G100-SS60 mix exhibited the highest compressive strength, recording nearly 18-20% higher strength than the control HSC mix, attributed to improved

particle packing, strong aggregate-paste bonding, and refined pore structure.

3. Split tensile strength of high-strength concrete improved with the partial replacement of natural river sand by alternative fine aggregates up to an particular level, Silica sand replacement at 60% yielded the highest tensile performance, showing an improvement of approximately 10-14% attributed to improved particle packing.
4. Quarry sand mixes exhibited optimum split tensile strength at 40% replacement, achieving a 7-10% increase over the base mix due to better interlocking arising from angular and rough particle surfaces.
5. Water absorption reduced with curing age and optimal aggregate replacement. Granite-based mixes showed lower absorption than limestone mixes due to their denser and less porous nature. Compared to the control mix, the G100-SS60 mix exhibited a reduction in water absorption of approximately 20-25%, indicating significant densification of the concrete matrix. Quarry sand mixes showed minimum absorption at 40% replacement, beyond which absorption increased slightly due to excess fines.
6. RCPT results confirmed substantial improvement in durability with optimal fine aggregate replacement. Granite mixes consistently allowed lower charge passage than limestone mixes.At 180 days, the G100-SS60 mix showed a reduction in charge passed of nearly 45-50% compared to the base granite mix (G100), demonstrating excellent resistance to chloride ingress. Similarly, QS mixes exhibited the lowest charge passed at 40% replacement, beyond which permeability increased marginally due to micro-void formation.
7. Abrasion resistance improved significantly with granite aggregates and optimal fine aggregate replacement. The G100-SS60 mix recorded the lowest depth of wear, showing an improvement of approximately 25-30% over the control HSC mix, attributed to the high hardness of granite aggregates and the dense surface matrix formed due to silica sand incorporation.

8. Compared to the control mix (Rs 7693.52/m³), the other high-strength concrete mixes showed **a** marginal cost increase of only 1.69-4.93%, while delivering substantially higher mechanical strength and durability performance.G100-SS60 mix, which exhibited the highest compressive strength improvement of 13.1% and maximum reduction in chloride permeability (42.6% at 180 days), incurred the highest cost increase of 4.93%, making it the most performance mix where durability is critical.
9. Mix L100-QS40 mix demonstrated a cost increase of only 1.69%, while still achieving notable improvements in durability (28-35% reduction in RCPT values at 180 days) and abrasion resistance, making it the most economical high-performance alternative among all mixes taken from each series.

5.3 General conclusions

The following conclusions have been reached in accordance with the research goals based on the discussion and analysis of the study's findings

5.3.1 Conclusion for objective 1:

To study the effect of granite and limestone as coarse aggregates along with silica sand and Quarry sand as fine aggregates on the mechanical properties of high-strength concrete.

i. Replacement of natural coarse aggregates with granite and limestone resulted in systematic improvement in mechanical performance, with granite-based mixes consistently exhibiting superior strength due to higher crushing resistance and enhanced mechanical interlock.

ii. At 28 days, complete replacement with granite aggregates (G100) achieved an increase of approximately 13.1% in compressive strength, whereas limestone aggregates (L100) yielded a comparatively moderate improvement of 7.6%, indicating the dominant role of aggregate hardness and angularity.

iii. Incorporation of silica sand significantly enhanced strength characteristics up to an optimum replacement level of 60%, beyond which marginal reductions were observed due to increased water demand and excess fines.

iv. The G100-SS60 mix demonstrated the highest overall mechanical performance, registering an improvement of nearly 18-20% in compressive strength and 10-14% in split tensile strength compared to the control mix, attributed to improved particle packing and aggregate-paste bonding.

v. Quarry sand replacement showed optimum mechanical performance at 40% replacement, where mixes such as L100-QS40 and G100-QS40 recorded 7-10% enhancement in split tensile and flexural strength, primarily due to improved interlocking from angular particles.

5.3.2 **Conclusion for objective 2:**

To test the durability of high-strength concrete mix.

i. Durability performance improved significantly with optimal aggregate combinations, with granite-based mixes exhibiting lower water absorption and permeability than limestone mixes owing to their denser and less porous aggregate structure.

ii. The G100-SS60 mix showed a reduction in water absorption of approximately 22% and a decrease in RCPT charge passed of about 45-50% at 180 days compared to the control mix, confirming substantial refinement of the pore structure.

iii. Quarry sand mixes exhibited minimum permeability and water absorption at 40% replacement, with L100-QS40 achieving a 28-35% reduction in RCPT values, beyond which durability performance declined slightly due to excess fines and micro-void formation.

iv. Abrasion resistance was notably enhanced in granite-based mixes, with G100-SS60 recording nearly 27% lower depth of wear than the control mix, attributed to the high hardness of granite aggregates and surface densification from silica sand.

5.3.3 Conclusion for objective 3:

To determine the cost of high-strength concrete mix thus arrived.

i. Best performing High-strength concrete mixes achieved substantial gains in strength and durability at a marginal cost increase of only 1.69-4.93% compared to the control mix, demonstrating favourable cost–performance efficiency.
ii. The G100-SS60 mix, despite a cost increase of 4.93%, delivered the highest mechanical strength and durability improvements, making it suitable for performance-critical applications such as marine and chloride-exposed structures.
iii. The L100-QS40 mix emerged as the most economical alternative, with only 1.69% increase in cost, while still providing meaningful durability enhancements, recommending its use in cost-sensitive high-strength structural applications.

5.4 Future Scope

- The present study may be extended by investigating the use of other alternative or recycled aggregates, such as recycled concrete aggregates or industrial by-products, in combination with limestone and granite to further enhance sustainability without compromising performance.
- Further selection of binder composition through varying proportions of silica fume, metakaolin, and water-binder ratio may be undertaken to develop performance-oriented high-strength concrete mixes suitable for different exposure conditions.
- Detailed rheological characterisation of fresh concrete, including parameters such as yield stress and plastic viscosity, may be explored to better understand the flow behaviour of mixes containing silica sand and quarry sand.

- Microstructural studies using advanced analytical techniques may be conducted to establish correlations between aggregate type, interfacial transition zone characteristics, and the observed mechanical and durability performance.
- Long-term durability performance under aggressive environmental conditions, including sulphate attack, carbonation, freeze-thaw action, and elevated temperatures, may be evaluated to assess service-life performance.
- Future work may also include field-scale trials and life-cycle cost and environmental impact assessments to support the practical implementation and economic viability of the developed high-strength concrete mixes.
- Future studies may incorporate detailed Life Cycle Cost Assessment (LCCA), considering initial construction cost, maintenance requirements, repair frequency, and service-life performance to provide a more comprehensive evaluation of the long-term economic feasibility of the developed high-strength concrete mixes.
- The suitability of granite aggregates obtained from different geological sources and regions may be investigated to assess the influence of variations on the mechanical and durability performance of high-strength concrete.
- Further research may be undertaken to establish the feasible range and optimum proportion of granite and limestone aggregates for the production of high-strength concrete, enabling the development of mix design recommendations for various structural and environmental conditions.

References

[1] M. P. Singh *et al.*, “Roads and Bridges,” *Earthq. Spectra*, vol. 18, no. 1_suppl, pp. 363-379, Jul. 2002, doi: 10.1193/1.2803920.

[2] P. C. Aïtcin, “Cements of yesterday and today: Concrete of tomorrow,” *Cem. Concr. Res.*, vol. 30, no. 9, pp. 1349-1359, Sep. 2000, doi: 10.1016/S0008-8846(00)00365-3.

[3] R. Hafizyar and M. Hunar Dheyaaldin, “Concrete Technology and Sustainably Development from Past to Future,” Sep. 2019, doi: 10.26392/SSM.2019.02.01.001.

[4] I. Baker, “Concrete,” *Fifty Mater. That Make World*, pp. 35-42, 2018, doi: 10.1007/978-3-319-78766-4_8.

[5] S. Subash, L. Parida, and S. Moharana, “Study on the Impact of Aggregate Size Gradation on Concrete: Mechanical, Durability and Microstructure Study,” *Int. J. Concr. Struct. Mater. 2025 191*, vol. 19, no. 1, pp. 114-, Nov. 2025, doi: 10.1186/S40069-025-00863-4.

[6] T. Kitanosono and S. Kobayashi, “Reactions in Water Involving the ‘On-Water’ Mechanism,” *Chem. - A Eur. J.*, vol. 26, no. 43, pp. 9408-9429, Aug. 2020, doi: 10.1002/CHEM.201905482;WGROUP:STRING:PUBLICATION.

[7] A. M. Mansor, R. P. Borg, A. M. M Hamed, M. M. Gadeem, and M. M. Saeed, “The effects of water-cement ratio and chemical admixtures on the workability of concrete,” *IOP Conf. Ser. Mater. Sci. Eng.*, vol. 442, no. 1, p. 012017, Nov. 2018, doi: 10.1088/1757-899X/442/1/012017.

[8] G. A. Khoury, “Effect of fire on concrete and concrete structures,” *Prog. Struct. Eng. Mater.*, vol. 2, no. 4, pp. 429-447, Oct. 2000, doi: 10.1002/PSE.51.

[9] L. O. Onundi, M. Ben Oumarou, and A. M. Alkali, “Effects of Fire on the Strength of Reinforced Concrete Structural Members,” *Am. J. Civ. Eng. Archit.*, vol. 7, no. 1, pp. 1-12, 2019, doi: 10.12691/ajcea-7-1-1.

[10] S. Y. N. Chan, G. F. Peng, and J. K. W. Chan, “Comparison between high strength concrete and normal strength concrete subjected to high temperature,” *Mater. Struct. 1996 2910*, vol. 29, no. 10, pp. 616-619, 1996, doi: 10.1007/BF02485969.

[11] A. Mwafy, N. Hussain, and K. El-Sawy, “Seismic performance and cost-effectiveness of high-rise buildings with increasing concrete strength,” *Struct. Des. Tall Spec. Build.*, vol. 24, no. 4, pp. 257-279, Mar. 2015, doi: 10.1002/TAL.1165;JOURNAL:JOURNAL:10991794;WGROUP:STRING:PUBLICATION.

[12] O. E. Gjørv, “High-strength concrete,” in *Developments in the Formulation and Reinforcement of Concrete*, Elsevier, 2008, pp. 153-170. doi: 10.1016/B978-0-08-102616-8.00007-1.

[13] C. French, A. Mokhtarzadeh, T. Ahlborn, and R. Leon, “High-strength concrete applications to prestressed bridge girders,” *Constr. Build. Mater.*, vol. 12, no. 2-3, pp. 105-113, Mar. 1998, doi: 10.1016/S0950-0618(97)00012-3.

[14] J. de Brito and N. Saikia, “Sustainable Development in Concrete Production,” *Green Energy Technol.*, vol. 54, pp. 1-22, 2013, doi: 10.1007/978-1-4471-4540-0_1.

[15] M. Soomro, V. W. Y. Tam, and A. C. Jorge Evangelista, “Production of cement and its environmental impact,” in *Recycled Concrete*, Elsevier, 2023, pp. 11-46. doi: 10.1016/B978-0-323-85210-4.00010-2.

[16] UN Environment Programme, *Sand and Sustainability: 10 Strategic Recommendations to Avert a Crisis*. 2022. [Online]. Available: https://www.unep.org/resources/report/sand-and-sustainability-10-strategic-recommendations-avert-crisis

[17] C. R. Hackney *et al.*, “River bank instability from unsustainable sand mining in the lower Mekong River,” *Nat. Sustain. 2020 33*, vol. 3, no. 3, pp. 217-225, Jan. 2020, doi: 10.1038/s41893-019-0455-3.

[18] C. R. Finch *et al.*, “International Journal of Vocational International Journal of Vocational,” *Training*, vol. 17, no. 2, pp. 89-95, 1993.

[19] M. Uwasu, K. Hara, and H. Yabar, “World cement production and environmental implications,” *Environ. Dev.*, vol. 10, no. 1, pp. 36-47, Apr. 2014, doi: 10.1016/J.ENVDEV.2014.02.005.

[20] R. M. Andrew, “Global CO2 emissions from cement production, 1928-2017,” *Earth Syst. Sci. Data*, vol. 10, no. 4, pp. 2213-2239, Dec. 2018, doi: 10.5194/ESSD-10-2213-2018.

[21] Andrew R.M., “Global CO 2 emissions from cement production.,” *Earth Syst. Sci. Data*, vol. 10, no. 4, pp. 1-20, 2018.

[22] T. R. Naik, “Sustainability of Concrete Construction,” *Pract. Period. Struct. Des. Constr.*, vol. 13, no. 2, pp. 98-103, May 2008, doi: 10.1061/(ASCE)1084-0680(2008)13:2(98).

[23] F. Canpolat and T. R. Naik, “Effect of curing conditions on strength and durability of high-performance concrete,” *Sci. Iran.*, vol. 24, no. 2, pp. 576-583, 2017, doi: 10.24200/sci.2017.2419.

[24] J. M. Feldman and G. Alfvin, “The killers of sand : A case study on how a shortage of sand is breaking down India from within,” 2019, Accessed: Dec. 07, 2025. [Online]. Available: https://urn.kb.se/resolve?urn=urn:nbn:se:su:diva-182506

[25] G. Psyrri *et al.*, “Abundant resources in an era of scarcity: Systemic aspects of the Global sand and gravel crisis,” *Resour. Conserv. Recycl.*, vol. 225, p. 108631, Jan. 2026, doi: 10.1016/J.RESCONREC.2025.108631.

[26] L. Aduda and L. Bolf, “The conflict potential of sand: Illegal sand mining on the African continent,” *Environ. Secur.*, vol. 2, no. 4, pp. 548-567, Dec. 2024, doi: 10.1177/27538796241230583.

[27] B. Lothenbach, K. Scrivener, and R. D. Hooton, “Supplementary cementitious materials,” *Cem. Concr. Res.*, vol. 41, no. 12, pp. 1244-1256, Dec. 2011, doi: 10.1016/J.CEMCONRES.2010.12.001.

[28] J. Skibsted and R. Snellings, “Reactivity of supplementary cementitious materials (SCMs) in cement blends,” *Cem. Concr. Res.*, vol. 124, p. 105799, Oct. 2019, doi: 10.1016/J.CEMCONRES.2019.105799.

[29] S. Samad and A. Shah, “Role of binary cement including Supplementary Cementitious Material (SCM), in production of environmentally sustainable concrete: A critical review,” *Int. J. Sustain. Built Environ.*, vol. 6, no. 2, pp. 663-674, Dec. 2017, doi: 10.1016/J.IJSBE.2017.07.003.

[30] Vikas, “Effect of Silica Fume and Metakaolin combination on concrete,” *Int. J. Civ. Struct. Eng.*, vol. 2, no. 3, Feb. 2012, doi: 10.6088/IJCSER.00202030017.

[31] A. 363R, “ACI 363 R-92 State-ofthe-Art Report on High-Strength Concrete Reported by ACI Committee 363,” vol. 92, no. Reapproved, pp. 1-2, 1998.

[32] H. G. Russell *et al.*, "State-of-the-Art Report on High-Strength Concrete Reported by ACI Committee 363," *Concrete*, vol. 92, no. Reapproved, pp. 1-2, 1997.

[33] BIS (Bureau of Indian Standards), "Concrete mix proportioning - Guidelines," *BIS 10262, New Delhi*, pp. 1-14, 2009.

[34] "The Role of Reinforced Concrete in High-Rise Construction - Barrow Mix Ready Mix Concrete Manchester." https://barrowmixconcrete.com/the-role-of-reinforced-concrete-in-high-rise-construction/ (accessed Dec. 09, 2025).

[35] Abdullahi, "Effect of aggregate type on Compressive strength of concrete," *Int. J. Civ. Struct. Eng.*, vol. 2, no. 3, Feb. 2012, doi: 10.6088/IJCSER.00202030008.

[36] K. P. Vishalakshi, V. Revathi, and S. Sivamurthy Reddy, "Effect of type of coarse aggregate on the strength properties and fracture energy of normal and high strength concrete," *Eng. Fract. Mech.*, vol. 194, pp. 52-60, 2018, doi: 10.1016/j.engfracmech.2018.02.029.

[37] H. Beshr, A. A. Almusallam, and M. Maslehuddin, "Effect of coarse aggregate quality on the mechanical properties of high strength concrete," *Constr. Build. Mater.*, vol. 17, no. 2, pp. 97-103, Mar. 2003, doi: 10.1016/S0950-0618(02)00097-1.

[38] H. Beushausen and T. Dittmer, "The influence of aggregate type on the strength and elastic modulus of high strength concrete," *Constr. Build. Mater.*, vol. 74, pp. 132-139, 2015, doi: 10.1016/j.conbuildmat.2014.08.055.

[39] S. Ahmad and S. A. Alghamdi, "A Study on Effect of Coarse Aggregate Type on Concrete Performance," *Arab. J. Sci. Eng.*, vol. 37, no. 7, pp. 1777-1786, 2012, doi: 10.1007/S13369-012-0282-6.

[40] H. Beushausen and T. Dittmer, "The influence of aggregate type on the strength and elastic modulus of high strength concrete," *Constr. Build. Mater.*, vol. 74, pp. 132-139, Jan. 2015, doi: 10.1016/J.CONBUILDMAT.2014.08.055.

[41] A. P. N. Siregar, M. I. Rafiq, and M. Mulheron, "Experimental investigation of the effects of aggregate size distribution on the fracture behaviour of high strength concrete," *Constr. Build. Mater.*, vol. 150, pp. 252-259, 2017, doi: 10.1016/j.conbuildmat.2017.05.142.

[42] P. P. Li, Q. L. Yu, and H. J. H. Brouwers, “Effect of coarse basalt aggregates on the properties of Ultra-high Performance Concrete (UHPC),” *Constr. Build. Mater.*, vol. 170, pp. 649-659, May 2018, doi: 10.1016/J.CONBUILDMAT.2018.03.109.

[43] A. P. N. Siregar, E. L. Pasaribu, and I. W. Suarnita, “The effect of coarse aggregate hardness on the fracture toughness and compressive strength of concrete,” *MATEC Web Conf.*, vol. 258, p. 04011, Jan. 2019, doi: 10.1051/matecconf/201925804011.

[44] I. Y. Hakeem, M. Alharthai, M. Amin, A. M. Zeyad, B. A. Tayeh, and I. S. Agwa, “Properties of sustainable high-strength concrete containing large quantities of industrial wastes, nanosilica and recycled aggregates,” *J. Mater. Res. Technol.*, vol. 24, pp. 7444-7461, May 2023, doi: 10.1016/J.JMRT.2023.05.050.

[45] F. J. Luo, L. He, Z. Pan, W. H. Duan, X. L. Zhao, and F. Collins, “Effect of very fine particles on workability and strength of concrete made with dune sand,” *Constr. Build. Mater.*, vol. 47, pp. 131-137, 2013, doi: 10.1016/j.conbuildmat.2013.05.005.

[46] H. Donza *et al.*, “‘ Strength of Concrete Containing Different Types of Fine Aggregate ,’” *Int. J. Mod. Eng. Res.*, vol. 3, no. 11, pp. 187-196, 2012.

[47] M. O. F. Engineering and S. Engineering, “Effect of Addition of Stone Dust As Fine Aggregate on Properties of Concrete Containing Rice Husk Ash As Cement”.

[48] R. Malathy, S. Ramachandran, R. Sentilkumar, and A. R. Prakash, “Use of Industrial Silica Sand as a Fine Aggregate in,” 2022.

[49] S. Bhanja and B. Sengupta, “Investigations on the compressive strength of silica fume concrete using statistical methods,” *Cem. Concr. Res.*, vol. 32, no. 9, pp. 1391-1394, Sep. 2002, doi: 10.1016/S0008-8846(02)00787-1.

[50] S. Park, S. Wu, Z. Liu, and S. Pyo, “The role of supplementary cementitious materials (Scms) in ultra high performance concrete (uhpc): A review,” *Materials (Basel).*, vol. 14, no. 6, pp. 1-24, 2021, doi: 10.3390/ma14061472.

[51] H. S. Kim, S. H. Lee, and H. Y. Moon, “Strength properties and durability aspects of high strength concrete using Korean metakaolin,” *Constr. Build.*

Mater., vol. 21, no. 6, pp. 1229-1237, 2007, doi: 10.1016/j.conbuildmat.2006.05.007.

[52] H. Donza, O. Cabrera, and E. F. Irassar, "High-strength concrete with different fine aggregate," *Cem. Concr. Res.*, vol. 32, no. 11, pp. 1755-1761, 2002, doi: 10.1016/S0008-8846(02)00860-8.

[53] M. A. Caldarone, "High-Strength Concrete : A Practical Guide," Apr. 2014, doi: 10.1201/9781482265842.

[54] M. A. Megat Johari, J. J. Brooks, S. Kabir, and P. Rivard, "Influence of supplementary cementitious materials on engineering properties of high strength concrete," *Constr. Build. Mater.*, vol. 25, no. 5, pp. 2639-2648, 2011, doi: 10.1016/j.conbuildmat.2010.12.013.

[55] M. Amin and K. Abu El-Hassan, "Effect of using different types of nano materials on mechanical properties of high strength concrete," *Constr. Build. Mater.*, vol. 80, pp. 116-124, Apr. 2015, doi: 10.1016/j.conbuildmat.2014.12.075.

[56] T. Lee, J. Lee, and H. Choi, "Assessment of Strength Development at Hardened Stage on High-Strength Concrete Using NDT," *Appl. Sci. 2020, Vol. 10, Page 6261*, vol. 10, no. 18, p. 6261, Sep. 2020, doi: 10.3390/APP10186261.

[57] K. A. Melo and A. M. P. Carneiro, "Effect of Metakaolin's finesses and content in self-consolidating concrete," *Constr. Build. Mater.*, vol. 24, no. 8, pp. 1529-1535, 2010, doi: 10.1016/J.CONBUILDMAT.2010.02.002.

[58] "(PDF) PARTIAL REPLACEMENT OF CEMENT WITH METAKAOLIN IN HIGH STRENGTH CONCRETE." https://www.researchgate.net/publication/306106684_PARTIAL_REPLACEMENT_OF_CEMENT_WITH_METAKAOLIN_IN_HIGH_STRENGTH_CONCRETE (accessed Dec. 12, 2025).

[59] S. I. Dorai, M. T. Student, and S. V. K. Viswes, "A Study on High Strength Concrete by using Metakaolin and Hybrid Fibers," vol. 8, no. 09, pp. 434-438, 2019.

[60] K. H. Younis, A. A. Amin, H. G. Ahmed, and S. M. Maruf, "Recycled Aggregate Concrete including Various Contents of Metakaolin: Mechanical

Behavior," *Adv. Mater. Sci. Eng.*, vol. 2020, 2020, doi: 10.1155/2020/8829713.

[61] S. U. Khan, M. F. Nuruddin, and N. Shafiq, "Strength development of concrete incorporating metakaolin and PVA fibres," *Appl. Mech. Mater.*, vol. 567, pp. 505-510, 2014, doi: 10.4028/www.scientific.net/AMM.567.505.

[62] P. Shen, L. Lu, W. Chen, F. Wang, and S. Hu, "Efficiency of metakaolin in steam cured high strength concrete," *Constr. Build. Mater.*, vol. 152, pp. 357-366, 2017, doi: 10.1016/j.conbuildmat.2017.07.006.

[63] J. Ahmad, A. Majdi, M. M. Arbili, A. F. Deifalla, and M. T. Naqash, "Mechanical, Durability and Microstructure Analysis Overview of Concrete Made with Metakaolin (MTK)," *Buildings*, vol. 12, no. 9, p. 1401, Sep. 2022, doi: 10.3390/buildings12091401.

[64] M. Mazloom, A. A. Ramezanianpour, and J. J. Brooks, "Effect of silica fume on mechanical properties of high-strength concrete," *Cem. Concr. Compos.*, vol. 26, no. 4, pp. 347-357, May 2004, doi: 10.1016/S0958-9465(03)00017-9.

[65] P. Smarzewski, "Mechanical and Microstructural Studies of High Performance Concrete with Condensed Silica Fume," *Appl. Sci.*, vol. 13, no. 4, p. 2510, Feb. 2023, doi: 10.3390/app13042510.

[66] H. G. Şahin, A. Mardani, and H. E. Beytekin, "Effect of Silica Fume Utilization on Structural Build-Up, Mechanical and Dimensional Stability Performance of Fiber-Reinforced 3D Printable Concrete," *Polymers (Basel).*, vol. 16, no. 4, p. 556, Feb. 2024, doi: 10.3390/polym16040556.

[67] U. Reddy, C. Vijendar Reddy, S. Lakhanpal, L. Kumar Tyagi, M. Muhsen, and I. Khan, "Use of silica fume as a replacement of cement in the concrete", doi: 10.1051/e3sconf/202452901036.

[68] A. Singh and N. Singh, "Mechanical properties of silica fume based concrete: A review," *Mater. Today Proc.*, May 2024, doi: 10.1016/J.MATPR.2024.05.037.

[69] E. Güneyisi, M. Gesolu, and E. Özbay, "Strength and drying shrinkage properties of self-compacting concretes incorporating multi-system blended mineral admixtures," *Constr. Build. Mater.*, vol. 24, no. 10, pp. 1878-1887, Oct. 2010, doi: 10.1016/J.CONBUILDMAT.2010.04.015.

[70] N. Van Tuan, G. Ye, K. Van Breugel, A. L. A. Fraaij, and D. D. Bui, "The

study of using rice husk ash to produce ultra high performance concrete," *Constr. Build. Mater.*, vol. 25, no. 4, pp. 2030-2035, Apr. 2011, doi: 10.1016/J.CONBUILDMAT.2010.11.046.

[71] "(PDF) Mechanical Properties of Ultra High Performance Concrete." https://www.researchgate.net/publication/305770268_Mechanical_Properties_of_Ultra_High_Performance_Concrete (accessed Dec. 12, 2025).

[72] T. Singh, R. Siddique, and S. Sharma, "Effectiveness of using Metakaolin and fly ash as supplementary cementitious materials in pervious concrete," *Eur. J. Environ. Civ. Eng.*, vol. 26, no. 15, pp. 7359-7382, 2022, doi: 10.1080/19648189.2021.1988715.

[73] M. Zuaiter *et al.*, "Effect of blending GGBS and silica fume on the mechanical properties of geopolymer concrete," *NatSR*, vol. 15, no. 1, p. 9091, Dec. 2025, doi: 10.1038/S41598-025-93637-7.

[74] Y. Wang, W. Zhang, J. Wang, R. Huang, G. Lou, and S. Luo, "Effects of coarse aggregate size on thickness and micro-properties of ITZ and the mechanical properties of concrete," *Cem. Concr. Compos.*, vol. 154, p. 105777, Nov. 2024, doi: 10.1016/j.cemconcomp.2024.105777.

[75] J. K. Periasamy, S. Sivalingam, A. Ponshanmugakumar, M. Jasmin, and G. Sheeba, "Experimental study on recycled coarse aggregate of concrete," *Mater. Today Proc.*, May 2023, doi: 10.1016/j.matpr.2023.05.110.

[76] C. Li, "Mechanical and transport properties of recycled aggregate concrete modified with limestone powder," *Compos. Part B Eng.*, vol. 197, p. 108189, Sep. 2020, doi: 10.1016/J.COMPOSITESB.2020.108189.

[77] C. Zhou and Z. Chen, "Mechanical properties of recycled concrete made with different types of coarse aggregate," *Constr. Build. Mater.*, vol. 134, pp. 497-506, Mar. 2017, doi: 10.1016/J.CONBUILDMAT.2016.12.163.

[78] M. E. Mitwally, A. Elnemr, A. Shash, and A. Babiker, "Utilization of steel slag as partial replacement for coarse aggregate in concrete," *Innov. Infrastruct. Solut. 2024 95*, vol. 9, no. 5, pp. 175-, May 2024, doi: 10.1007/S41062-024-01464-Y.

[79] A. A. ; E. ; Radwan *et al.*, "The Use of Plastic Waste as Replacement of Coarse Aggregate in Concrete Industry," *Sustain. 2024, Vol. 16, Page 10522*, vol. 16,

no. 23, p. 10522, Nov. 2024, doi: 10.3390/SU162310522.

[80] I. Y. Hakeem, M. Alharthai, M. Amin, A. M. Zeyad, B. A. Tayeh, and I. S. Agwa, "Properties of sustainable high-strength concrete containing large quantities of industrial wastes, nanosilica and recycled aggregates," *J. Mater. Res. Technol.*, vol. 24, pp. 7444-7461, May 2023, doi: 10.1016/j.jmrt.2023.05.050.

[81] P. P. Li, Q. L. Yu, and H. J. H. Brouwers, "Effect of coarse basalt aggregates on the properties of Ultra-high Performance Concrete (UHPC)," *Constr. Build. Mater.*, vol. 170, pp. 649-659, May 2018, doi: 10.1016/j.conbuildmat.2018.03.109.

[82] M. Aslam, P. Shafigh, M. Alizadeh Nomeli, and M. Zamin Jumaat, "Manufacturing of high-strength lightweight aggregate concrete using blended coarse lightweight aggregates," *J. Build. Eng.*, vol. 13, pp. 53-62, Sep. 2017, doi: 10.1016/J.JOBE.2017.07.002.

[83] M. Kalra and G. Mehmood, "A Review paper on the Effect of different types of coarse aggregate on Concrete," *IOP Conf. Ser. Mater. Sci. Eng.*, vol. 431, no. 8, 2018, doi: 10.1088/1757-899X/431/8/082001.

[84] A. J. Alsaad, W. S. Alyhya, and M. S. Radhi, "A Novel Approach in the Utilization of Waste Plastic with Enhanced Surfaces as Fine Aggregates in Concrete Production," *Eng. Technol. Appl. Sci. Res.*, vol. 15, no. 4, pp. 24486-24492, Aug. 2025, doi: 10.48084/ETASR.11361.

[85] M. Nuruzzaman, J. Almeida, M. T. E. Amin, and P. K. Sarker, "Performance of Sustainable Green Concrete Incorporating Quarry Dust and Ferronickel Slag as Fine Aggregate," *Materials (Basel).*, vol. 17, no. 10, 2024, doi: 10.3390/ma17102326.

[86] Y. M. Hong and S. R. Choudhury, "The Substitution Effect of the Fine Aggregate in Concrete with Oyster Shell," *Mater. 2024, Vol. 17, Page 6148*, vol. 17, no. 24, p. 6148, Dec. 2024, doi: 10.3390/MA17246148.

[87] A. Umara Shettima, Y. Ahmad, M. Warid Hussin, N. Zakari Muhammad, and O. Eziekel Babatude, "Strength and Microstructure of Concrete with Iron Ore Tailings as Replacement for River Sand," *E3S Web Conf.*, vol. 34, p. 01003, Mar. 2018, doi: 10.1051/E3SCONF/20183401003.

[88] Z. Z. Ismail and E. A. AL-Hashmi, “Recycling of waste glass as a partial replacement for fine aggregate in concrete,” *Waste Manag.*, vol. 29, no. 2, pp. 655-659, Feb. 2009, doi: 10.1016/J.WASMAN.2008.08.012.

[89] K. Vardhan, R. Siddique, and S. Goyal, “Influence of marble waste as partial replacement of fine aggregates on strength and drying shrinkage of concrete,” *Constr. Build. Mater.*, vol. 228, p. 116730, Dec. 2019, doi: 10.1016/J.CONBUILDMAT.2019.116730.

[90] G. Cabanillas Hernandez, J. M. García Chumacero, L. M. Villegas Granados, G. G. Arriola Carrasco, and N. H. Marín Bardales, “Sustainable use of wood sawdust as a replacement for fine aggregate to improve the properties of concrete: a Peruvian case study,” *Innov. Infrastruct. Solut. 2024 97*, vol. 9, no. 7, pp. 233-, Jun. 2024, doi: 10.1007/S41062-024-01567-6.

[91] N. Singh, M. Mithulraj, and S. Arya, “Influence of coal bottom ash as fine aggregates replacement on various properties of concretes: A review,” *Resour. Conserv. Recycl.*, vol. 138, pp. 257-271, Nov. 2018, doi: 10.1016/J.RESCONREC.2018.07.025.

[92] N. Jayasimha, B. Sujini, and B. P. Annapurna, “A study on durability and strength properties of high strength concrete with partial replacement of iron ore tailings with fine aggregates,” *Mater. Today Proc.*, vol. 65, pp. 1922-1929, Jan. 2022, doi: 10.1016/J.MATPR.2022.05.163.

[93] N. Sakthieswaran, N. Moorthy, M. Renisha, and M. Chinnadurai, “Optimization of Strength Properties of Reactive Powder Concrete by Response Surface Methodology,” *J. Shanghai Jiaotong Univ. 2023 295*, vol. 29, no. 5, pp. 900-908, Jun. 2023, doi: 10.1007/S12204-023-2612-0.

[94] G. Singh *et al.*, “Incorporation of Silica Fumes and Waste Glass Powder on Concrete Properties Containing Crumb Rubber as a Partial Replacement of Fine Aggregates,” *Sustain. 2022, Vol. 14, Page 14453*, vol. 14, no. 21, p. 14453, Nov. 2022, doi: 10.3390/SU142114453.

[95] L. Gautam, J. Kumar Jain, T. Alomayri, N. Meena, and P. Kalla, “Performance evaluation of self-compacting concrete comprising ceramic waste powder as fine aggregate,” *Mater. Today Proc.*, vol. 61, pp. 204-211, Jan. 2022, doi: 10.1016/J.MATPR.2021.08.063.

[96] T. U. Mohammed *et al.*, “Alternative Fine Aggregates to Natural River Sand for Manufactured Concrete Ensuring Circular Economy,” *Constr. Mater. 2024, Vol. 4, Pages 640-654*, vol. 4, no. 4, pp. 640-654, Oct. 2024, doi: 10.3390/CONSTRMATER4040035.

[97] S. Mundra, V. Agrawal, and R. Nagar, “Sandstone cutting waste as partial replacement of fine aggregates in concrete: A mechanical strength perspective,” *J. Build. Eng.*, vol. 32, p. 101534, Nov. 2020, doi: 10.1016/J.JOBE.2020.101534.

[98] A. Gamieldien, B. Dookee, H. Beushausen, and M. Alexander, “Feasibility of Utilizing Fine Recycled Concrete Aggregates as a Dune Sand Replacement in Concrete Production,” *RILEM Bookseries*, vol. 59, pp. 630-639, 2025, doi: 10.1007/978-3-031-75507-1_60.

[99] C. M. Yun, M. R. Rahman, K. K. Kuok, A. C. P. Sze, K. J. K. Zhiing, and M. K. Bin Bakri, “Glass Waste as Fine Aggregate Filler Replacement in Concrete Addition of Superplasticizer,” *Eng. Mater.*, pp. 45-61, 2022, doi: 10.1007/978-3-030-98812-8_3.

[100] D. Ganvir and B. Kumar, “Effect of Jarosite as Partial Replacement of Fine Aggregate in Pavement Quality Concrete Mixes,” *Lect. Notes Civ. Eng.*, vol. 218, pp. 223-229, 2022, doi: 10.1007/978-981-16-9921-4_16.

[101] M. Soundararajan, S. Jayaprakash, S. K. Maniarasan, and R. Gobinath, “Predicting Strength Properties of High-Performance Concrete Modified with Natural Aggregates and Ferroslag under Varied Curing Conditions,” *Adv. Civ. Eng.*, vol. 2023, pp. 1-16, Jun. 2023, doi: 10.1155/2023/9960412.

[102] D. Sau, A. Shiuly, and T. Hazra, “Utilization of plastic waste as replacement of natural aggregates in sustainable concrete: effects on mechanical and durability properties,” *Int. J. Environ. Sci. Technol.*, vol. 21, no. 2, pp. 2085-2120, Jan. 2024, doi: 10.1007/s13762-023-04946-1.

[103] S. Singh, R. Nagar, V. Agrawal, A. Rana, and A. Tiwari, “Sustainable utilization of granite cutting waste in high strength concrete,” *J. Clean. Prod.*, vol. 116, pp. 223-235, 2016, doi: 10.1016/j.jclepro.2015.12.110.

[104] A. Carlos, I. Masumi, M. Hiroaki, M. Maki, and O. Takahisa, “The effects of limestone aggregate on concrete properties,” *Constr. Build. Mater.*, vol. 24, no.

12, pp. 2363-2368, Dec. 2010, doi: 10.1016/J.CONBUILDMAT.2010.05.008.

[105] A. R. Murthy, N. R. Iyer, and B. K. R. Prasad, "Evaluation of mechanical properties for high strength and ultrahigh strength concretes," *Adv. Concr. Constr.*, vol. 1, no. 4, pp. 341-358, Dec. 2013, doi: 10.12989/ACC2013.1.4.341.

[106] L. Scheinherrová *et al.*, "Mechanical and Basic Physical Properties of High-Strength Concrete Exposed to Elevated Temperatures," *Key Eng. Mater.*, vol. 760, pp. 108-113, 2018, doi: 10.4028/WWW.SCIENTIFIC.NET/KEM.760.108.

[107] A. A. Zende *et al.*, "Mechanical Properties of High-Strength Self-Compacting Concrete," *ACS Omega*, vol. 8, no. 20, pp. 18000-18008, May 2023, doi: 10.1021/ACSOMEGA.3C01204.

[108] N. M. Ibrahim *et al.*, "Compressive Strength of Concrete from Lightweight Bubbles Aggregate," *Appl. Mech. Mater.*, vol. 754-755, pp. 348-353, Apr. 2015, doi: 10.4028/WWW.SCIENTIFIC.NET/AMM.754-755.348.

[109] R. de S. Castoldi, L. M. S. de Souza, and F. de Andrade Silva, "Comparative study on the mechanical behavior and durability of polypropylene and sisal fiber reinforced concretes," *Constr. Build. Mater.*, vol. 211, pp. 617-628, Jun. 2019, doi: 10.1016/J.CONBUILDMAT.2019.03.282.

[110] C. Mansilla, M. Pradena, C. Fuentealba, and A. César, "Evaluation of Mechanical Properties of Concrete Reinforced with Eucalyptus globulus Bark Fibres," *Sustain. 2020, Vol. 12, Page 10026*, vol. 12, no. 23, p. 10026, Dec. 2020, doi: 10.3390/SU122310026.

[111] W. Wang and Q. Yue, "The Time Variation Law of Concrete Compressive Strength: A Review," *Appl. Sci. 2023, Vol. 13, Page 4947*, vol. 13, no. 8, p. 4947, Apr. 2023, doi: 10.3390/APP13084947.

[112] B. S. Divsholi, T. Y. D. Lim, and S. Teng, "Durability Properties and Microstructure of Ground Granulated Blast Furnace Slag Cement Concrete," *Int. J. Concr. Struct. Mater. 2014 82*, vol. 8, no. 2, pp. 157-164, May 2014, doi: 10.1007/S40069-013-0063-Y.

[113] C. Alexandridou, G. N. Angelopoulos, and F. A. Coutelieris, "Mechanical and durability performance of concrete produced with recycled aggregates from

Greek construction and demolition waste plants," *J. Clean. Prod.*, vol. 176, pp. 745-757, Mar. 2018, doi: 10.1016/j.jclepro.2017.12.081.

[114] L. Wang, H. Yong, J. Lu, C. Shu, and H. Wang, "Influence of Coarse Aggregate Type on the Mechanical Strengths and Durability of Cement Concrete," *Coatings 2021, Vol. 11, Page 1036*, vol. 11, no. 9, p. 1036, Aug. 2021, doi: 10.3390/COATINGS11091036.

[115] C. K. Valenzuela-Leyva, M. Soto-Felix, J. R. Gaxiola-Camacho, O. F. Ojeda-Farias, J. M. Herrera-Ramirez, and C. Carreño-Gallardo, "Improving Durability and Compressive Strength of Concrete with Rhyolite Aggregates and Recycled Supplementary Cementitious Materials," *Build. 2025, Vol. 15, Page 2257*, vol. 15, no. 13, p. 2257, Jun. 2025, doi: 10.3390/BUILDINGS15132257.

[116] M. Bravo, J. De Brito, J. Pontes, and L. Evangelista, "Durability performance of concrete with recycled aggregates from construction and demolition waste plants," *Constr. Build. Mater.*, vol. 77, pp. 357-369, Feb. 2015, doi: 10.1016/J.CONBUILDMAT.2014.12.103.

[117] F. Rezaei, A. Memarzadeh, M. R. Davoodi, M. A. Dashab, and M. Nematzadeh, "Mechanical features and durability of concrete incorporating recycled coarse aggregate and nano-silica: Experimental study, prediction, and optimization," *J. Build. Eng.*, vol. 73, p. 106715, Aug. 2023, doi: 10.1016/J.JOBE.2023.106715.

[118] S. Jamil, M. Idrees, A. Akbar, and W. Ahmed, "Investigating the Mechanical and Durability Properties of Carbonated Recycled Aggregate Concrete and Its Performance with SCMs," *Build. 2025, Vol. 15, Page 201*, vol. 15, no. 2, p. 201, Jan. 2025, doi: 10.3390/BUILDINGS15020201.

[119] F. Faleschini, M. Alejandro Fernández-Ruíz, M. A. Zanini, K. Brunelli, C. Pellegrino, and E. Hernández-Montes, "High performance concrete with electric arc furnace slag as aggregate: Mechanical and durability properties," *Constr. Build. Mater.*, vol. 101, pp. 113-121, Dec. 2015, doi: 10.1016/j.conbuildmat.2015.10.022.

[120] K. Shyam Prakash and C. H. Rao, "Study on Compressive Strength of Quarry Dust as Fine Aggregate in Concrete," *Adv. Civ. Eng.*, vol. 2016, pp. 1-5, 2016, doi: 10.1155/2016/1742769.

[121] M. ; Almeida *et al.*, “Performance of Sustainable Green Concrete Incorporating Quarry Dust and Ferronickel Slag as Fine Aggregate,” *Mater. 2024, Vol. 17, Page 2326*, vol. 17, no. 10, p. 2326, May 2024, doi: 10.3390/MA17102326.

[122] D. O. Nduka, O. I. Fabgenle, O. Joshua, A. O. Ogunde, and I. O. Omuh, “Comparative analysis of concrete strength utilizing quarry-crushed and locally sourced coarse aggregates,” *Int. J. Mech. Eng. Technol.*, vol. 9, no. 1, pp. 609-617, 2018.

[123] C. Shi, D. Wang, L. Wu, and Z. Wu, “The hydration and microstructure of ultra high-strength concrete with cement-silica fume-slag binder,” *Cem. Concr. Compos.*, vol. 61, pp. 44-52, 2015, doi: 10.1016/j.cemconcomp.2015.04.013.

[124] F. Faleschini, M. Alejandro Fernández-Ruíz, M. A. Zanini, K. Brunelli, C. Pellegrino, and E. Hernández-Montes, “High performance concrete with electric arc furnace slag as aggregate: Mechanical and durability properties,” *Constr. Build. Mater.*, vol. 101, pp. 113-121, Dec. 2015, doi: 10.1016/J.CONBUILDMAT.2015.10.022.

Annex-A

This annexure presents the detailed methodology adopted for the optimization of the high-strength concrete control mix (CM) used in the present research work.

The control mix (CM) used in the experimental work was not arrived at arbitrarily, but a multi-stage optimisation framework was employed to obtain a concrete mix satisfying both strength and workability requirements. The procedure consisted of the following stages:

Stage I: Preliminary exploration Trials

In this stage, a series of preliminary trial mixes was prepared to study the influence of individual parameters on concrete behaviour. Separate preliminary trial sets were conducted to understand the effect of Superplasticiser, water binder, silica fume and metakaolin content

The objective behind this was to identify feasible parameter ranges and practical limits for achieving adequate workability and strength. Apart, from this, many other trials outside this shown preliminary trial window were also conducted to understand the effect of materials. Details of the various relevant preliminary trial mixes and the observations are presented in Table A.

Table A1: Details of the preliminary trials for determining feasible ranges

Trial ID	Cement (Kg/m^3)	SF (Kg/m^3)	MK (Kg/m^3)	Water (Kg/m^3)	SP (Kg/m^3)	w/b	Slump (mm)	Strength (MPa)
T1	475	26	26	148	4.2	0.28	72	56.6
T2	475	26	26	148	5.3	0.28	102	58.34
T3	475	26	26	148	6.32	0.28	112	62.21
T4	475	26	26	148	7.4	0.28	125	60.54
T5	475	26	26	174	6.32	0.33	136	56.25
T6	475	26	26	168	6.32	0.32	128	58.44

T7	475	26	26	158	6.32	0.3	116	60.65
T8	475	26	26	148	6.32	0.28	113	62.21
T9	462	26	26	148	6.32	0.28	118	61.25
T10	448	26	39.5	148	6.32	0.28	116	62.5
T11	435	26	52.7	148	6.32	0.28	111	64.75
T12	422	26	65.9	148	6.32	0.28	108	64.91
T13	409	26	79.1	148	6.32	0.28	106	64.82
T14	448	26	52.7	158	6.32	0.30	117	63.5
T15	435	39.5	52.7	158	6.32	0.30	110	64.8
T16	422	52.7	52.7	158	6.32	0.30	102	64.82
T17	409	65.9	52.7	158	6.32	0.30	90	64.87

Stage II: Taguchi Optimisation

A Taguchi L9 orthogonal array was adopted, considering three control factors, i.e., Silica Fume, Metakaolin and Water binder ratio. Every factor has three levels, details of which are given as follows in Table A2.

Table A2: Factors and Levels used in Taguchi optimisation

Factor	Level 1	Level 2	Level 3
A - SF (%)	5	7.5	10
B - MK (%)	5	10	15
C - w/b	0.28	0.30	0.32

The details of the orthogonal array used for the Taguchi design of experiments (DOE) is given in Table A3.

Table A3: Taguchi orthogonal array with factors, levels and mix details

Trial	A	B	C	SF (%)	MK (%)	w/b
T1	1	1	1	5	5	0.28
T2	1	2	2	5	10	0.30
T3	1	3	3	5	15	0.32
T4	2	1	2	7.5	5	0.30
T5	2	2	3	7.5	10	0.32
T6	2	3	1	7.5	15	0.28
T7	3	1	3	10	15	0.32
T8	3	2	1	10	10	0.28
T9	3	3	2	10	15	0.30

The S/N ratio for various trials as obtained from Taguchi analysis is given in the Table A4.

Table A4: S/N ratio obtained from the Taguchi method for orthogonal matrix

Trial	A (SF%)	B (MK%)	C (w/b)	C.S	S/N ratio (dB)
T1	5	5	0.28	63.8	36.0964
T2	5	10	0.30	64.2	36.1507
T3	5	15	0.32	63	35.9868
T4	7.5	5	0.30	65.5	36.3248
T5	7.5	10	0.32	66.8	36.4955
T6	7.5	15	0.28	67.4	36.5732
T7	10	15	0.32	63.2	36.0143
T8	10	10	0.28	65	36.2583
T9	10	15	0.30	64	36.1236

The response table for mean S/N ratio, delta and factor ranking as obtained after Taguchi analysis by DOE is given in Table A5.

Table A5: Response table for mean S/N ratio, delta and factor ranking

Level	A (SF%)	B (MK%)	C(w/b)
1	36.08	36.15	36.31
2	36.46	36.3	36.2
3	36.13	36.23	36.17
Delta	0.39	0.16	0.14
Rank	1	2	3

The main effect plot after analysis in DOE for SN ratios is shown in Figure 1A.

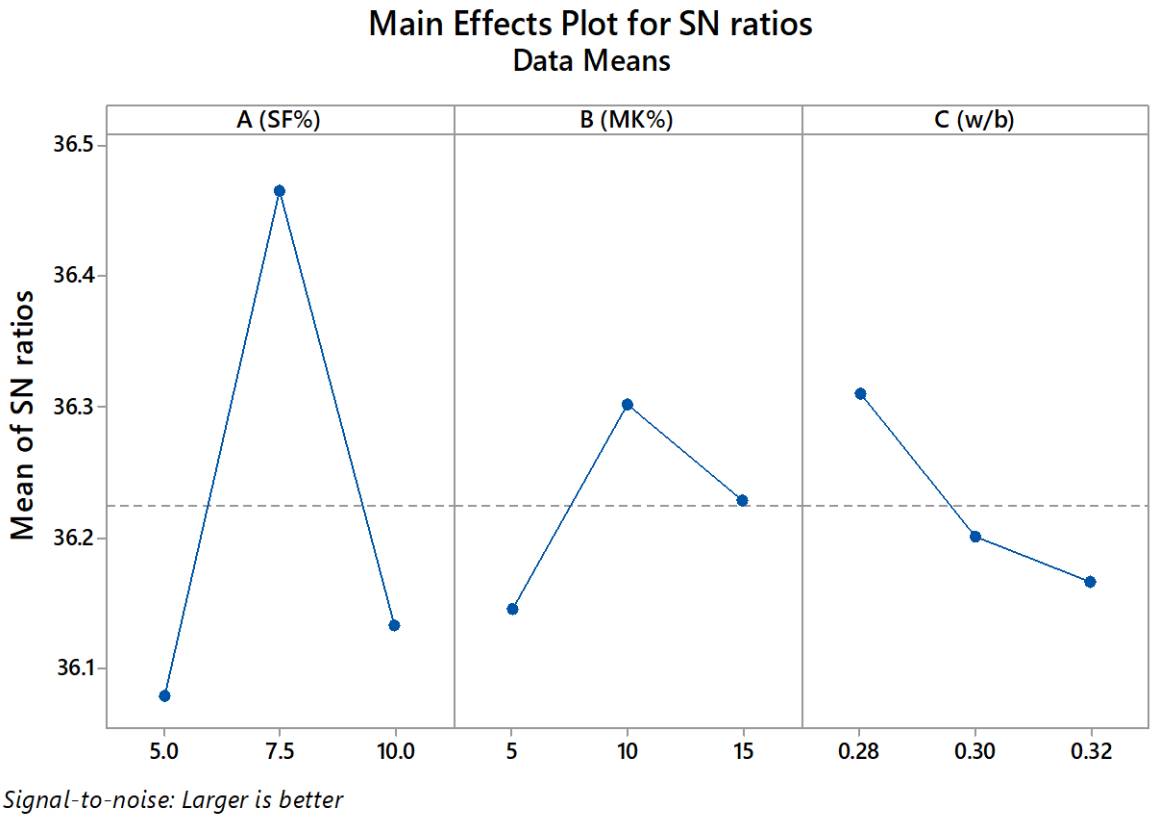

Fig A1: Main effect plot for mean SN ratios

Signal-to-noise ratio analysis and mean response analysis were carried out to determine the optimum factor levels. The optimal level for each factor is the one with the highest mean S/N ratio. From the main effect plot and response table, it is clear that factor A attains the peak at level 2 (7.5%), factor B attains the peak at

level 2 (10%), and factor C attains the peak at level 1 (0.28). Hence, the optimum combination given by Taguchi optimisation came out to be A2B2C1.

The optimised factor combination, i.e., A2B2C1, obtained from the Taguchi analysis, was used to prepare an experimental confirmation trial mix, which was further tested, further validating the Taguchi predicted optimum, confirming that the control mix was giving better strength and workability results within the acceptable limits.

Analysis of variance was used after the Taguchi analysis and the results of Analysis of variance are shown in table A6.

Table A6: Analysis of Variance

Source	**DF**	Adj SS	Adj MS	F Value	P Value
A (SF%)	2	14.8200	7.4100	45.37	0.022
B (MK%)	2	2.0467	1.0233	6.27	0.138
C (w/b)	2	1.8867	0.9433	5.78	0.148
Error	2	0.3267	0.1633		
Total	8	19.800			

The Analysis of variance confirms that Factor A (SF) is the most significant parameter (P = 0.022), while the low error mean square (0.1633) and high R^2 = 98.29% validate that the experimental results are reliable with minimal error, confirming the adequacy of the Taguchi L9 optimisation for the present study. The ANOVA conducted through Minitab's Taguchi DOE module yielded a model R^2 of 98.29%. The summary of the Model results obtained is shown in the table A7.

Table A7: Result Summary of the Model

S	**R-sq**	**R-sq(adj)**
0.404	98.29%	93.15%

The standard deviation of residuals (S = 0.404 MPa) is negligibly small relative to the response range, indicating excellent model fit with minimal unexplained error.